On-site Autonomous Fabrication at Architectural Scales

Levi Cai

B.S.E. Computer Science, University of Pennsylvania (2012)
M.S.E. Robotics, University of Pennsylvania (2015)

Submitted to the Program in Media Arts and Sciences,
School of Architecture and Planning
in partial fulfilment of the requirements for the degree of

Master of Science in Media Arts and Sciences
at the
MASSACHUSETTS INTITUTE OF TECHNOLOGY
June 2018

© Massachusetts Institute of Technology 2018. All rights reserved.

Signature redacted

Signature of Author: _____
Program in Media Arts and Sciences
May 4, 2018

Signature redacted

Certified by: _____
Neri Oxman
Professor of Media Arts and Sciences
Program in Media Arts and Sciences
Thesis Supervisor

Signature redacted

Accepted by: _____
Tod Machover
Academic Head
Program in Media Arts and Sciences

MASSACHUSETTS INSTITUTE OF TECHNOLOGY
JUN 27 2018
LIBRARIES
ARCHIVES

On-site Autonomous Fabrication at Architectural Scales

Levi Cai

Submitted to the Program in Media Arts and Sciences,
School of Architecture and Planning
in partial fulfilment of the requirements for the degree of
Master of Science in Media Arts and Sciences

Abstract

Recent developments in digital fabrication tools and materials have pushed how fast, how well, and in what forms products can be made. The construction industry has been interested in using these automated technologies, however, material and machine constraints prevent them from being adopted at the scales that are demanded. This thesis is focused on how we might automate construction, especially when physical human intervention may be difficult. What approaches can we pursue now? What approaches should we aim for in the future? How can we achieve high scalability and maintain sustainability throughout? I will focus on how methodologies in controls and design must shift, but will also discuss how materials, sensors, and structural and machine morphologies inform these decisions and must be jointly developed to create robust autonomous construction systems.

Climate change has instituted the need to reduce waste and use environmentally-friendly materials. Refugee crises have created severe housing shortages in remote and dangerous parts of the world. Growing curiosity about extra-terrestrial exploration have captured our imaginations about fabricating off-world habitats. These scenarios have further encouraged the development of novel platforms, that are not only autonomous, but can fabricate site- and task-specific structures, on-site and in unstructured environments.

I present a pathway through which we can explore and feasibly implement this research at every step. I propose we begin by (1) modifying and automating combinations of existing construction processes and materials. These systems, however, are not simply scaled, for which I present (2) strategies for developing new types of inherently parallelizable systems that use different materials, and are designed from scratch. And finally, inspired by nature, I speculate about (3) a truly sustainable, scalable, and inter-species cooperative future for construction. For this I explore the relation of social behaviors to fabrication and how to create them in both biological and artificial contexts, in the present.

Thesis Supervisor: Neri Oxman
Title: Professor of Media Arts and Sciences

On-site Autonomous Fabrication at Architectural Scales

Levi Cai

Signature redacted

Thesis Reader: _____

Joseph A. Paradiso
Alexander W. Dreyfoos (1954) Professor, MIT Media Lab
Associate Academic Head, Program in Media Arts and Sciences

On-site Autonomous Fabrication at Architectural Scales

Levi Cai

Signature redacted

Thesis Reader: _____

Radhika Nagpal
Fred Kavli Professor, Harvard University
Wyss Institute for Biologically Inspired Engineering

Acknowledgements

In my first weeks at MIT, Prof. Neri Oxman told me "not to look for problems to solve, but to find possibilities to explore," and has shaped my entire experience here and my ambitions going forward. From diving robots into the Charles River, building awesome robots to build awesome structures, to putting experiments on 0G flights, it's been a remarkable two years.

I want to thank Dr. Steven Keating and Julian Leland for the craziest introduction to MIT while in California working on the DCP, and to Dr. Markus Kayser, Sara Falcone, and Nassia Inglessis for a whirlwind tour with the Fiberbots (and Mark Feldmeier for the advice). I also want to thank the entire Mediated Matter family, past and present, (Andrea Ling, Tim Tai, Rachel Smith, Dr. Jean Disset, João Costa, Christoph Bader, Sunanda Sharma, Josh Van Zak, Barrak Darweesh, Daniel Lizardo, Michael Stearn, Chikara Inamura, Nicolas Hogan, Jorge Duro-Royo, Dominik Kolb, Kelly Donovan, Natalia Casas, Viirj Kan, Dr. James Weaver, Robert Garriga, Jami Rose, and Melinda Szabo) for being the most diverse and talented team I've worked with and for always being there for me and each other (and keeping me caffeinated).

I wish to acknowledge my readers Profs. Radhika Nagpal and Joseph Paradiso for inspiring me to be better both technically and morally.

Thanks to Ariel Ekblaw and Katy Bell, and the Space and Ocean Initiatives, for showing me what it really means to explore and carve your own path. Thanks as well to my friends and mentors who helped me get here in the first place and the friends I have made here who kept me sane, in my cohort and the extended Media Lab community, especially my food buddies Andrea Ling, Dan Levine, Stefania Druga, and Devora Najjar.

Finally, I want to express my gratitude to my family, Mom, Dad, and Angela for their unwavering support and my partner in crime, Susan Sheng, for the many adventures we've had together and those to come!

Table of Contents

1 Introduction to On-site Autonomous Construction

Growing interest in construction for refugee, remote, or even extra-terrestrial, situations have pushed the construction industry to look for new technologies to aid in these extreme domains. Often, due to the hostile and dynamic nature of these regions, a manual workforce can be difficult, and even dangerous, to utilize. In these scenarios it can be ideal to use automated solutions that can operate directly on-site and be used to create site- and task-specific structures ad-hoc. However, few construction processes are currently automated, and those that are, are difficult to use in on-site circumstances. This thesis will introduce possible approaches to the questions: what are the ideal, autonomous construction systems we would like to have, and how might we introduce them in practice, quickly, safely, and feasibly?

In this thesis, I will explore how to automate construction systems that can operate, with minimal human intervention, on-site in unstructured environments. These systems will be mobile, so that they can build structures much larger than themselves. I will present a series of improvements that can gradually be investigated and ultimately implemented in the real-world. I begin by demonstrating how existing platforms and material processes can be augmented with controls systems to automate them and achieve large-scale autonomous fabrication in the present. Then I will introduce strategies to parallelize and improve material processes, so that they can be more efficient in terms of speed and material usage. Finally, I will speculate on the development of an entire construction ecosystem, where designers, fabrication systems, and material processes are efficient and sustainable as a whole.

1.1 Motivation & Background

In terms of large-scale, sustainable, building strategies, nature provides us with potential sets of techniques to strive for. Eusocial organisms, which include ants, bees, termites, and wasps, are able to build habitats, must larger than the individual insects, that accomplish a wide range of objectives and function in various environments, all while using ad-hoc processes and materials. These processes are holistically sustainable, including the materials used, the methods that achieved them, and even the fabricators themselves. However, many of these capabilities are difficult to match with current technology.

For now, digital fabrication, especially 3D printing, has ushered in a new era of technology to produce products with new geometries, lower costs, less waste, and at much faster rates. Naively, these technologies could be used to assist in construction to obtain the same benefits while also minimizing danger to workers. However, the construction industry has not adopted many of these innovations because they do not use common construction materials and are difficult to scale in terms of size, speed, cost, and reliability. Furthermore, as these technologies are introduced into a remote and construction-oriented setting, new control and operation strategies need to be introduced and incorporated.

Several groups have begun to tackle these questions on a variety of fronts, focusing on either machine morphology, the underlying fabrication process, materials, automation and interface strategies, or some combination of them. Some earlier examples of scaling digital fabrication techniques were the developments of Big Area Additive Manufacturing (BAAM), by Oak Ridge National Laboratory, Lockheed Martin, and Cincinnati Incorporated [1], and 3D-printable concrete-like material used in conjunction with a large gantry crane, by Contour Crafting and USC [2]. BAAM focused on fundamental advances in material deposition processes to increase the deposition size and extrusion rate of traditional plastic filament deposition model (FDM printing) and enabled print sizes of up to 12' x 6' x 6' and a deposition rate of 80lbs/hr. Contour Crafting similarly developed a novel material with an affiliated material extrusion process and demonstrated one of the first instances of fully automated concrete-like extrusion with the explicit goal to automate aspects of the construction site.

1.1.1 Size Considerations

Since then, numerous other attempts have been made to scale either the speed or the size of possible prints. On the perspective of size, two approaches have emerged. The first is to develop larger, stationary machines capable of handling larger work volumes, as is the case in [2]–[5]. This approach is appealing, especially for gantry-based platforms, because they are relatively easy to create and control. However, they have strict limits before assembly becomes necessary, where large portions are built off-site, shipped on-site, and then assembled. This can often be a fast way to produce high quality components in tightly-controlled environments. On the other hand, it may require additional manual labor or a new set of automation techniques. They can also be difficult to use in an on-site context.

A second is to create mobile systems that can re-position around or on the structures as they build them, which has been explored by groups as in [6]–[17]. The latter approach draws inspiration from builders found in nature such as bees, beavers, termites, birds, and more. These systems rely on the ability to move about their structures to enable nearly limitless work volume, so long as the structure itself is traversable by the builder. However, mobile systems introduce additional complexity in terms of mobile mechanisms that can handle surface variations and obstacles, as well as localization. Some systems rely on aerial platforms [9], [10], [18] instead, and perform assembly tasks across a structure. This provides immediate, large work-volumes and allows for high mobility across the structure. It is important to note, though, that they have thus far required substantial infrastructure to manage power, localization, and environmental disturbances caused by the robots themselves. [9], [19] used motion capture systems and [18] used fiducials attached to a ceiling to provide high accuracy localization for the drones, which restricted them to indoor environments. Furthermore, because of both electrical and mechanical power restrictions, aerial systems have been limited to using light-weight materials like custom foam blocks, small plastic beams, and resin-coated fibers. Other systems, such as [6], [8], [11], [12], [16] have focused on ground-based vehicles with manipulators in order to perform placement and extrusion tasks. These follow strict layer-by-layer construction, but have used a larger variety of materials.

1.1.2 Speed Considerations

Two general tactics have also been employed in order increase fabrication rates. The first, as in the case of BAAM, is to find strategies for increasing the deposition rate of a machine. These strategies range from novel chemical and process developments, as with BAAM and its novel thermal innovations, and mechanical developments, such as simply having faster actuators for brick laying. A severe downside to this is if a process runs into fundamental scientific limits, either requiring new types of motors or materials and processes to be developed.

The primary alternative is to parallelize as many operations as possible. One demonstration of this idea, in construction, was in Longyan, China, earlier in 2018, to replace a stretch of train track in under nine hours [20]. 1500 workers, 23 diggers, and seven trains were organized into seven teams to complete tasks simultaneously. It is important to note the amount of careful planning and logistics that were necessary to accomplish this feat. Some work has been done in the automation community to achieve

these types of performance gains [3], [9], [11], [16], [19], [21] some of which use a team of independent mobile agents [11], [16], [19] and others use multiple arms on a gantry [3], [21]. In these situations, careful coordination and collision avoidance within a shared workspace becomes crucial, and is still an active area of research both in- and outside of the fabrication community. To address this, [9], [12], [19] only have one robot operating within the structure workspace at any given moment, which reduces the potential for collisions or interference. In gantry systems, it can be difficult to properly separate out motions, as the gantry itself constrains and couples actuators together, though it will vary depending on the type of actuation. In the case of [3], [21], where multiple arms operate on a single gantry, it becomes clear that parts must be discontinuous and need additional developments to handle part joints where one gantry ends and the neighbouring one begins. It is thus interesting to observe that assembly-oriented processes are frequently more straight-forward to parallelize as joinery is inherent in the process. Within continuous extrusion processes, advantages in mechanical and chemical bonds in a single piece is lost, or not naively achieved, when one machine encounters another. [11], [16], [22] have attempted assembly-based methods to develop novel algorithms and robotic systems that are able to operate in a shared workspace, and in the case of [23] able to cooperate directly by jointly manipulating components.

1.1.3 Material and Process Considerations

Initial material choices constrain the possible fabrication processes as well as the scaling strategies that are available. The list of combinations of materials, starting phases, and possible processes is vast, but only a handful are used in construction.

At the moment, materials that are code certified by the International Building Code [24] are the ones that dominate the construction industry. These materials include concrete, glass, wood, and some plastics, and have undergone rigorous testing for different use-cases, such as exterior and internal finishing or piping. These stringent requirements, which are necessary to ensure safety, are some of the primary reasons new materials are difficult to introduce into the market.

Other groups have begun to introduce new materials, or new ways of using old materials, into the architectural domain. MX3D [25] has begun to build a full-scale pedestrian bridge using welded metal, fabricated using a robotic arm to create organic shapes. This process requires a fully connected circuit in order for welding to occur and can be extremely slow. Composites are an increasingly popular class of materials used

in architectural settings for their lightweight, high strength properties that can require less material waste. Instances can be seen in practice such as the SFMOMA façade or in Menges' pavilions [13], [18], [26], however, these materials still do not see widespread usage, as they are complicated to control and have not passed all safety criteria.

Perhaps the most pertinent question is one of assembly vs. continuous materials and methods. Strategies involving the assembly of discrete, pre-fabricated modules provide natural strategies for scaling, as modules usually only need to be stacked or attached [9], [16], [17], [19], [22], [23], [27], [28]. Depending on the process, they can also be simpler to reverse and even re-use, removing a module and placing it somewhere else is generally more straightforward than cutting, melting, etc., reprocessing and then re-extruding. However, this can lead to questions on what are the appropriate "bricks" for each situation? These approaches can also increase the complexity of fabrication, as bricks need facilities to be pre-fabricated and transported to the assembly site.

Continuous fabrication, however, if material properties and their outputs are well understood, can offer higher resolution and higher degrees of tunability or adaptability, and in certain circumstances, reduced usage of material and need for transportation. Generally, these can be considered assembled processes if observed at a much smaller, or chemical, scale, and may even have their own lattice-like structures. Systems that require high-performance across several parameters, such as aerospace and automotive applications, often turn to continuous methods of fabrication over assembled in specific parts, as questions about bonding agents and methods can raise concerns over structural stability and performance. When scaling these methods further, an issue of print or part segmentation can ensue, leading to a hybrid assembly of large continuously printed parts, as seen in [2], [5], [29], where parts of walls are first printed, then shipped, and finally assembled on-site.

For completeness, I will briefly mention self-assembled systems. These serve as an alternate approach to the previous, where the agents *themselves* are the assembled modules. They are found ubiquitously across nature, as almost all living systems are composed of self-assembled and self-organized cells or larger organisms, and whose strategies are actively being studied and artificially mimicked [30]. These can take advantage of either (mostly) passive [31]–[35] or active approaches [15], [36]–[43] to control and determine form. These systems are especially effective in temporary situations, where immediate reconfigurations are desirable. However, to limit scope,

they will not be explored as thoroughly in this thesis, though are certainly applicable and worth a further discussion.

1.1.4 Bio-inspiration

Nature inspires through its creative, yet immensely successful, approaches to solving some of the most difficult challenges, some of which are still out of reach to humanity. Throughout this thesis, I will continually draw from bio-inspired solutions to address issues in scalability, robustness, and sustainability.

Biology has produced some of the world's most successful fabricators, from termites to birds to beavers. Of these, eusocial insects have been of primary inspiration to researchers in automated construction. This is because they are, relatively, easily studied and provide simple solutions to the problem of cooperative construction that can be adapted to autonomous systems.

In addition, all of these organisms operate in robust and sustainable ways, using only environmentally friendly materials, and constructing structures ad-hoc in a wide range of environments that can be adapted to various circumstances.

1.1.5 On Interfaces, Automation, and Controls

As fabrication machines become increasingly complex, so do the techniques that are used to control them. This issue is compounded when considering multiple perspectives, one from the viewpoint of increasing machine or agent capabilities, and another from the perspective of the designer or user who will ultimately interact with the machines. Users of CNC machines with greater than 3 degrees of freedom are familiar with this, as the machine themselves can allow for more complex geometries and features, such as double curvature, but toolpath generation and potentially mounting of stock material can increase in complexity. This often leads to a churn in the design process, where the designer models new parts, usually in some form of CAD software, and verifies that the machine can fabricate it by generating CAM toolpaths and confirming that the paths are traversable by the machine. This process can be time consuming depending on the complexity of the part, and as machines become increasing complex, so will the design process.

This burden can sometimes be alleviated from the perspective of the designer if particular decisions can be made on the machine side, and from the perspective of the designer of the machine itself, if aspects can be automated. However, this can require

sophisticated controls software and mechanical systems, such as handling redundancy and singular conditions in high-DOF robot arms or complex end-effector tool changers, respectively.

In this thesis I will attempt to outline the effects of system design decisions on each of these perspectives and how one might approach balancing them, or at least, highlighting their impacts. This discussion becomes especially necessary when dealing with multi-agent systems where possible control parameters exponentially increases with additional agents, due to the additional parameters and the interactions between every pair of agents that must be considered. This can be overwhelming, either from the automation perspective or from the perspective of the designer. While I do not solve these issues within the span of this thesis, they will be considered throughout.

1.2 Approach & Methodology

While this thesis will focus on the design and development of controls and interfaces for autonomous construction systems, few aspects of a fabrication system exist in isolation. Design changes to any part of it can dramatically affect each other portion. Within this thesis, I will explore the interactions across four primary facets of autonomous construction systems: the **designers** who place requirements on the structure, the output **structure** itself, the **materials** used in it, and the **agent(s)** that built it. Here the structure is the final geometry that is left on-site once the construction process has ended. The materials can include both that of which the structure is composed of, but also those that are incorporated as part of the build process, such as scaffolding and support materials. The agents are the system that manipulate and modify the materials—either through subtractive, additive, formative, or assembled means—and ultimately does not remain once the structure is complete.

Each of these facets dictates, and is informed by, the decisions made in the other facets. This interplay is what creates complexity in deciding how to proceed when designing novel construction systems. The assumption embedded within this thesis is that all facets must be discussed in conjunction with one another to make decisions clear and co-development across several facets can be made together to make substantial progress compared with individual improvements.

For instance, say we are designing a new fabrication system that purely uses materials from standard, prismatic wood stock. This generally limits us to machines that are capable of subtractive, cutting and sanding, or assembly, gluing and bolting,

procedures. It also means that mostly rectangular, or at least cornered, structures are far simpler and faster to create than organic ones, though these are certainly possible with sufficient cutting, sanding, and layering. These suggest that autonomous systems will likely need to sense, or at least plan for, existing raw materials and their configurations relative to the machine.

For the remainder of this thesis I thus lay some foundational choices that will steer the design of the systems discussed. At the highest level, the goal is to develop fully autonomous fabrication systems that can operate in extreme and remote environments and build at architectural scales. These systems will ideally be low-cost and highly scalable, so that they can be used for a wide-range of purposes and environmental conditions. Each system proposed should be feasible to create, and usable by designers. And overall, I hope to encourage movement in the direction of a truly sustainable future for architecture and fabrication.

To get there however, several innovations must be accomplished and addressed in a step-by-step fashion. The approach taken in this thesis is to incrementally introduce changes to material selection, agent morphology and capabilities, designer interactions, and the systems necessary to automate them.

I propose to start the automation process by combining existing material systems with existing platforms and technologies, with the idea that regulation and overall safety are the crucial bottlenecks towards introducing. Once these systems begin to be implemented, it is worthwhile to explore newly emerging materials that reduce waste and increase structural capabilities, such as the case in composites. At the same time, in order to achieve scale, we need systems that can build cooperatively without incurring complexity costs on design and fabrication. And finally, we need to eventually move to truly sustainable strategies, and work closer with natural materials and fabrication systems that use environmentally-friendly materials and processes.

Most of these systems are biased towards ground-based mobility to expand the work envelope of each system, and as opposed to aerial systems, to reduce infrastructure and increase the range of material systems we can work with. These systems will also focus on additive manufacturing approaches using continuous extrusion methods, because they generally enable a wider range of possible geometries and can be more adaptable on-site.

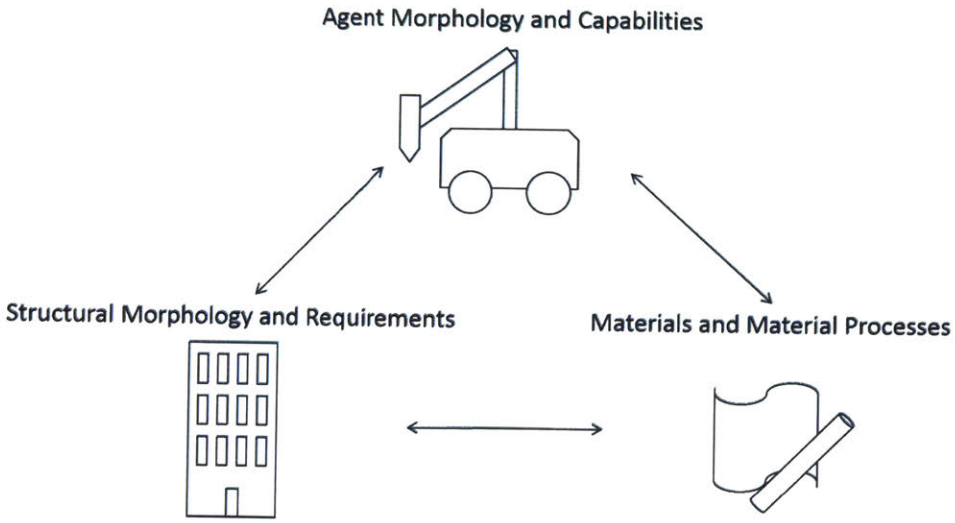

Figure 1: The facets that designers engage with in any fabrication system

1.3 Thesis Organization

This thesis will be organized into 3 primary chapters, followed by a chapter containing overall concluding remarks and discussion. Of these core chapters, chapter 2 will focus on strategies for automating construction that can happen **now** by combining existing platforms and technologies in novel ways. Chapter 3 will explore how **near-term** autonomous systems can be developed to exploit parallelism and composite be used to scale construction in both size and speed. Chapter 0 will be more speculative and explore what properties an ideal autonomous construction system in the **far future** should have. These will emphasize environmentally-friendly (or completely natural) approaches to fabrication and material selection, and what steps can be taken to study and implement these technologies now. Within every chapter, I will emphasize experimental, as opposed to theoretical, results on separate platforms that I have helped develop to demonstrate the feasibility of these ideas. While the primary focus will be on designing autonomy, electronics, and software interfaces, I will provide sufficient preface of the material and hardware systems that motivate the decisions being presented.

	Today	Tomorrow	The Future
Materials	Existing	Composites	Natural
Systems	Single robot from pre-existing systems "easier"	Custom-made, multi-robot systems "harder, but better"	Biological systems with swarms "hardest, but ideal"
Implementations	DCP v.2 	Fiberbots 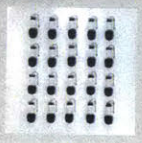	Silkworm Swarms 

Table 1: Overview of the thesis, top row indicates the time-scale and corresponding chapter. Then describes the materials systems, fabrication methods, and case studies explored within each chapter.

2 Today, Monolithic with Existing Platforms and Materials

2.1 Background & Approach

Several groups have already started to try to commercialize various aspects of autonomous, large-scale fabrication units. Most of these systems attempt to use new materials alongside large, monolithic systems, that are easier to work with from an automation standpoint. For instance [2], [5], [44] all work with a new form of 3D-printable concrete, which allows them to directly extrude concrete without the need for formwork. This concrete can then be extruded via large gantry or arm-style systems. Hadrian [8] uses a large, mobile, compound arm to do brick assembly, but also uses a specialized adhesive, rather than traditional mortar, which may prevent fast commercial viability in some regions. Built Robotics [45] instead focuses on automating a traditional construction vehicle, the track loader, for general material relocation tasks, such as digging or foundation, but is unable to perform overall fabrication.

Because safety is a key concern, and is a primary bottleneck for the introduction of certain construction techniques into industry, we focus on using materials and platforms that are familiar to the industry. However, these are not trivial to use, as indicated by predecessors and highlighted in the next two sections.

2.1.1 Existing Methods and Materials

Existing materials for construction include concrete, glass, wood, some plastics, and foams. Each of these materials can be difficult to work with in an automation context. Concrete typically requires some type of mould or formwork in which to cure, and is generally very fluid, and thus difficult to directly 3D print. Glass requires tightly controlled environments that can handle extreme temperatures, which makes it difficult to scale, and especially apply in an on-site context without assembly. Wood can potentially require sophisticated manipulations during assembly operations. And plastics have yet to be scaled, as seen in BAAM. We must then find a material strategy that can scale and be used easily with autonomous systems.

2.1.2 Existing Platforms

Construction sites are already populated with a large variety of equipment and vehicles that are specifically built to operate in these types of environments. It is thus tempting

to simply attach sensors and automate existing vehicles this way. However, these vehicles were not built for automation. Driven primarily by diesel and hydraulic valves, precise maneuvers, which are generally required for automated fabrication systems, can be difficult to achieve.

On the other hand, large-scale automation and fabrication tasks are already widely used by the automotive industry. However, these systems are meant to be operated in highly controlled environments where each task is explicit and highly repetitive. Construction sites tend to be significantly less structured, and so naively adopting large robotic arms is non-trivial as well.

Some groups have adopted a hybrid approach, such as [6]–[8], and are able to assemble structures on-site, using high-precision robot arms in conjunction with existing construction vehicles. This strategy seems the most promising, but there are still challenges to address in how to combine and control these types of systems.

Case Study: The Digital Construction Platform v. 2

Figure 2: The Digital Construction Platform v.2 with spray foam end-effector and trailer attachment, during a large-scale print. The orange arm is a KUKA KR10 R1100, the white vehicle is an Altec AT40GW aerial boom truck.

In this section I will dive into the development of a platform, the Digital Construction Platform v.2 (DCP), that highlights the process and analysis for converting existing construction equipment into an autonomous system that can be used for large-scale fabrication. This work was done in collaboration with Dr. Steven Keating, Julian Leland, Dr. Neri Oxman, and aided by undergraduate researchers Damien Martin and Selam Gano. Much of the software and controls systems were developed by myself along with Julian Leland. This section will review critical aspects of the development of the system as they relate to this thesis and the overall discussion of automating large-scale construction by augmenting existing platforms. Much of this work is published in *Science Robotics* [46], and additional details in [47], [48]. All control software for the system can be found in [49].

2.1.3 Platform Overview

The original Digital Construction Platform (DCP v.1) was developed by Keating et al. [50], [51] in 2012-2014 and a second variation, based on the same concepts, was developed in 2016-2018, known as DCP v.2 and presented in [46]–[48], which will be the focus of this discussion.

The DCP is an autonomous robotic platform developed to perform large-scale, on-site construction tasks, as shown in Figure 2. By changing the end effector, the DCP was shown [46], [47] to be able to perform subtractive and additive tasks, such as digging and 3D printing, perform basic environmental sensing, as well as gathering raw materials. The system was designed to automate near-term, and large-scale, construction tasks by utilizing certified materials, fabrication processes, and existing platforms that are familiar to the current construction industry.

The hardware is composed of two parts, a custom aerial lift coupled with an industrial robot arm. The base portion is a re-purposed AT40GW Altec Articulating Boom Lift, generally used for elevated work platforms for construction and maintenance tasks. This provided a track-based mobile platform along with an articulated, 6-DOF hydraulic arm, though the DCP only takes advantage of the first four joints, named J1-J4. The boom arm was customized and equipped with sensors along each hydraulic joint and the hydraulic levers were adapted to allow for programmatic control. At the end of the boom arm, a KUKA KR10 R1100 sixx WP electric robotic arm was attached. The combination of the boom arm with the KUKA arm creates a micro-macro serial-link manipulator configuration. Generally, the micro manipulator—the KUKA—is used for

more accurate and dexterous motions while the macro manipulator—the boom arm—is used for larger and faster motions. Refer to Table 2 for technical specifications.

A retractable track system at the base of the aerial lift provides mobility, and increases the possible lateral work volume. The retraction allows the platform to fit between standard doorways over 34 inches in width and, by stowing the arm, over 9 feet tall. By extending the tracks outwards, the system can increase the stability of the platform during rather sharp turns. These features make the DCP v.2 versatile to navigate and build within relatively standard construction sites.

Additional features of the DCP v.2 are a custom battery system, developed by Altec, so that the DCP can run purely on electrical power, whereas standard systems are diesel driven. The battery can also be charged via solar panels that were mounted on the system, so the DCP is self-sufficient in terms of energy and can fully operate in remote environments, as long as there are construction materials available and sunlight.

	DCP v.2				
	AT40GW				KUKA
	J1	J2	J3	J4	
Pose Repeatability (ISO 9283)	55mm				0.06mm
Max Joint Speed	8 deg/s	6 deg/s	6 deg/s	120 mm/s	225 deg/s
Joint Resolution	0.05 deg	0.15 deg	0.15 deg	3 mm	0.005 deg
Max Radial Reach	9.1 m				1.48 m

Table 2: Technical overview of the DCP, updated from [47]

2.1.4 The Material Process (Print-in-Place)

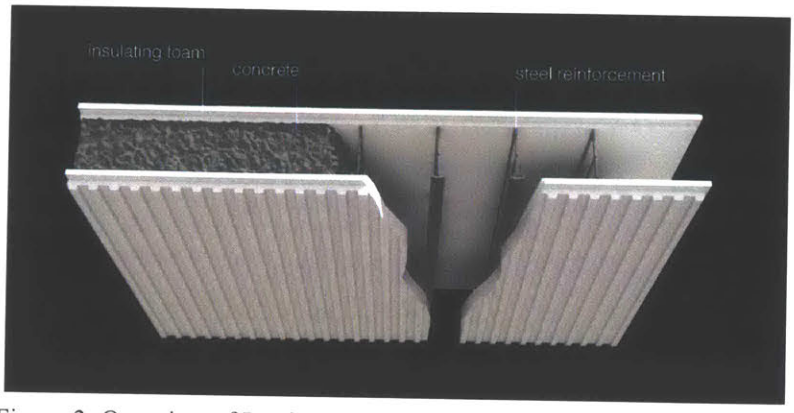

Figure 3: Overview of Insulating Concrete Forms (PC: Barrak Darweesh)

While the overall DCP system is proposed as a material and process agnostic platform—that it can perform additive, subtractive, and sensing tasks—its primary use was to extend the work volume of the Print-in-Place (PiP) fabrication process [50].

The PiP method was developed as an extension of Insulating Concrete Forms (ICF), which is a code certified method for doing concrete fabrication [52] as shown in Figure 3. In traditional concrete construction, moulds, often wooden, with steel rebar ties are placed on the construction site. Concrete is then poured into the moulds and once it has hardened, the moulds are removed, and insulation is then added to the interior of the structure. Here, the process of adding and removing moulds wastes both time and mould material. ICFs instead use the insulation material itself, such as polyurethane foam, as a mould that is then left as part of the final output structure. ICFs typically consist of foam blocks with steel reinforcement inside, that are then stacked like LEGO-bricks. Once stacked, concrete is poured inside them, allowed to harden, and the building process with insulation is complete. This process of concrete fabrication assumes fairly rectilinear structures, as they are generally assembled from rectilinear blocks.

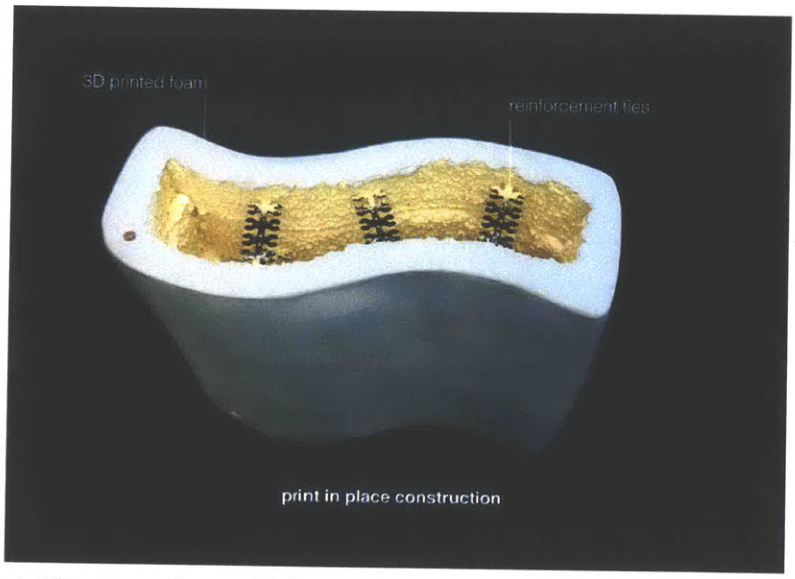

Figure 4: This shows the mould that can be created via Print-in-Place construction. Spray foam is deposited layer-by-layer via a 3D printing platform. Reinforcement ties (rebar) are then added throughout the process, and surface finishing can be applied afterwards. Finally, not shown, traditional concrete can be poured into the mould. PC: Steven Keating [47]

PiP, as shown in Figure 4, modifies the ICF process by replacing the insulating blocks with a sprayed insulation foam. This foam can be deposited via CNC means, such as a traditional 3D printer, or a robotic arm. Here the end-effector would be a foam spraying nozzle. This allows for more "organic" geometries and doubly curved surfaces to be created, while adhering closely to overall building certification standards.

The DCP acts as the robotic platform by which insulation foam is deposited, sprayed, on the construction site. This sprayed material must be able to withhold liquid concrete mixtures, verified in [50], and must be double walled to form a mould. Once the foam has cured and several layers have been deposited, steel reinforcement can be added, and then desired concrete mixtures can be poured.

2.1.5 Automating the DCP v.2 (Controls and Interfaces)

In traditional filament deposition-style 3D printing, deposition path accuracy, resolution and layer-to-layer adhesion are defining characteristics of the capability of a 3D printer. This requires that material feed rate, deposition bead size, nozzle position and nozzle velocity are all accurately and precisely controlled. In addition, reasonable paths that do not incur collisions between the part and the printer, and fall within the dynamic and

kinematic constraints of the printer, must be generated. These requirements dictate the design and development of the controls system for the DCP as well, which uses a custom spray foam nozzle, in this case of PiP, instead of a traditional plastic extruder.

Once the two portions were combined, several steps remain before the system is usable as a functioning, autonomous platform that is capable of PiP-style fabrication. The steps followed are listed below and published in detail in [46]–[48], we will summarize on certain aspects for completeness:

Automation:

1. Mounting sensors to the AT40GW for state feedback, including the arm and the mobile base
2. Generating kinematic and dynamics models: forward kinematics (FK), inverse kinematics (IK), and jacobians, that can be computed in near real-time
3. Creating controllers for AT40GW
4. Decide on interface and communication schemes between the AT40GW platform and the KUKA
5. Create a material handling system

Usability:

1. Decide on CAD capabilities
2. CAD to Cartesian-space waypoints and trajectories
3. Simulations for verification

Kinematics (AT40GW)

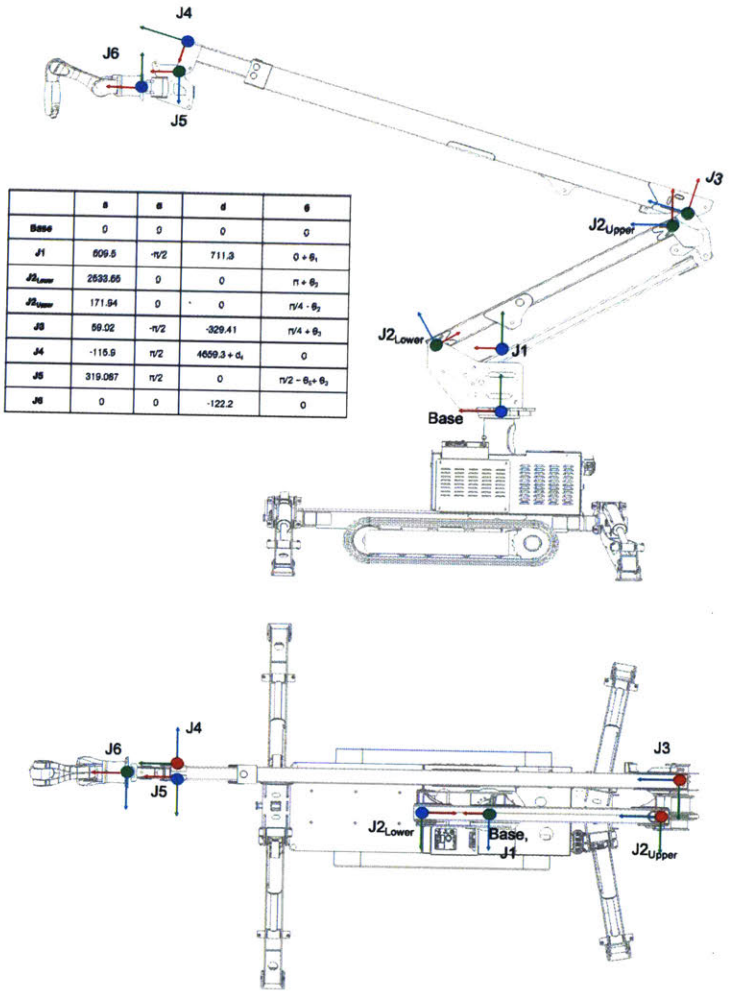

	a	α	d	θ
Base	0	0	0	0
J1	509.5	-π/2	711.3	$0+\theta_1$
$J2_{Lower}$	2533.65	0	0	$\pi+\theta_2$
$J2_{Upper}$	171.94	0	0	$\pi/4-\theta_2$
J3	59.02	-π/2	-329.41	$\pi/4+\theta_3$
J4	-115.9	π/2	$4659.3+d_4$	0
J5	319.067	π/2	0	$\pi/2-\theta_5+\theta_3$
J6	0	0	-122.2	0

Figure 5: DH parameters with corresponding frames of reference. J1-6 are the actuatable joints provided by the stock AT40GW. J1-3 and J5-6 are rotational and J4 is prismatic, also published in [48].

The AT40GW consists of 6 moveable joints that are referred to as J1 through J6, as labelled in Figure 5. It has a RRRPRR configuration, however, only J1-J4 are provided with 500Hz PWM-enabled control interfaces on the hydraulic valve drivers. For this reason, we do not use J5 and J6 in typical autonomous operation.

A forward kinematics model was derived using DH parameters with notation specified in [53]. This generated a number of matrices used to compute rotations between the base frame of the AT40GW to all intermediate frames through J4 and to the mounting position of the KUKA. The rotation matrices associated with the intermediate joints were used, by pre-multiplying with the rotation matrices of previous joints, as part of a simulator to visualize the state of the robot.

Figure 6: Light painting using control system preceding FK, IK, and trajectory generation optimizations. Points were specified roughly 1 m apart and controlled in joint space, which results in the "waves" between points.

The Jacobian, using J1-4, was computed using MATLAB's built-in jacobian function and was combined with a custom iterative inverse kinematics solver with a fixed step size function. All of these matrices were first computed using the MATLAB's symbolic toolbox. Generally, solving for intermediate states using the symbolic toolbox is inefficient, as resolving symbols is slow, and can result in run-times of several seconds per conversion between task and joint space coordinates. This can severely restrict how the controllers can be implemented (as these conversions cannot occur at run-time), as shown in Figure 6. By vectorizing and functionalizing (using MATLAB's matlabFunction command) each of these methods, we were able to achieve end-effector controllers that could coordinate all joints in task space running at 100Hz. These were further improved in later work by Leland in [48].

It is also important to note that the automated use of J2 was generally restricted in order to simplify the kinematics solution and reduce possibilities of singularities. J2 was primarily used to temporarily extend the reach of the arm for larger operations when required.

Sensors and Electronics

Many 3D printers in operation use stepper motors which can be controlled using position, velocity, and acceleration profiles, all simultaneously, with high accuracy and can be purely feed-forward driven as long as slippage can be prevented [54]. Unfortunately, construction machines are not designed to be precise or automatable. Their high-torque and force requirements restrict the ability to use motors resembling steppers, and even worse, their linkages are often flexible [55], [56] which makes their dynamics difficult to model or predict overall behavior during motions. While human operator readily account for these errors, most robotic systems with similar configurations to the AT40GW are equipped with sensors to provide state feedback and react to disturbances instead. However, the stock AT40GW, as it is not meant to be automated, is not equipped with any form of digital feedback.

We thus attached a series of linear and rotary sensors to provide feedback for controls. Balluff magnetostrictive linear sensors, which output absolute position measurements from -10 to 10V, are attached to the hydraulic cylinders on J2-4 [57]. These are mapped to rotational motions for J2 and J3, with resolutions of 0.15°, and standard linear motion for J4, with 3 mm resolution. A YUMO relative rotary encoder was mounted to J1 with 1024 counts/rotation resolution. These sensors are connected to LabJack T7 PRO DAQ analog-to-digital converters and allows us to read the sensors from MATLAB.

All devices, including the KUKA, coordinated with a central desktop computer, iMac, running MATLAB. The mobile tracks and outriggers (4 large "legs" used to stabilize the AT40GW during arm motions) were also modified so that they were controllable using PWM signals, but no feedback is currently available for them.

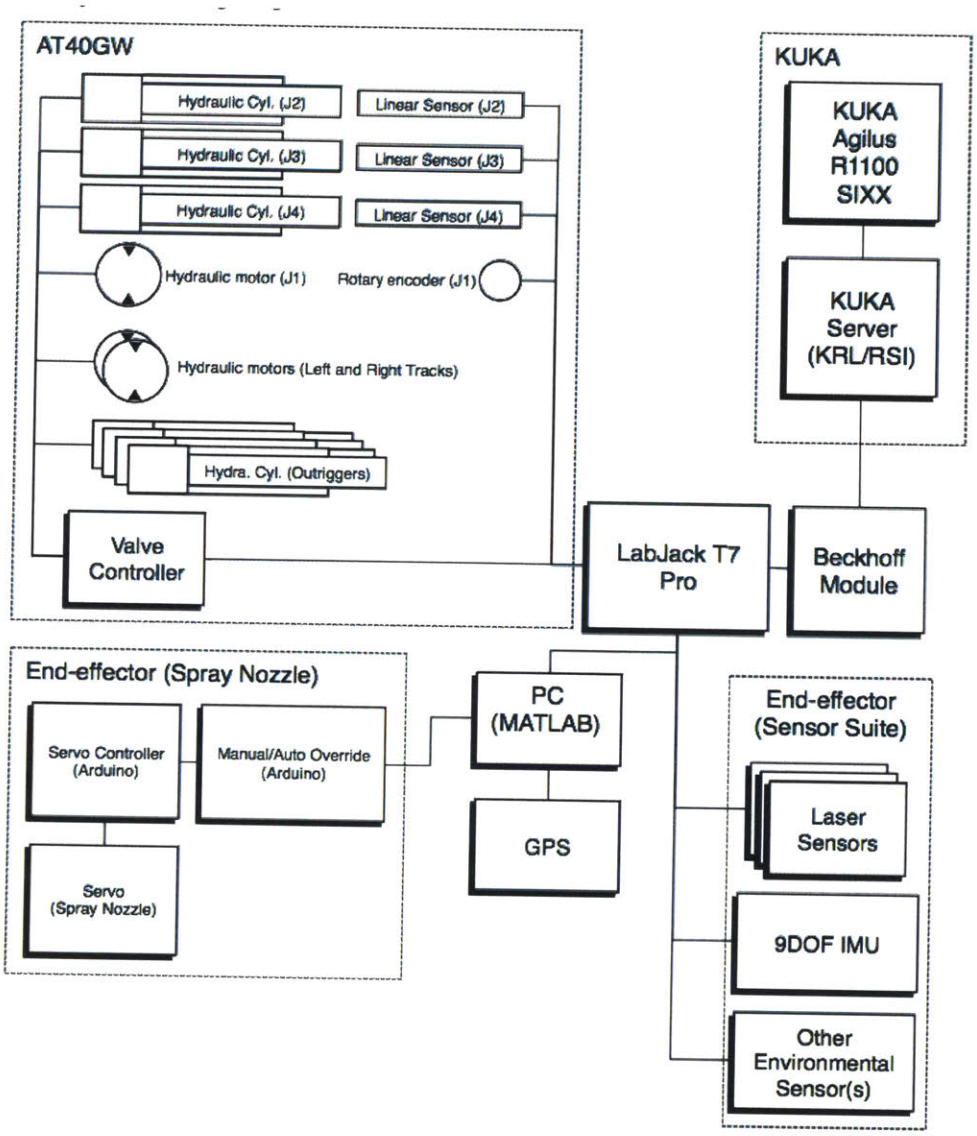

Figure 7: Overall software communication architecture of the DCP v.2, originally published in [46], [47]. The AT40GW, KUKA, and end-effector systems are all coordinated via a central PC running MATLAB.

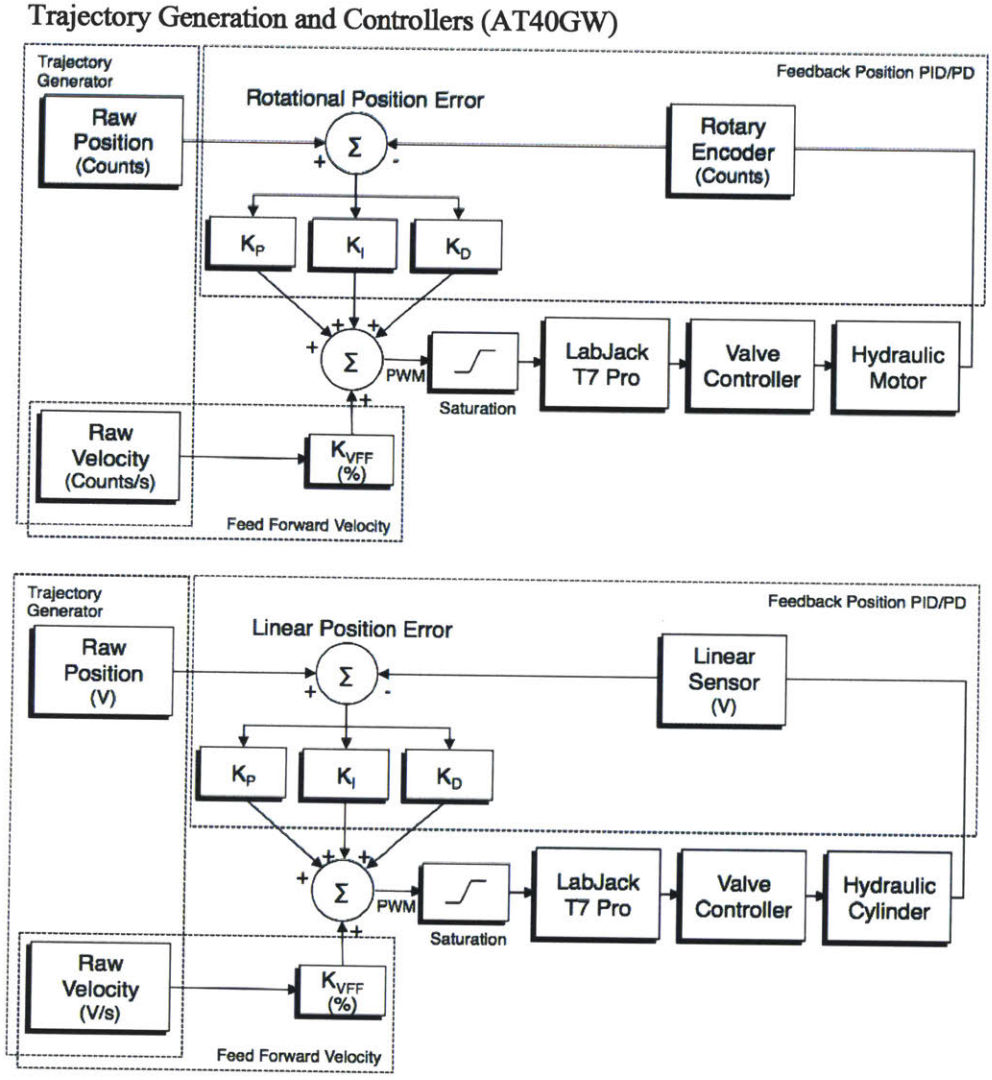

Figure 8: Controller block diagrams for positional PID controller with feed-forward velocities on each of the joint types for the AT40GW. Developed and run in real-time in MATLAB at 100Hz. Diagram originally published in [46].

For motions involving the AT40GW arm, it was necessary to generate trajectories. Note that the AT40GW arm was only used for 3D end-effector positioning, and the KUKA was responsible for the additional 3 degrees of freedom if orientation of an end-effector was required. Unlike a 3D path, trajectories also include velocity and acceleration information along the path. First, waypoints are generated in the space, either manually or from the output of a slicer program (similar to a traditional slicer program used in 3D

printers). A task-space (or 3D Cartesian space in this case) acceleration profile is specified for all the waypoints and a desired velocity to be maintained throughout the path. The task-space velocity must remain as constant as possible in order to ensure reliable print outputs, as it directly affects the print bead size. Any deviations in velocity during the path may result in bead sizes that are too small to allow necessary adhesion in the next layer. This can be difficult in high-DOF arm systems where translation from task-space velocities into appropriate joint-space velocities and back can introduce errors.

Once the waypoints, acceleration, velocities, and timestep have been selected, we used the mstraj function from Peter Corke's RVC Toolkit, with slight modifications to return velocities and other related information [58]. While generally used to generate joint-space trajectories where all joints should arrive at their destinations at the same time, we used it as a task-space trajectory generator for 3D motions, consisting of linear motion between waypoints and parabolic splines between them to account for acceleration profiles. Points were sampled along the trajectory assuming 100Hz, 0.01sec, time increments.

From here we created positional PID controllers with feed-forward velocities to track the generated trajectories at a fixed rate of 100Hz to match the sample rate of the trajectories. A separate controller was used and tuned for each of the 4 actuated joints. The controllers operated in joint space, so all task-space trajectory profiles were converted to joint-space preceding execution.

One additional issue in developing the controller is that a feed-forward mapping between PWM commands and desired velocities for each joint were required so that appropriate commands can be sent to the DCP. However, even though the PWM signals control the velocity of the hydraulic valves, the relation is highly non-linear. Hydraulic valves have a large deadband region, where a non-zero PWM signal generates 0 motion, and have tight saturation bounds, where a larger PWM signal does not generate faster motions. Both of these situations can cause large errors to occur between the desired control inputs and the controller outputs, and hence cause additional problems such as system jerking or lack of motion. We empirically mapped physical velocities to PWM signals by driving each motor at fixed PWMs and measuring the output velocities. Once a discrete and coarse profile was mapped, any PWM points that fall inside these ranges is linearly interpolated to retrieve a corresponding velocity, or vice versa. It is also notable that this method is still inaccurate, and does not account for couplings between

linkages and joints. For instance, if J4 is fully extended, it could adversely affect J3 motions as there is a longer mass to move. Details of these mapping methods and explanations are covered in [48], but samples are shown in Figure 9 and Figure 10.

We found that overall, our system could generally operate between 50 mm/s to 350 mm/s in Cartesian space over most trajectories that lay inside its overall workspace. Speeds that were faster caused severe oscillations in the arm that are not addressed in our current system and anything slower often reached deadband issues in one or more joints so incorrect resulting motions would occur.

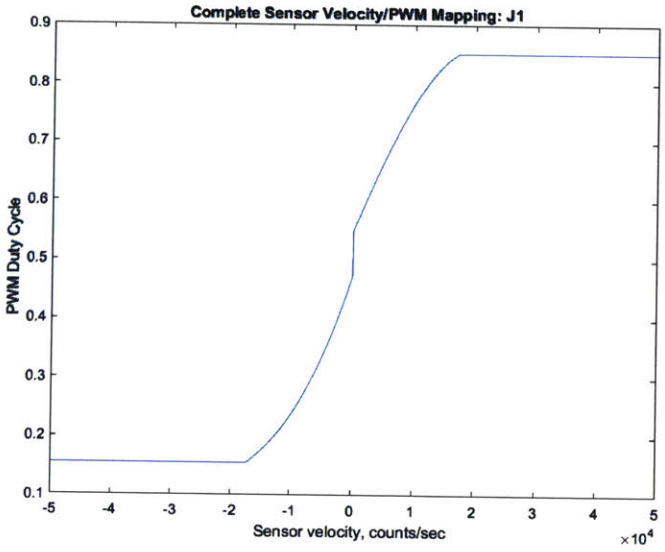

Figure 9: Mapping between PWM signal to velocity for J1. The perfectly vertical segment between PWM duty cycle 0.45 to 0.55 indicates a deadband region, and the horizontal regions indicate saturation areas.

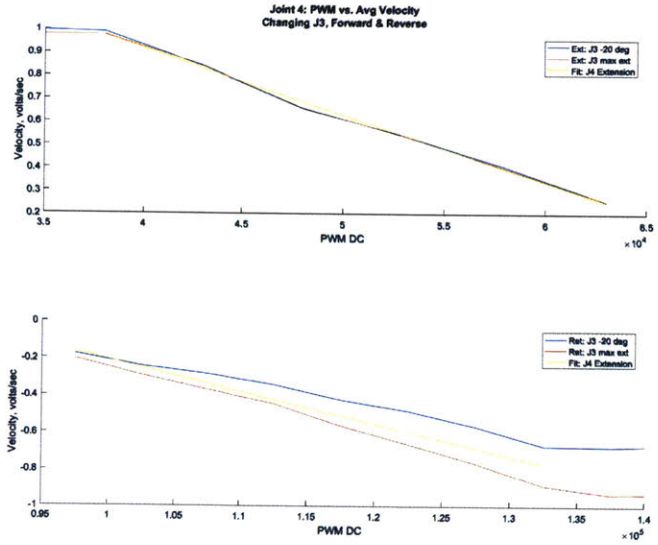

Figure 10: Shows the PWM to velocity mapping for J4, highlights the issue of the coupling between joints affecting the motions of other joints adversely as J4 mappings change when J3 begins to move at the same time. We primarily assume that these joints are not coupled in the controller, and treat these deviations as noise that the controller can compensate for. However, better mappings will improve performance.

Simulation

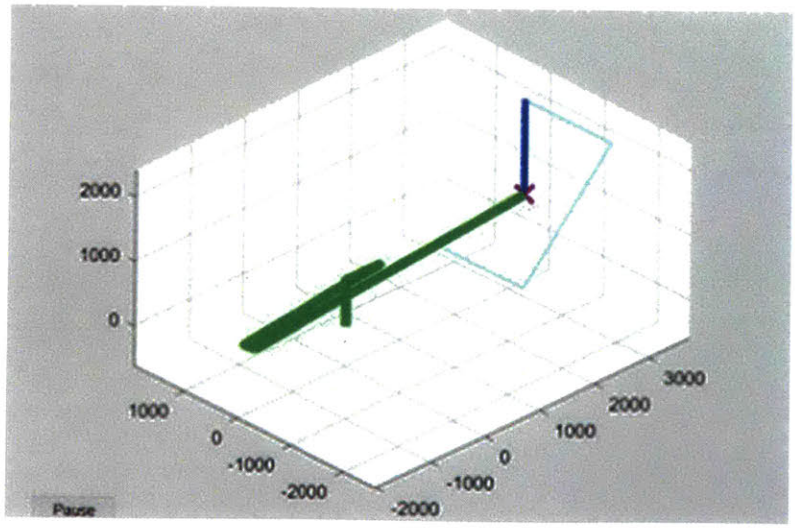

Figure 11: Example of the simulator, the green represents the current configuration of the AT40GW arm, the light blue line is a trajectory, the dark blue represents the current segment

being followed and the cross is the location of the desired point in the trajectory. Significant drift or error has occurred if the desired point deviates from the end-point of the AT40GW arm.

A simulator, show in Figure 11, was built to assist in both offline and online visualization and testing for development. This simulation, when in offline mode, simply tracked a virtual set of joint states of the robot, which could then be displayed using forward kinematics. In this mode, it was used to aid development of waypoint generators, trajectory generators, and controllers, and could fully simulate all of these functions. By adding Gaussian noise to the arm motion during controller simulations, basic empirical tests could be made to understand robustness by seeing if errors accumulated over time between desired tracking points and the end-effector location. Note however that this simulator did not contain any physics models, so could not be used to resolve more complex issues based on dynamics.

When used online, the simulator could be fed current joint positions, and was used to monitor progress and current state of the system. The simulator ended up being a crucial component to fast development and logical testing for the system since preparing and running full-scale real tests on the DCP were extremely time-consuming, often taking up to an hour to setup.

Material handling

As with any additive manufacturing process, the deposition rate and material bead size often dictate how the entire rest of the system must behave. We used a two-part polyurethane foam, Dow Chemical Froth-Pak Foam Insulation, that was deposited via a spray nozzle. The polyurethane foam was stored in large pressurized containers, roughly 4000lbs. for each part, on a trailer hitched to the DCP itself. The polyurethane foam, once mixed, takes approximately 30 seconds to cure and expands to several times its original volume depending on how much was deposited. The spray nozzle itself, as shown in Figure 12, provided a spray nozzle that could be programmatically controlled. However, the control was not well modelled and highly non-linear in terms of spray rate and bead size compared to the control inputs. In order to understand the coupling of all these behaviors, empirical test, shown in Figure 13, were performed to select an ideal set of parameters for a large-scale print. In the future, better models of these parameters and their relations would vastly improve possible performance.

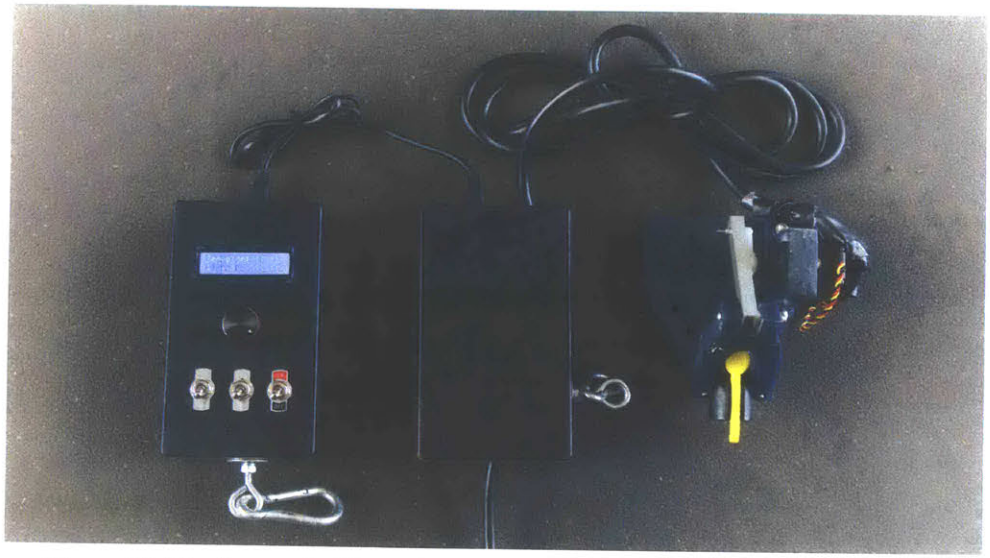

Figure 12: The foam end-effector for PiP test print. Allows for basic control over foam spray rates both manually and programmatically by adjusting the position of a servo motor. The bead size and spray rate varies highly non-linearly with the position of the servo motor.

Figure 13: Many empirical tests were performed to find mappings between Cartesian speed of the end-effector, the distance of the nozzle from the print height, and the spray nozzle settings, and their effects on bead size and overall material deposition rate.

2.1.6 Control of Dual Arms

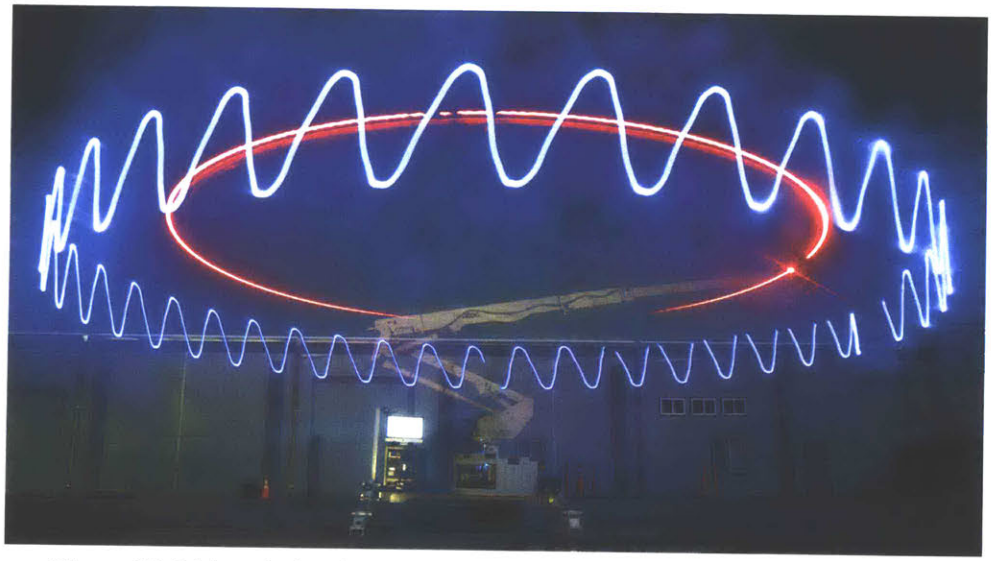

Figure 14: Light painting demonstration of a parallel operation motion using separate KUKA (in blue) and AT40GW boom arm (in red) motions while executing a single trajectory.

Once the AT40GW has control capabilities, it must then be augmented with the KUKA system. The KUKA has 3 primary means of programmatic interfaces, all of which rely on its internal proprietary modes of control to execute programs. The first, and most commonly used in our applications, is to send motion commands via UDP sockets to the KUKA Robot Sensor Interface. This requires a custom C++ UDP server implementation and runs at 83.3Hz maximum, but can be used to command arbitrary task-space positions to the KUKA in near real-time. Second, is to use direct inputs from external sensors into the KUKA, which requires some custom code to be operating the KUKA to read and react to sensors. This was used by Keating et al. in [47] to create basic position error compensation tests using the KUKA, which effectively maintained a specific height from the ground. It used a SICK DT35 laser to determine ground height. One issue with this method, however, is that the KUKA cannot be commanded from an external source to change behaviors. And thirdly, KUKA provides a the KUKA Robot Language (KRL) interface, which can run custom code on the KUKA directly. By having the KUKA read from digital input lines, it can respond to external commands, but requires substantial additional code to support a wide variety of responses. Details on the implementations of these modes can be found in [47], [48].

In addition to the KUKA's many interfaces, the coupled control of the KUKA and the AT40GW boom arm can be implemented in several different strategies as well. All of the strategies can be summarized by the use of the KUKA to perform dexterous and/or fine motions while the AT40GW boom is used for large-scale, coarse motions.

1. Serial Operation – This mode of operation treats both robots independently. Waypoint goals are specified as either AT40GW motions or KUKA motions, and are executed in sequence. As an example, we implemented this mode by having the KUKA move if motions were under 2 m from the current end point. Otherwise, it was considered an AT40GW motion. This can be implemented during trajectory generation phases and commanded to the KUKA via the UDP server implementation.
2. Macro-Micro Operation – As outlined in [55], [56], in this mode, the micro manipulator, the KUKA, is used for error compensation while all motions are performed by the macro manipulator, the AT40GW. Currently, this has been implemented in small scale demonstrations using SICK DT35 sensors for 1D distance compensation on our system. Larger use-cases require precise external feedback in order to compute an error from the desired end-point configuration with the current configuration of the robot. We can achieve this to some extent using the forward kinematics of the combined AT40GW through KUKA system based on the encoder readings, but this does not take into account beam bending behaviors of the AT40GW's large steel arms.
3. Parallel Operation – Parallel operation, as shown in Figure 14, is a broad class of operations, and can include macro-micro operations. At a more abstract level, trajectories can be assigned to both the macro and micro manipulators separately and are then executed at the same time. This has been termed a "hand-finger" setup and explored by [59], but is still an active area of research. One can imagine generating trajectories that minimize oscillations, or energy expenditures, or maximizes speed.

2.1.7 Design to Print Workflow

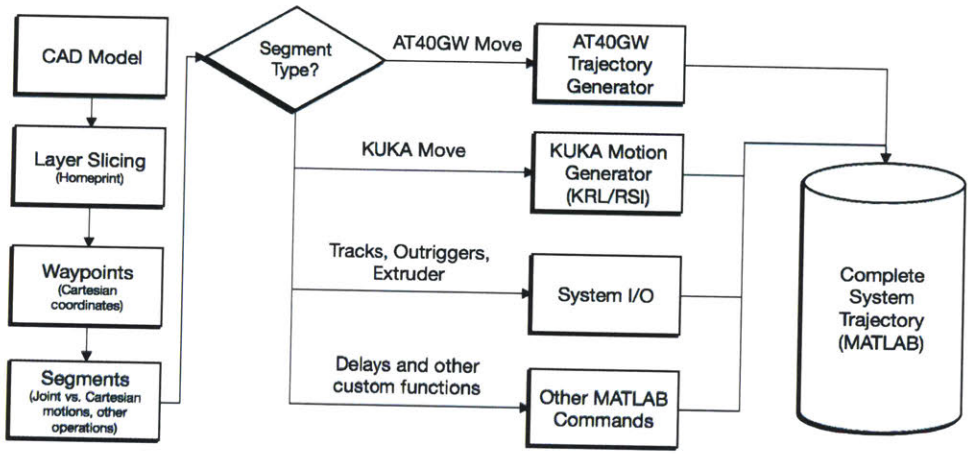

Figure 15: A generalized sample workflow from design to print using the DCP.

Once a control strategy has been implemented, a design to fabrication workflow must then be developed. The most straight-forward implementation of this workflow is to treat the DCP as a traditional, large-scale 3D printer, in the case of PiP fabrication. An abstract representation of this process is outlined in Figure 15. This expects designers to use a typical CAD tool, such as Rhino © or SolidWorks ©, to design a 3D output structure. Once complete, the structure is exported via standard STL format and then sliced into thin layers along the Z-axis. These layers are then converted into trajectories that the DCP can then follow using one of the methods proposed in the dual arm control section. This is the current standard procedure for interfacing with the DCP and is outlined in greater detail in [47].

While simple to implement, this workflow does not provide designers with access to the entire set of capabilities of the DCP. The slicing strategy assumes that the nozzle is always pointed downward, and trajectories are provided in 3D, rather than 6D to include potential changes in nozzle orientation. While simpler, if the nozzle orientation is fixed downward, this likely require support material to be used in the 3D print in the case of large overhangs in the print. Thus, for our large-scale experiments that contained overhangs, we created custom trajectories that would adjust the orientation of the nozzle using the KUKA. Furthermore, this slicing strategy also obscures the fact that extremely large prints may not fit in the stationary work volume of the DCP. This would require

some segmentation of the 3D print, which can either be handled entirely by the human operator, but is preferably handled by an automated slicer.

2.1.8 Results

Several tests were conducted to characterize the system and understand its viability as an overall autonomous, on-site construction system. I will present a selection of the key results here as they relate to the controllability of the system as well as those that highlight its usability for PiP construction specifically. All of these were presented in *Science Robotics* [46].

Characterization and Verification of AT40GW Controls

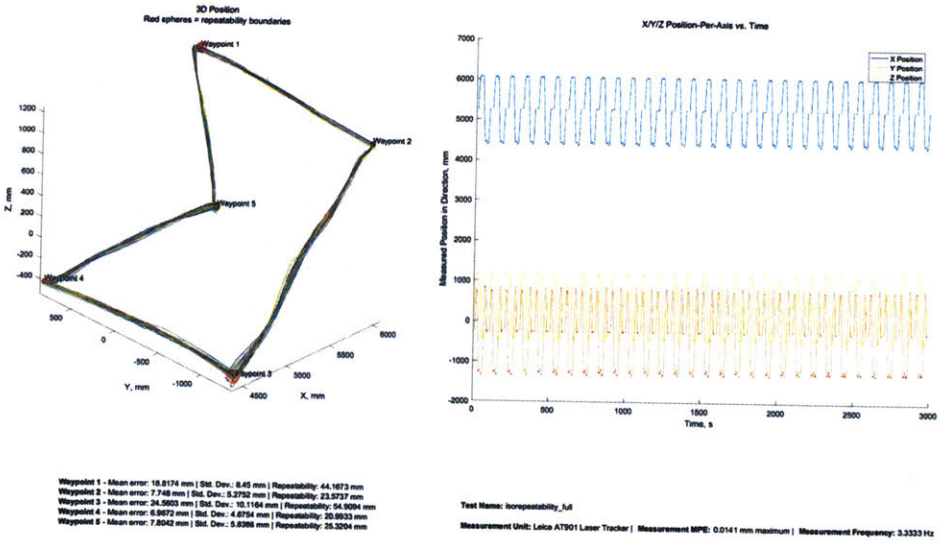

Figure 16: ISO9283 test to characterize pose repeatability of the system. This test requires the arm visit a specific set of waypoints, 30 times each, shown on the left. The edges of the enclosing square are 2 m in length. ISO9283 measures the precision (standard deviation) of the end-point once it arrives at each waypoint, which we found to be under 5mm. Published in [46].

The first set of experiments were performed to understand the capabilities and limitations of the controllers we implemented for the AT40GW boom arm. We first used a Leica Geosystems Absolute Tracker AT901 laser tracker system that operated at 3.3Hz with an error range of 500μm. A ball mirror was attached to the end of the AT40GW, which served as a reference for the laser tracker. The AT40GW was then instructed to follow

Cartesian-space trajectories and stop along 5 waypoints for 30 times in succession. We measured the standard deviation around the resting location of the AT40GW end-point and found that the pose repeatability of the system is about 5mm, the results are shown in Figure 16. This test demonstrates only that the system can reasonably repeat position tracking behaviors, but does not indicate performance on general trajectory following or absolute accuracy.

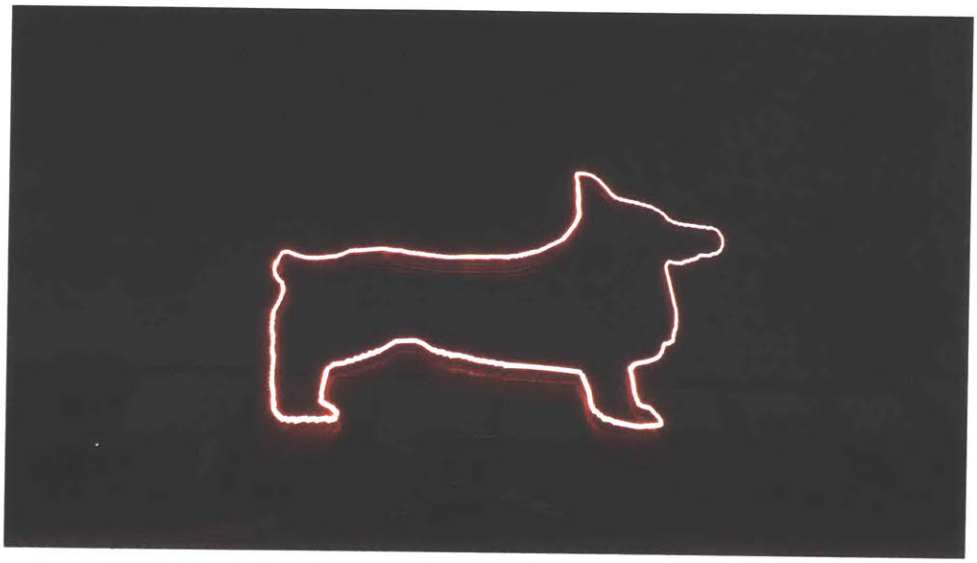

Figure 17: Light painting demonstrating curved trajectory following of the AT40GW arm, 4m in length corgi. Published in [46].

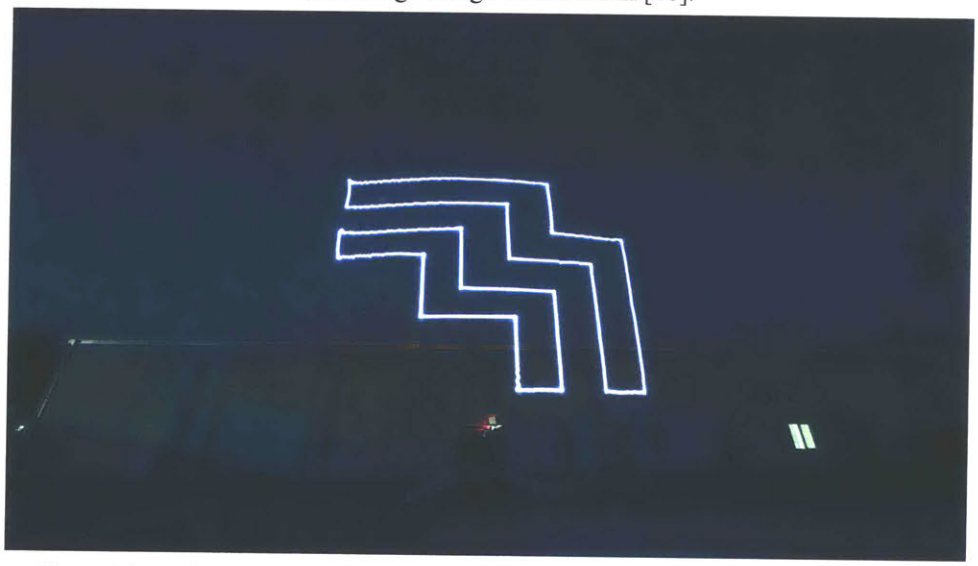

Figure 18: Light painting demonstrating rectilinear trajectory following of the AT40GW arm, 3m Mediated Matter logo. Published in [46].

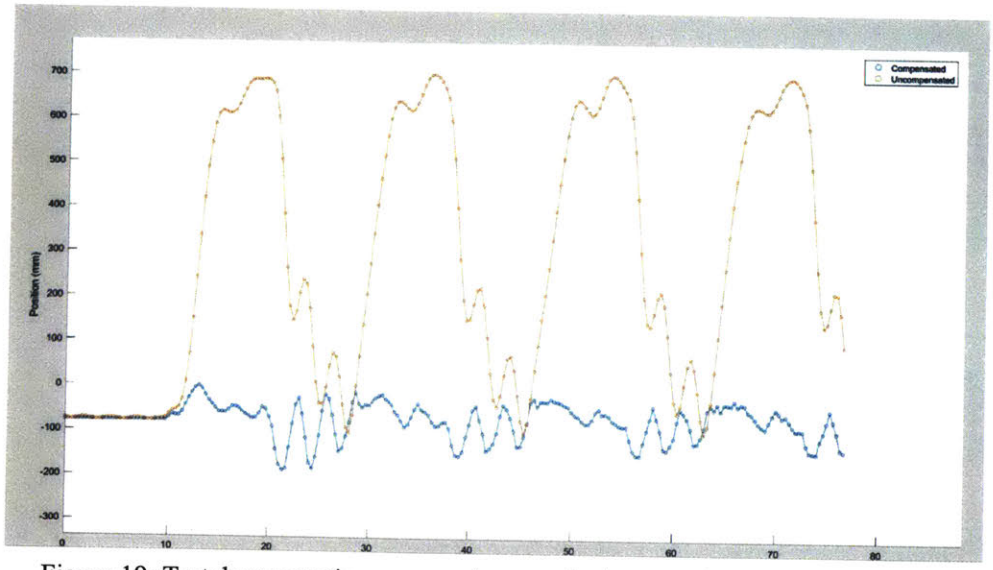

Figure 19: Test demonstrating macro-micro manipulator configuration where the micro manipulator is used for error compensation, the x-axis is time (s) and y-axis is height of the KUKA end-effector in mm. A laser was attached to the KUKA end-effector and directed at the ground and commanded to maintain a fixed distance from the ground. The macro manipulator was then commanded to move up and down. The orange shows errors when not-correct, and the blue shows when the KUKA compensation is active. This performance is correlated with sensor accuracy and response rate of the KUKA.

We also verified that the AT40GW controllers were capable of both curved and rectilinear trajectory following at large-scales using light paintings. The results are shown in Figure 17 and Figure 18, further tests need to be done to determine accuracy and controllability of the velocity and oscillatory behaviors of the boom arm.

Finally, we tested a small-case scenario for a macro-micro manipulator configuration where the KUKA was used for error compensation and shown in Figure 19. A SICK DT35 laser distance sensor was attached to the KUKA end-effector and pointed downwards. The AT40GW arm was then commanded to move up and down. In the first sequence, shown in orange, no error compensation is used and the height of the KUKA end-effector also oscillates. After, the error compensation is activated and shown in blue, which significantly reduces error, however, there are still some oscillations present. Further exploration into improving this accuracy was carried out by Julian Leland in [48].

Large-scale Experiment

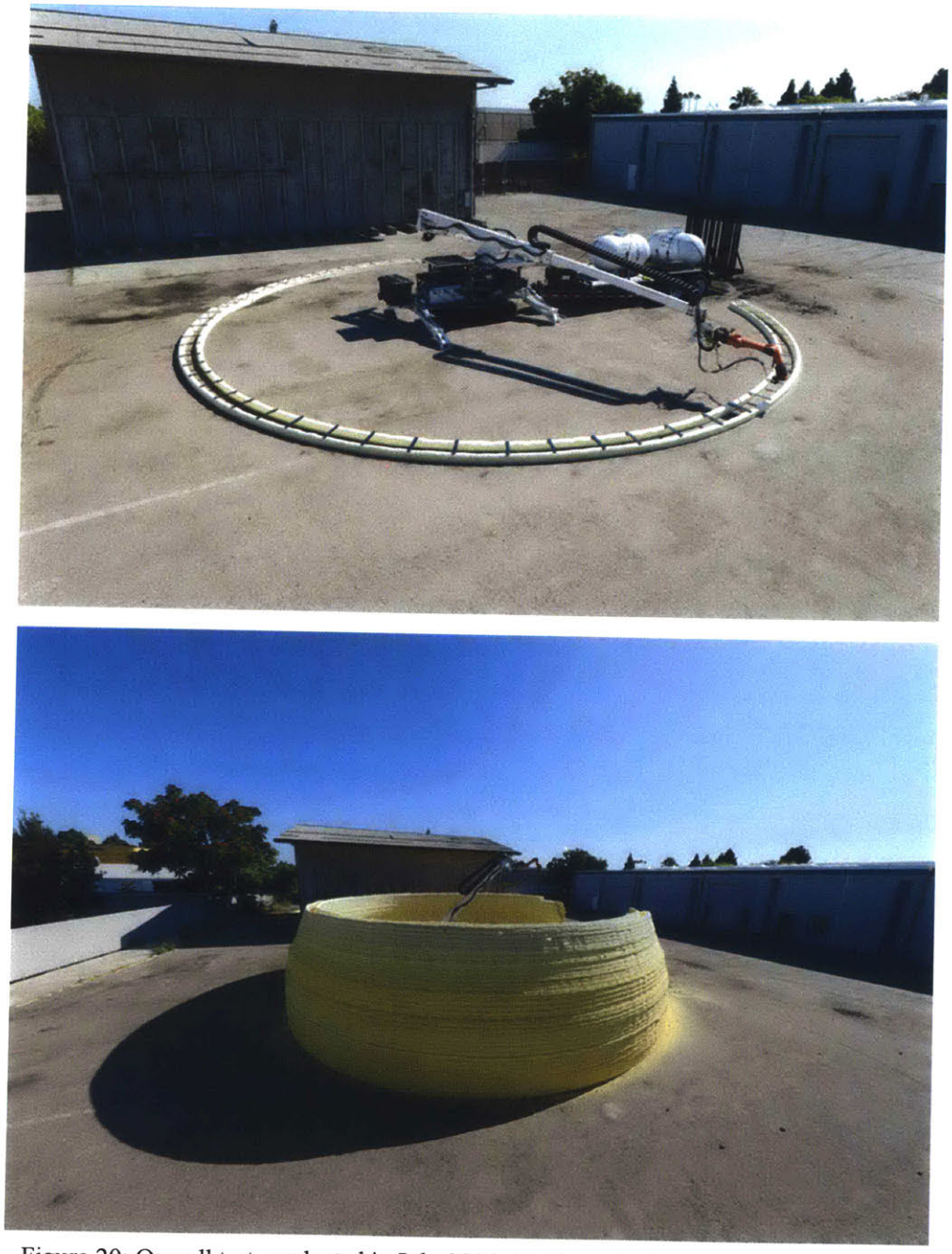

Figure 20: Overall test conducted in July 2016, 13.5 hour total print time, 14.6 m diameter, 3.7 m tall, with 306 layers. Walls had double curvature and used no support material.

The entire development process culminated in a large-scale print test, completely autonomously and on-site, to demonstrate the full capabilities of the system as a PiP construction platform. A half-dome was created with double walls, as a PiP mould, and plastic rebar ties were manually added throughout the process (shown in black in Figure 20). The DCP v.2 was fitted with 2 tanks, each containing 1 component of Dow Froth-Pak 2-part polyurethane spray foam. The system was primarily used in a serial configuration, the large arc motions were conducted by the AT40GW, and the small connecting motions executed by the KUKA. The trajectory for the dome was customized to enable the KUKA to adjust orientation throughout the print so that the nozzle was always tangent to the surface of the dome at each layer. This allowed the avoidance of support material while achieving overhang features. The entire print time was roughly 13.5 hours, and the final dome was 14.6 m in diameter and 3.7 m tall. No concrete was filled to avoid demolition issues.

2.1.9 Discussion & Conclusion

Figure 21: Top shows a vision for the future using collaborative DCP systems for remote environments. Bottom shows recent, not yet published, work exploring external sensing to produce maps of unstructured print environments.

The DCP v.2 highlights the potential to adapt existing construction and robotic systems towards autonomous fabrication platforms. By adding off-the-shelf sensors and building custom control software, the DCP v.2 is already capable of performing basic

autonomous construction tasks, on-site, and in the near-term. Though not discussed in this thesis, we did demonstrate basic capabilities in gathering materials on-site as well such as gravel and straw [46], [47]. Further investigations are necessary to improve the control accuracy and external sensing capabilities, such as LIDAR, of the platform if it is to be used in more remote or complex construction tasks, some of which is has been conducted by Julian Leland [48] and Barrak Darweesh, respectively. Additionally, the demonstrations performed are only conducted within the *stationary* build volume of the DCP v.2. More research should be done towards print segmentation, large-scale controls of flexible manipulators, and using the mobile system autonomously with external sensing, such as performed in [6], [60]. Additionally, research done in the mobile manipulator community, though generally proposed for in highly-controlled environments, could be adapted for use here as well [61]–[63].

Finally, and as a segue into the next sections of this thesis, truly scalable autonomous fabrication, on the order of entire construction sites or cities, can be enabled by using several platforms like the DCP in cooperation. This vision is shown in . However, there is significant research that must be conducted before these visions can become reality. The computational complexity of a single mobile manipulator system is already quite large, though there has been some progress on how to resolve this. This problem is exacerbated when there are several such systems that must coordinate or avoid one another as they operate in the same workspaces.

3 Tomorrow, Multi-robots with Composites

3.1 Background & Approach

Systems resembling the DCP v.2 can provide a reasonable infrastructure for initial forays into autonomous, large-scale fabrication. However, as autonomous fabrication platforms progress, we would like them to be increasingly scalable, fast, efficient, and provide more design flexibility. Cooperative autonomous systems, those consisting of multiple robots working together on a single output structure, have been identified as a potential strategy for achieving faster build speeds by taking advantage of parallelism. An additional benefit of multi-robot systems is that redundancy of robot hardware can help in cases of failures of some of the robots.

At the same time, currently available construction materials are not necessarily the best for all situations. In nature, many organisms utilize a hierarchical material design strategy to create lightweight, high strength structures. For instance, arthropod shells [64], wood, and bone [65] use specially organized fibrous materials at multiple layers to obtain adaptive and robust structural behaviors. These same principals are exploited in composite materials used in the automotive and aerospace industries. Even more recently, composite materials are an emerging class of materials within the digital fabrication and construction industries, and some have been recently approved for use in some construction scenarios [66]. These materials can combine desirable properties of several materials at once to produce high-performance and light-weight structures that may also reduce overall material consumption, and hence waste.

In this chapter I will discuss the emergence of composite materials at the architectural scale and how they can be combined with multi-robot systems to create increasingly scalable autonomous construction systems. I will highlight potential benefits and dig into the challenges that prevent them from being used in current processes. And I will conclude with a case study that implements some of these ideas and shows how they might be possible to achieve.

3.1.1 New Materials: Composites for Construction

Advancements in composites and multi-material 3D printing have opened new doors to high-performance materials, that are available at lower costs and can be used in conjunction with new design techniques. These enable designers to easily create parts

with tunable, anisotropic features that were previously difficult to manufacture. Fiber-reinforced polymers (FRP) or fiber-based composites are a sub-class of these materials and are widely used in aerospace and automobile industries. Only recently have they been identified as a class of materials that can help unlock new form factors and structural performance in digital fabrication and architecture [66]. Several architectural projects have looked to composites as a surprisingly affordable method to create new facades, such as for SFMOMA [26], or structural components such as tubular bridges [67].

One major issue with composites is the requirement that a mould, or mandrel, is used to shape and cure it, such as through heat or light. Once a mandrel is in place, fibrous materials are combined with a bonding agent or matrix, such as plastic, and wound around the mandrel before being cured.

Groups such as Markforged, Impossible Objects, and the Lewis Lab [68]–[70], have looked into different uses of fiber composites without the need of a mould, such as mixing in pieces of fiber rather than a continuous strand. This strategy has been shown to reinforce and improve existing non-composite parts, but is difficult to scale, and does not provide the full benefit on continuous strands of fiber that cross the entire object.

In response, other groups such as NASA and Menges et al. [4], [13], [18] use robot arms to achieve unique winding patterns while using long, continuous strands of fiber at a large scale. However, these demonstrations are still limited in the potential scales they can achieve.

3.1.2 New Platforms: Multi-robot Systems

In addition to new material system, as discussed earlier, multi-robot systems are being pursued to increase construction speeds. Inspired by natural systems, such as eusocial organisms, the primary argument is that teams of robots can build in parallel and provide redundancy in case of failures. In cooperative circumstances, they may even be able to help with various aspects of construction as in the Minibuilders project [12]. Most of these systems are mobile [9], [11], [14], [16], [18], [19], some have focused on algorithmic contributions, and other material systems. However, few of these have been able to build at architectural scales, as development can be complex. Both Menges et al. [18] and Augiliaro et al. [9] achieved architectural scales, and in the case of Menges et al. [13], [14], several projects have used the combination of a multi-robot system with fiber-based composites, however, each of these systems required substantial

infrastructure. Our system hopes to avoid the large costs incurred by assembly and infrastructural needs by most mobile, multi-robot fabrication systems.

Some key challenges in enabling parallel prints are part segmentation – how is the structure divvied to robots, a shared workspace while avoiding collisions, and communication—what forms of coordination are possible.

3.1.3 New Design Techniques: Fabrication-aware & Multi-objective Optimization

Finally, the designers who use multi-robot platforms must be considered. In modern fabrication, introducing new platform capabilities also tends to come with additional challenges for the designer. For instance, while 3-axis CNC machines are commonly found and used in machine shops, 4- and 5- axis machine usually require special training and CAM software in order to utilize them. This can create a burden on the designer. This problem is exacerbated in the case of multi-robot systems, where the degree of freedom exponentially increase with each additional robot, and the interactions of each robot with each previous robot. Creating toolpaths for such systems, or verifying that a structure can be produced, would be intractable with traditional CAD-style approaches.

Some groups have begun to investigate the use of fabrication-aware design approaches, where geometric constraints of fabrication tools is checked for during the CAD process [71]–[74]. In parametric design contexts, where part relations are specified, automatic optimization is possible, and has been conducted using standard optimization techniques, including neural networks and evolutionary algorithms [75]–[77]. Nooks et al. [78] has looked specifically into structural design through simulating multiple agents, but are fabricated through more traditional means after the fact. The most compelling has been the TERMES project [16], where the robotic fabrication platform was co-designed with an algorithm that guarantees fabricability of the structure by the robots. However, this approach was limited to assembly of system-specific bricks that cannot be used in general construction.

3.2 Case Study: The Fiberbots

Figure 22: (Top-left) shows a single Fiberbot, (top-right) shows a single Fiberbot as it is winding a fiberglass tube, and (bottom) the entire Fiberbot system, using 16 robots, as it creates a large, "woven" architecture in parallel.

The work done in this section was a collaboration with Dr. Markus Kayser, Sara Falcone, Nassia Inglessis, Christoph Bader, and Dr. Neri Oxman, with the assistance of undergraduates Robert Garriga, Jami Rose, and Melinda Szabo. The software, controls, and electronics were designed by myself with assistance from Melinda Szabo.

3.2.1 Overview

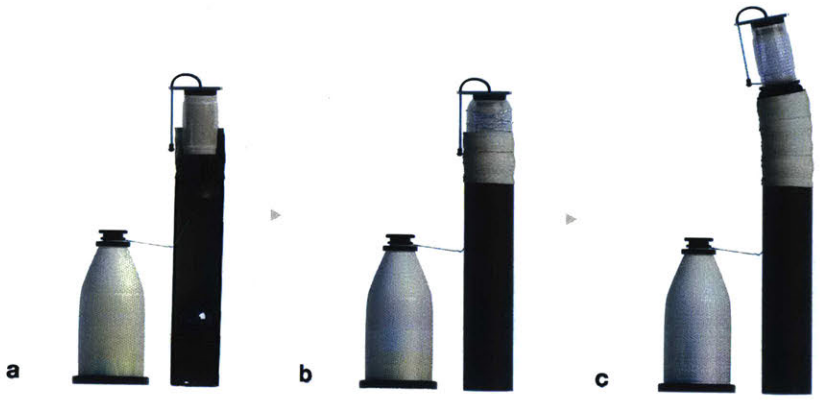

Figure 23: Demonstrates the operation of a single Fiberbot creating a single segment of its own tube. (a) shows a cross-sectional view of a Fiberbot in its initial, deflated, configuration and how material is fed to the robot. (b) shows the Fiberbot once it has inflated its mandrel and begun winding a new segment of tube. (c) shows the robot deflated once again, drives up along the just-completed segment, and tilts itself to create local curvature in the next segment of tube. PC: Barrak Darweesh

The *Fiberbot* system is developed to explore the combined use of fiber-reinforced polymer materials in an architectural setting along with an autonomous and fully-parallel construction method. Ideally, the system would allow structures to be created in remote environments without the need for human intervention, such as placing or removing scaffolding. This construction method relies on a team of identical robots that can climb on their own structures as they build and is co-designed with a custom design language, in place of traditional CAD software. The ability to climb provides the robots with an effective build volume much larger than themselves. The robots operate by each creating a large, tubular structure out of fiberglass composites. The tubes are built in parallel and can curve around one another to create larger "woven" architectures.

As an example application, a team of robots would be placed on one side of a river in a remote area. Users would specify that the robots should attempt to build a densely woven pattern across the river, and that the final structure should remain fairly flat, like a bridge. The robots would then proceed by "growing" fiberglass tubes, weaving around one another as they proceeded.

Users first specify high-level design parameters, such as regions in the construction area to avoid, areas of attraction, or volumes where additional strength (gained by increased tube density and interweaving) are needed. The user then applies these specifications to our custom structure generator. This generator simulates robots as agents, similar to the boids model used in flocking, where agents are attracted to, repulsed from, or directed alongside one another or obstacles in the environment [79]. We extend this model by adding behaviors such as desired curling, to encourage agents to curl around other tubes and increase density. These virtual agents are initialized on the ground plane, and begin to navigate the world according to these parameters, and as they move, they effectively leave behind a trail of tubes. This trail serves as the trajectories for the Fiberbots, and are then processed into commands that can be executed by the real physical robots.

Each physical robot builds a self-supporting composite tube segment-by-segment. Its body is cylindrical and operates by fixing itself to a base structure and winds fiberglass filament saturated with a UV-curing resin around itself and cures the resin as it winds. Once a segment is complete, the robot will detach itself from the just-built segment, drive further along it, fix itself again, and repeat the procedure. To produce curvature in the tube as it creates it, the robot can tilt its body, right before it fixes itself in place, to create a local "kink". By creating many kinks over many segments, a gradual, controlled curve can be achieved. This process is shown in Figure 23. Because the tubes are self-supporting, overhang features are possible, though future iterations may allow for non-self-supporting tubes.

To our knowledge, we have designed and developed one of the first demonstrations of parallel construction by multiple crawling robots operating in the same workspace that succeeded in building at architectural scales. The hardware system required novel developments in creating a flexible composite fabrication system that allowed for tunable fiber winding behaviors and a re-usable mould system. We also introduce a unique swarm-based design process, in place of traditional CAD, that was co-designed with the hardware and helps simplify the job of designers and allows them to focus on

high-level specifications of the structure. The model is then compiled into specific trajectories that the Fiberbots follow at construction time. They reproduce the designs as closely as possible, using dead-reckoning (integrating internal sensors, an IMU and encoders) for localization. Collision avoidance is handled at design-time, so no external sensors are currently on-board the robots, though we hope to include them in future versions to create more ad-hoc structures and behaviors.

This section will begin by introducing the Fiberbot hardware platform, which includes the composite winding and mobile driving systems, in 3.2.2. The design process for the output structure will be covered in 3.2.3, the software architecture and automating principals will be discussed in 3.2.4, and finally experimental results and conclusions will be presented.

3.2.2 Hardware Platform

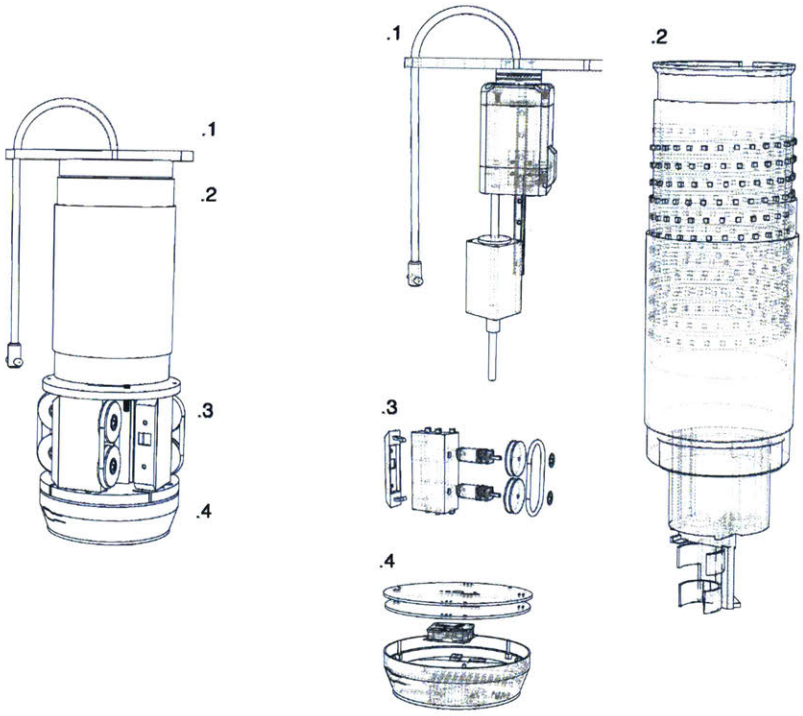

Figure 24: On the left, one Fiberbot is shown. On the right are the sub-assemblies, (1) is the winding arm, (2) is the mandrel with UV LEDs, (3) is 1 of 4 track cartridges that make up the drive system, and (4) is the electronics housing.

The purpose of a single robot is to build a self-supporting fiber composite tube with controlled curvature and large specified lengths. The majority of the hardware for the Fiberbots was designed by Dr. Markus Kayser and Sara Falcone, with modifications from the author in order to improve controllability, and the electronics and software by the author with assistance from Melinda Szabo. The history and overall iterations of the project can be found in Dr. Kayer's doctoral thesis. The development was separated into two major subsystems: (1) the fiber composite handling subsystem and (2) the mobile subsystem. Here I will describe the final subsystems in detail, and how they enable the creation of self-supporting composite tubes with controlled curvature and arbitrary

length. Note that these apply to a single robot at a time, and how they are used in parallel will be covered in a later section.

Fiber-composite Handling System

The fiber composite handling subsystem is responsible for creating a single segment of fiberglass tube at a time, up to 93 mm in length and between 96.52 mm to 114.3 mm in diameter. The segment must be anchored to the previous segment to be structurally stable, and the fiber patterning, thickness, and resin saturation can be tunable throughout the segment.

Traditional tubular fiber-glass winding systems are used to create large composite tubes of fixed size and shape. These systems consist of spools of dry fiberglass material, a bath that wets or saturates the fibers with resin, and a cylindrical mandrel that acts as a mould for saturated and uncured fibers. A nozzle is responsible for effectively squeezing or scraping excess resin from the fibers and then depositing it onto the mandrel, known as pultrusion. Throughout the operation, the nozzle generally travels up and down along the transverse axis of the cylindrical mandrel while the mandrel rotates, the combination creates a winding motion. By changing the relative speeds of the rotation and linear motions, different fiber alignments, or patterns, can be set. The design of the nozzle and resin bath can be used to adjust fiber saturation, or the fiber-to-resin ration. Fibers that are aligned along the transverse axis provide maximum tensile strength and increase stiffness. Those that are more radially aligned help maintain the overall shape of the tubes. Thus the fiber alignment and fiber saturation parameters can tune the overall structural properties of the final tube [80].

As traditional systems primarily focus on tubes of fixed size and shape, with one exception in [81], the desire to control curvature and build near-arbitrary length tubes required us to design a novel filament winding process for the Fiberbot system. We created a custom re-usable mandrel, filament saturation and curing process, and winding technique, which will be described in detail.

The Mandrel

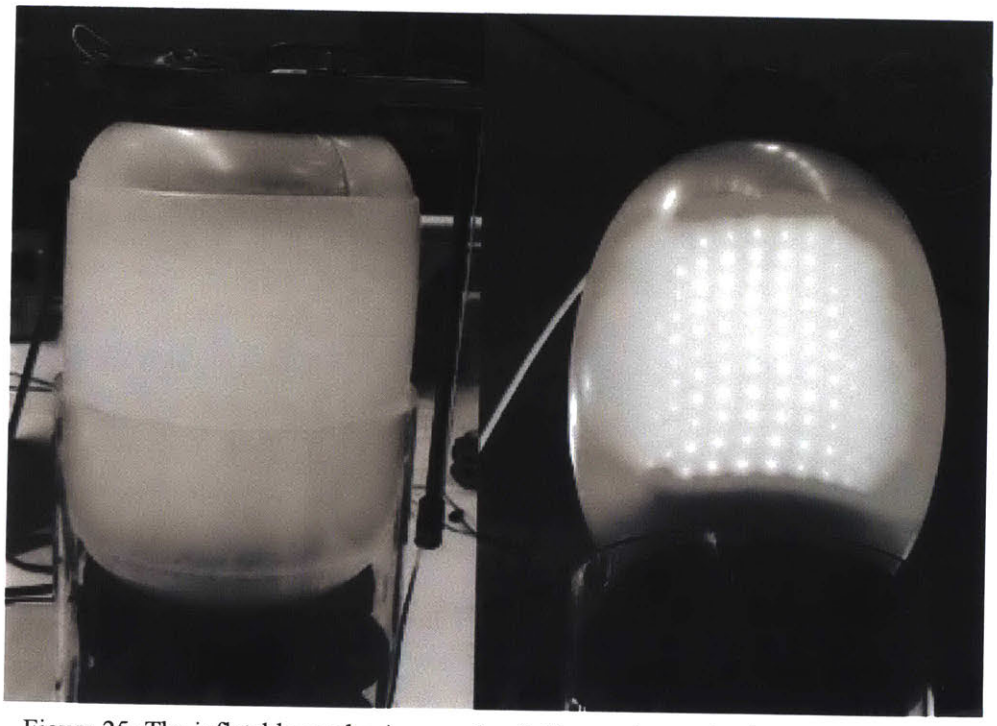

Figure 25: The inflatable mechanism, made of silicone sheets, for the re-usable/collapsible mandrel is shown here. On the left is completed mandrel using 2 layers of silicone in order to create cylindrical tubes. On the right, if only 1 layer is used, it bulges, and would cause more rippled effects in the overall tube.

The mandrel, as in other filament winding systems, acts as a mould for wetted fibers to cure on. However, unlike most other systems, our mandrel is flexible and re-usable to assist in the production of tubes of varying diameter, curvature, and lengths. To achieve this, the mandrel is made from a layer of silicone sheet and is coupled with pneumatics to make it inflatable. When inflated, it serves a dual purpose, as both a mould for the fibers, but also anchors the robot to the already-built tube. This anchoring provides an overlapping region between the in-progress region of the tube with the already-built tube. The in-progress region then is cured over the existing tube to create a solid bond, and thus extends the tube outwards by a small amount. The mandrel can delaminate and separate itself from the structure by deflating. This allows it to be re-used immediately, and frees the robot to be able to drive up the tube and continue with the build process. By inflating slightly more or less, the mandrel can provide, to a limited degree, varying radii. The cylindrical part of the mandrel is 100 mm in length, and 80 mm in diameter when deflated. When inflated, we can create tubes with inner diameter between 96.5 mm

to 114 mm. The maximum thickness of the tube is determined by the distance from the inner diameter of the tube to the inner edge of the nozzle, which is 35 mm away from the deflated mandrel. This maximum thickness will also change depending on the curvature of the tube, as highlighted in Figure 27.

During typical operation outdoors, the resin can be cured using UV from the sun. However, in cases where there is not sufficient solar exposure, UV-LEDs within the robot are used. The silicone sheet is clear and UV-LEDs are placed inside of the mandrel itself. This design allows the robot to be fairly compact and keeps everything on the interior of the tube. Previous versions of the robot placed the LEDs on the winding arm itself, but this added complexity and mass to the winding arm, which is undesirable and will be discussed in a later section.

The Material Feed

Each tube is created from a single strand of fiberglass thread and a tank of UV-curing resin, which can be seen in Figure 23. The material is kept at the ground level and fed up, through the center of the tube, into the robot. The robot then feeds the material through its own center and winds it on its exterior before depositing onto the mandrel. The fiber is kept separate from the resin until it reaches the nozzle located at the end of the winding arm.

The resin is UV-curing, which means it must be isolated from any UV exposure until it has reached the mandrel. A peristaltic pump, located at the ground next to the resin tank, pushes resin from the ground up to the robot through a small conduit of fixed length. The pump is a stepper motor and is controlled by the robot via step commands that are sent to the ground across a tethered wire. The length of the conduit determines the maximum length that is possible to produce for the overall tube, unless another mechanism is introduced to splice additional lengths of conduit mid-build. The rate of resin flow is controlled by varying the speed of this resin pump. We kept the pump on the ground, rather than inside the body of the robot, primarily due to its size and weight. Because the pump is located at the base, there is a delay between when a flow command is changed and when it affects the rate of flow at the nozzle of the robot. This means that a command to stop the flow of resin must be sent several seconds, up to a minute, before the flow of resin is required to stop. The delay incurred depends on the length and diameter of the conduit, and so must be adjusted each time a new tube that requires a longer conduit is required.

The fiberglass thread is kept on a spool on the ground. The thread is passed through a hole in the tube, which is smoothed to ensure minimal friction and prevent cutting of the thread as it travels up the tube. The thread is pulled by the winding robot arm during the fiber winding process, known as pultrusion. To minimize friction, and hence tension, on the winding arm, the fiber is kept dry until it has reached the exterior of the winding arm, and so is fed up the tube separately from the resin.

The Winding Arm

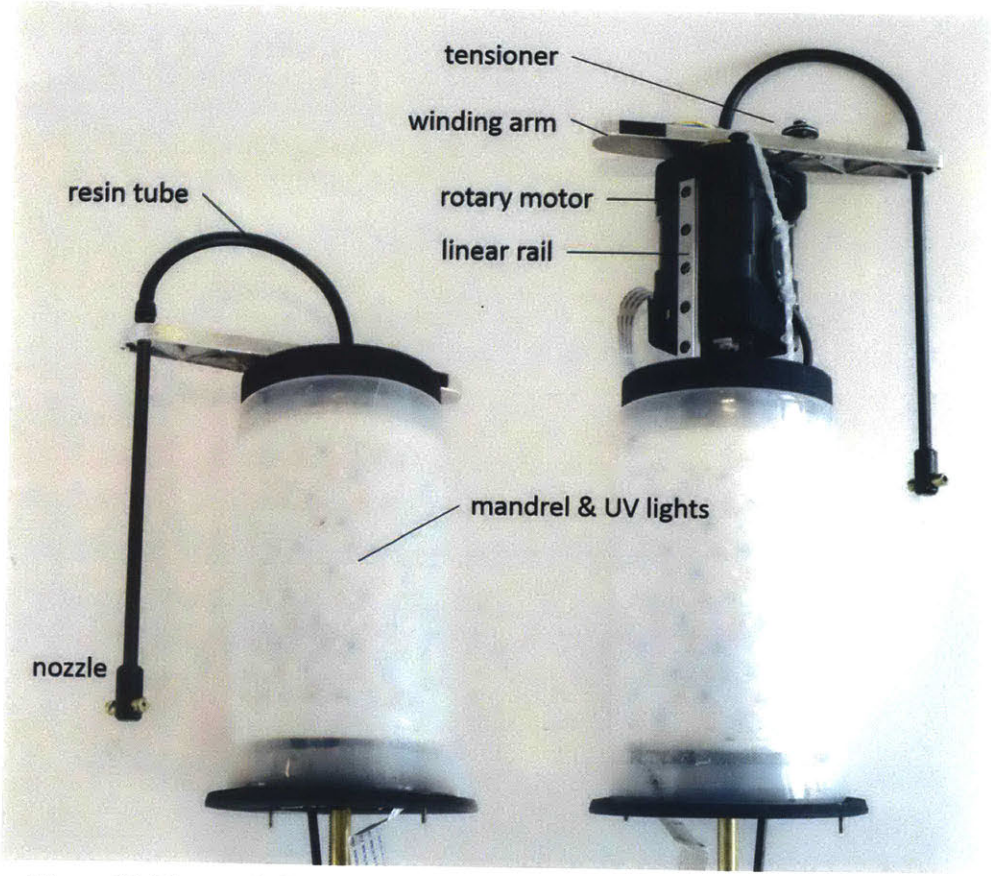

Figure 26: The mandrel and winding arm sub-assembly (mobile carriage is removed) are shown here. On the left, the winding arm is fully retracted, on the right, it is fully extended, and shows the range of linear motion. The black component on the right is the rotary motor with a rotary fluid union and electrical slip ring attached to it.

The winding arm is responsible for saturating the fiberglass thread with resin and controls the fiber alignment as it deposits it onto the mandrel. In many alternative

filament winding systems, the mandrel rotates and the nozzle travels linearly along the transverse axis of the cylinder. In the Fiberbot system, however, the mandrel is completely stationary during the fiber winding process. This is because the mandrel must also act as an anchor to the preceding segment. Thus the winding arm moves the nozzle both rotationally and linearly around the mandrel. It consists of one rotational stepper motor that is mounted along a rail to another linear stepper motor. These motors provide precise control over both position and velocity of the winding motion. The travel distance of the linear motor is 93 mm, and the radius of the wind arm is 78 mm from the axis of rotation to the center of the nozzle. The maximum speeds achievable are about 70 mm/s linear and 110 rpm rotary, though this changes depending on the tension applied. These could be controlled precisely, at least 0.025 mm per step for the linear actuator (before microstepping) and at least 1.8° per step for the rotational (before micro-stepping). We generally operated with a microstep of 16, giving 0.00156 mm linear resolution and 0.1125° rotational resolution.

To keep the design of the system simple, the arm itself is a static piece of aluminum and does not have any additional actuation. In the future, however, it may be useful to allow the arm to retract into the body of the robot, or extend outward, in order to help resolve potential collisions with other tubes and robots. Because it is static, and the fact that the arm protrudes out from the tube, it becomes the limiting factor in determining a collision radius around the robot. The collision radius also determines the minimum radius, or gap, that two or more tubes can be next to each other. In order to shrink the gap, the arm would have to be made shorter. On the other hand, if the length of the arm is too short, the robot would not be able to wind a tube with any additional curvature, as shown in Figure 27.

Once the tube is sufficiently long, the robot inside effectively acts as a large weight at the end of a cantilevered rod. The winding motion of the arm exacerbates this effect, and if dramatic enough, could apply large, undesirable forces on the tube and cause severe oscillations. To counteract this, the arm is kept as light as possible and is also counter balanced Figure 26.

Mobility

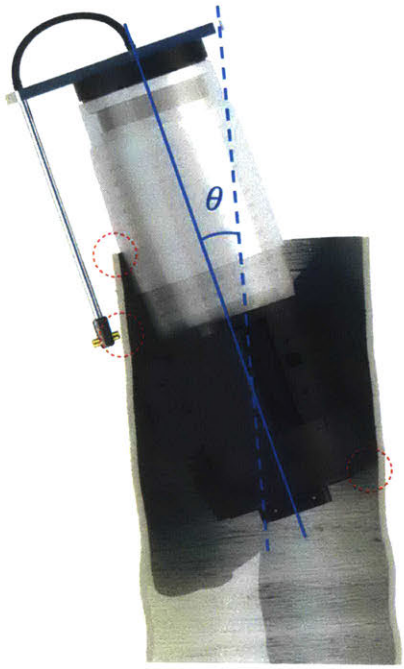

Figure 27: This shows how local curvature is achieved, and what the limitations are. The Fiberbot tilts (solid blue line) relative to the preceding segment (dotted blue line) by a controlled angle θ. This is achieved by spinning the tracks in opposite directions. Θ_{max} is limited to 2.5° because of the robot colliding with its own tube, determined by 3 locations, as shown by the dotted red circles. PC: Barrak Darweesh

While the fiber handling system creates single segments of tube at a time, the mobile system is what allows the Fiberbots to build full tubes of near-arbitrary length with controlled curvature. The mobile system allows the robots to crawl forward and backward along the length of the tube so that they can extend it to near-arbitrary lengths. It also allows the robots to tilt, which creates curvature, as shown in Figure 27. The mobile system is fully contained within the tube that it creates to decrease the collision radius around the robot.

The mobile system is track-based to increase traction along the tube. There are four tracks, organized so that pairs of them are situated opposing one another in a cross configuration. Two are easily visible and seen contacting the tube in Figure 27. To tilt, each pair of tracks is turned in opposite directions, giving 2-DOF, roll and pitch. To crawl along the tube, all four tracks are turned in the same direction. A 6 degree of

freedom IMU is fixed in the mobile base, and high-resolution magnetic encoders are attached to the wheels on each track. These sensors give feedback so that tilt angles and distance travelled along the tube can be precisely controlled. This is also how the current Fiberbots localize, using an odometry or dead-reckoning approach.

Each track is housed in a cartridge that consists of two DC motors and is mounted to the robot using a rail and two springs, which form a simple suspension mechanism. The suspension is necessary to allow the robot to easily traverse the tube regardless of curvature or changes in diameter. It also keeps the robot fixed to the tube no matter the orientation, even if the tube is pointed directly at the ground.

Electronics

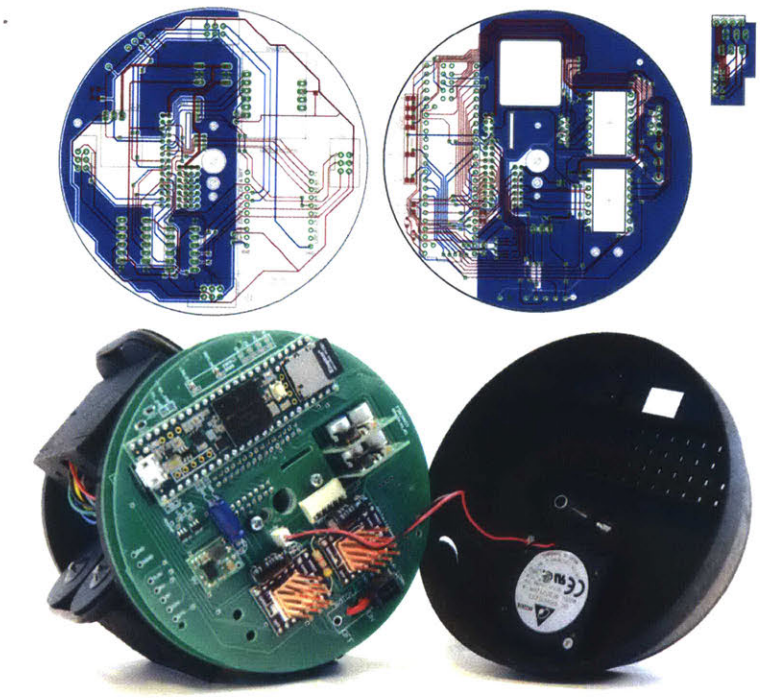

Figure 28: All logic-oriented electronics are housed at the bottom of the mobile carriage (pictured here) to provide easy access. Ground planes were carefully designed (above) in order to isolate noise affects on logic lines from the DC motors. Previous versions of the Fiberbot packaged the electronics inside the mandrel, but made it difficult to debug. The lid (on the right) is designed to increase airflow of the fan, which is used to cool the stepper drivers.

Each Fiberbot is equipped with a Teensy 3.6, which contains a 180MHz ARM Cortex-M4 processor, that handles all on-board processing and control. The electronics went

through several iterations, and were originally packed into the main body of the robot. The current version placed them at the bottom of the robot along with the mobile carriage so that they are easier to access and cool. There are 2 primary boards that are stacked and route logic between the Teensy and controller breakout boards.

4 wires are sent between the ground base station and the robot, one is a 24V power supply, a GND, and 2 signals to control the speed and direction for the resin pump stepper motor at the base. To increase performance, the stepper motors are all run at 24V, and all other components use switching regulators to step down the voltage for their own operation. Because this 4-wire tether, coupled with the conduit for resin, are what determine the final tube's maximum length, they were simultaneously made and cut, and were made as long as possible. This length, usually over 10 m, meant that resistance went up across a thin wire, so large gauge wire (14 AWG minimum) were used to minimize resistance and ensure that no ground plane separation effects occurred.

An ESP8266 chip, using the Adafruit HUZZAH breakout board, was used for wireless 802.11 communication between each Fiberbot and the central computer. A BNO055 9-DOF IMU, which reads at a maximum of 100Hz, was used to provide angular feedback over I2C to the Teensy. However, only 6-DOF, a gyro and accelerometer, were used due to the severe drift incurred by the magnetometer readings since tests were located near other buildings. To provide the necessary roll, pitch, yaw readings, from the 6-DOF input, the BNO055 uses an on-board ARM Cortex-M0 that computes a sensor-fused reading using proprietary algorithm. To track distance travelled, Pololu magnetic encoders were attached to micro metal gear motors, with 12 count-per-revolution magnets, and were monitored with interrupt handlers and a 4X counting scheme to provide bidirectional and high-resolution readings.

For actuation, the Teensy sent digital direction and step commands, with 16^{th} microstepping, to each of the 3 stepper motors (rotary, linear, and resin pump) running at roughly 400kHz. The DC motors were controlled using PWM signals across Pololu DC motor controllers and the UV LEDs, solenoids, and airpump used for the mandrel were all controlled via MOSFETs.

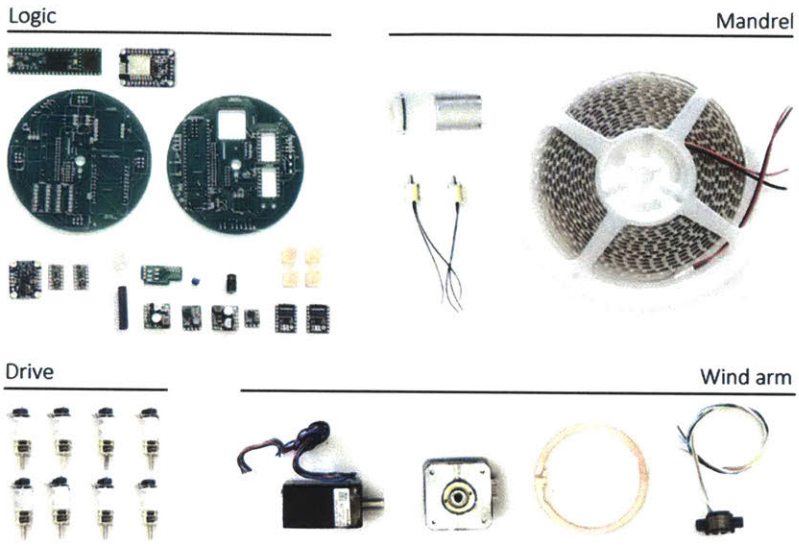

Figure 29: The electronics used for each sub-system. The mandrel consists of an air pump, 2 solenoids to direct air in and out of the membrane, and UV lights. The drive consists of 8 high-torque DC motors with magnetic encoders, 2 motors per track. The wind arm has 1 linear stepper, 1 rotary stepper, and a slip ring to enable future sensors to be attached on the outside of the winding arm.

3.2.3 Hierarchical Design (Pre-print)

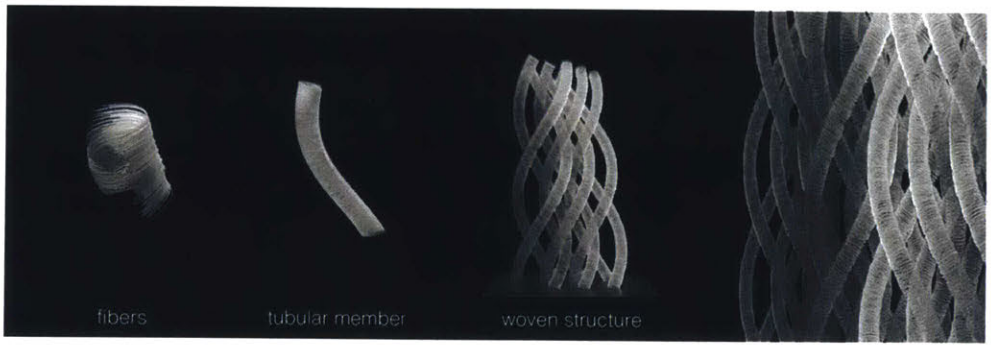

Figure 30: Illustrates the hierarchical levels of the design strategy. At a local-level, the fiber patterning and thickness controls local strength of a single segment. This can be graded along the length of a single tubular member by varying patterns across segments. Finally, each tube can be thought of as a thread in a larger "woven" architecture, which is designed with high-level descriptors. PC: Christoph Bader

While the goal of the Fiberbot system is to be able to create buildings ad-hoc and respond to environmental cues and obstacles, the current system instead relies on pre-designed structures. These structures follow a hierarchical design strategy outlined from local to global, from left to right, in Figure 30. At a local level, within a single segment, we are able to control fiber alignment, fiber-to-resin ratios, and segment thickness. Along a single tube, curvature and radii can be tuned, and segment properties can be changed along the tube. Finally, at the highest-level, the tubes can curl around one another, creating a "woven" architecture. Parameters such as density, amount of curling, number of robots, etc. can be used to modify and control designs.

These design strategies get increasingly complex with each additional robot in the system. It is difficult to imagine a designer using traditional CAD software to model each individual tube, each curve, and each segment. We thus sought to relieve this burden by co-designing a CAD-like system that allows a human user to specify only high-level design parameters and the system will automatically ensure fabricability of the final structure, without additional human effort.

Local Fiber Wind Patterning

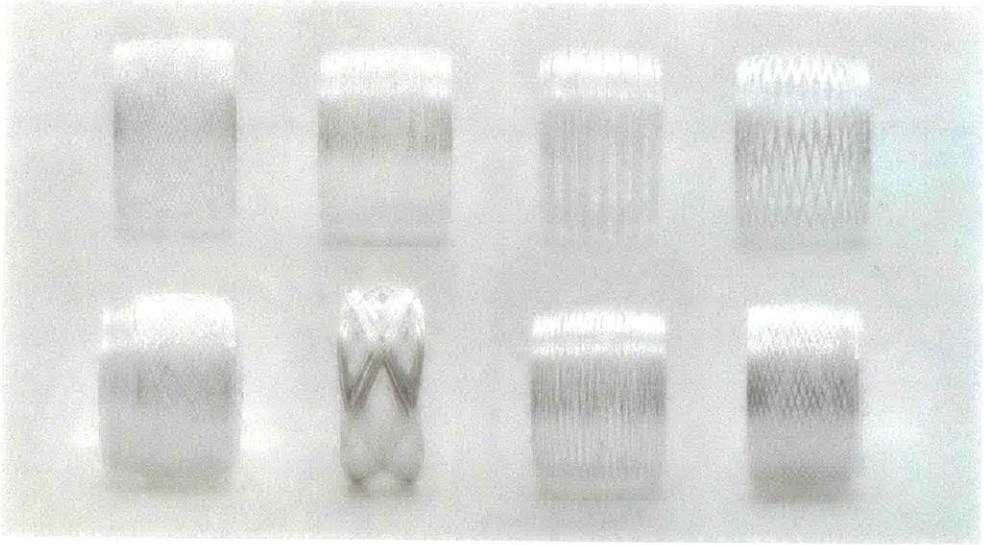

Figure 31: Wind patterns can be specified and controlled for single segments at a time by varying the ratio between the linear and rotational speeds. Here are some samples with varying patterns produced. PC: Nassia Inglessis.

A crucial aspect for all composite tubes is the winding pattern, which determines the strength of the tube [80], [82]–[84]. It was thus important that our system provide high-

resolution control over the wind pattern along each segment. Certain wind patterns can even provide controlled flexibility, but this strategy was not exploited in our current system. Wind patterns are typically defined by the wind angle, the angle of a single strand relative to the transverse axis of the mandrel, and how much the tube is covered. The wind angle can be controlled by:

$$\tan\theta = \frac{dl}{dr}$$

Where dl and dr are the linear speed and rotational speed (mm/s) respectively. Because the ratio is the determining factor we can run the wind at maximum speed and get the same desired pattern. To find the correct speeds, we can choose a desired θ, find the ratio by setting $dr = 1$ and then scaling dr by the ratio amount:

$$dl_a = \tan\theta$$
$$dr = \frac{dl_{max}}{dl_a}$$

Note that patterning is also dependent on the height of the pattern (which sets the period). Most composite filament winding systems use a similar equation to the following in order to determine how many times the linear actuation must travel the full length before the entire mandrel is fully covered once [80], [82]–[84]:

$$n = \frac{2\pi r \cos\theta}{w}$$

Where θ is the pattern angle, r is the mandrel radius, and w is the width of the fiber strand.

Nassia Inglessis empirically found desirable patterns by building a separate, stand-alone platform for wind tests. This was effectively just the fiber composite handling portion of the Fiberbot with the mobile carriage removed. It used the same electronics and basic mandrel, though some portions were reconfigured to make it easier to remove the wound tubular segment. This setup could only wind one segment at a time and was stationary.

Figure 32: Standalone test bench for finding local wind patterns. PC: Nassia Inglessis.

Structure and Fabrication Constraints

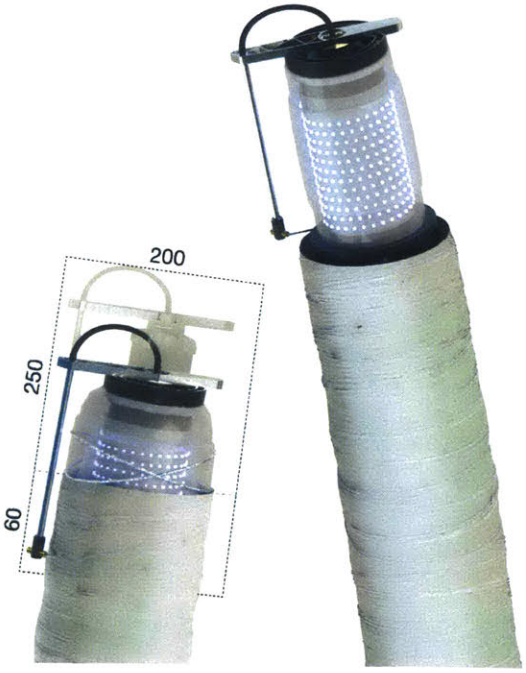

Figure 33: The current Fiberbots are unable to create tubes that touch. This gap is determined by the protrusion of the wind arm as the robot winds, which creates a cylindrical collision avoidance volume, with a diameter of 200 mm and 250 mm above the opening of the tube as the robot winds. This fabrication constraint is included in the design of the structure.

Several constraints were used to inform the design and fabricability of a structure. These can be summarized by collision avoidance of a robot with its own tube and collision avoidance of a robot with other tubes. The former issue is illustrated in Figure 27, and the latter in Figure 33. The former restricts local angle changes to 2.5°, which limits the minimum turn radius that a tube can have. The latter restricts how small the gap can be between tubes, the closer the more ideal, but the higher risk of collision. Because localization is odometry-based, and not highly accurate, additional buffer was provided, for a total cylindrical collision volume that extended 250 mm passed the top of the current tube and 200 mm diameter around the robot. By incorporating these constraints into the design process, we can ensure fabricability of the structure.

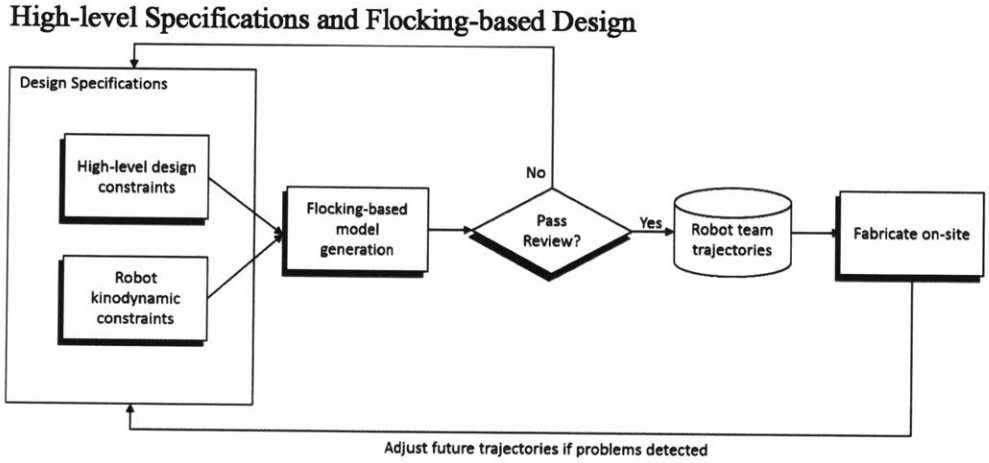

Figure 34: Workflow of the entire Fiberbot system, from specifying high-level constraints for the design, compiling to robot-specific instructions, and then building.

A high-level design language was created to allow designers to model output structures without increasing their burden when using additional robots. This design system was created primarily by Christoph Bader with some input from the author. The details will be published in a later paper, but a high-level description will be provided here for completeness. This design system is based on Reynold's flocking behaviors [79]. Here, each robot is simulated as a point, initialized as they would be in the physical world, at fixed points on the ground. Each robot has a set of attributes, the list is available in Table 3, that govern its behavior. At each time step in the simulation, the robot iteratively computes a new direction, which is fully defined by a linear, weighted combination of the attributes, such as bias towards curling around other tubes, attraction

to other robots, repulsion from robots, etc. This angle between this new position and the previous position is restricted by the constraint in Figure 27. To guarantee fabricability, at every step, a collision cone is extended from the robot to neighboring tubes, using the constraints specified in Figure 33. Once a new direction has been computed, the robot traverses in that direction by a fixed distance. To ensure overlap between segments, this distance must be less than the maximum length of a segment, which is 93 mm. When the robots have reached a specified height, the simulation is stopped. If the design is satisfactory, then trajectories for each robot are saved and converted into local commands specifying the angle (roll and pitch) in global coordinates, and a relative distance to travel between each point.

It is important to note that this design process does not have guarantees that the robots will not. Drifting during localization error is also only handled by a static buffer, and may become extreme in large tubes without additional localization correction of some form.

Table 3: List of parameters available to designers to specify high-level behaviors

Algorithmic parameters	Effect on robot paths	Effect on overall structure
Number of robots	Interactions with neighboring robots via other parameters	Determines size, build speed, and potential density
Starting position	Initial density	Controls density at bottom of structure
Adhesion	Instructs robots to approach each other	Increases potential weaving and density
Alignment	Steers robots in similar direction	Decreases weaving
Separation	Steers robots away from each other	Decreases density and weaving
Curling bias	Instructs robots to curl around other tubes	Controls amount/tightness of weaving in a region of space
Vector field	Biases tube alignment with vector field	Controls overall shapes
Virtual walls	A virtual surface to avoid and/or follow	Rigidly controls overall shapes
Max angle	Limits curve radius of a tube	Limits tightness of weave
Collision margin	Volume around robot to prevent collisions	Limits tightness of weave

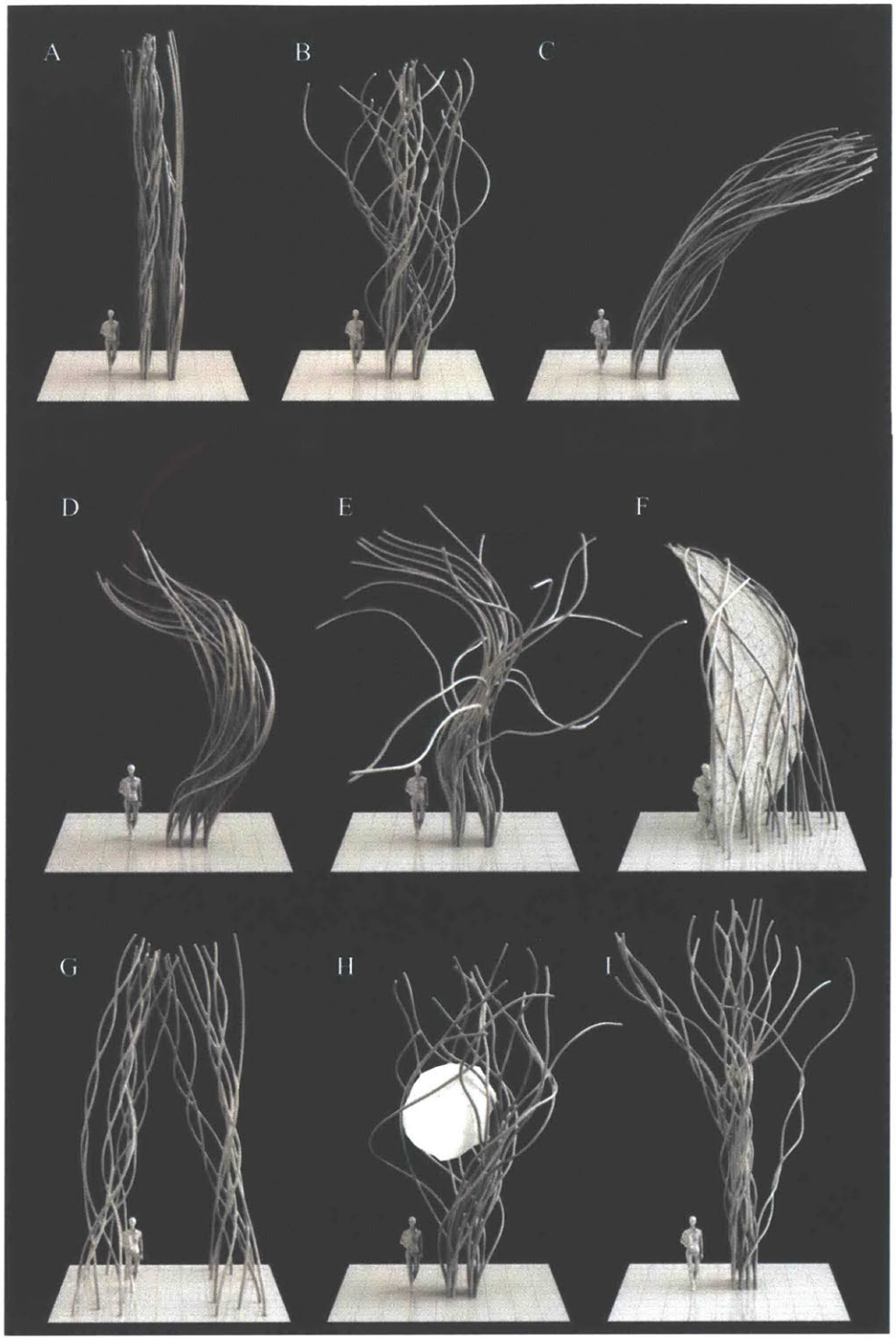

Figure 35: Panels (A)-(I) show variations in parameters from . (A) shows high alignment with low curling bias, (B) high curling bias with low alignment, (C) has high alignment with a

global goal, (D) shows steering along a path (E) shows potential fields being used to guide alignment, (F) shows alignment along a barrier or surface and (G)-(H) are further experiments. PC: Christoph Bader.

3.2.4 Controls and Coordination (During Print)

Once a global design has been established, each trajectory is compiled into a list of distances and pairs of angles (roll, pitch) relative to a global reference frame that is shared by all tubes. Each list is then assigned to a robot and translated into commands that the robot can execute.

Because the current robot system only has internal sensing (IMU and encoders), real-time collision avoidance is not possible. Therefore, all collision avoidance is handled during the pre-design process, and then followed as closely as possible by the robots at build-time. To do this, a custom set of commands was developed for the Fiberbots, which is similar in style to "G-code" used by most 3D printers and allows setting of parameters, requesting data and state from the robot, and executing motions.

One crucial component is that all Fiberbots that will be working in a shared workspace must be initialized with a shared global frame of reference. Throughout the print, in case of robot failures, this frame of reference must be tracked at all times, and be able to be shared among other robots in case a replacement is required.

A central controlling computer runs a multi-threaded custom server that coordinates commands to each robot and provides a human-interface for interacting with the robots in real-time. It is interesting to note that a "decentralized" version of this system, where each robot is sent all commands ahead of time and instructed to execute them, so the central computer is only used for monitoring, is nearly the same architecture. However, one difference is that for certain designs, the order in which robots begin fabrication is important and a central system would be needed to at least begin the fabrication process, and depending on the rate that lengths of tube are created, may need additional coordination. At the moment, this order checking is performed manually.

In the remained of this section, I will briefly discuss the high-level software architecture and how parallel execution is achieved.

Embedded Software (Control of a Single Robot)

Table 4: List of "G-code-like" commands available for each Fiberbot. The true list is significantly longer and more detailed, many of which are used to monitor and set properties, this provides an overview of the major ones used during fabrication.

Cmd	Name	Parameters	Description
w	wind	positions along mandrel, speeds, time to wind	winds a segment
drv	drive	distance	drives up/down tube by distance
a	align	3D unit vector or roll, pitch	aligns transverse axis of robot with vector specified in global reference frame, or locally relative move by roll and pitch degrees
h	home	homes wind steppers	homes the rotational and linear steppers
wref	world reference		sets the current IMU frame as the global reference frame
i/d	inflate/deflate		inflates or deflates mandrel

Each Fiberbot uses a Teensy 3.6 on-board, which contains a 180MHz ARM Cortex-M4 processor. The outer control loop typically runs at around 400kHz and maintains a state machine. The software is setup to take either serial or wireless commands directly through the Teensy serial port or by connecting and communicating via UDP with the ESP8266 which forwards messages to the Teensy and back to the original sender. It produces a 1Hz heartbeat message, which contains information about the current state and the last command received, these are used by the central coordinator to monitor the progress and state of all robots, as well as to track what commands to send next and if a lapse in communication has occurred.

The on-board processor also handles interpreting and executing commands, some of which are listed in Table 4. These commands are used to change between states or request information from the robot. All of the motion commands can be sent in either absolute or relative motions. During fabrication of a typical tube segment, a common sequence of commands is to inflate, wind, deflate, drive, align, home, and then repeat for the next segment. Before construction begins, the "wref" command is used to setup a global frame of reference, which will be discussed in the next section.

Localization in a Shared Workspace

The Fiberbots navigate by executing drive and alignment commands. Localization is only provided by integrating sensor readings during these motions. Both commands are implemented using PID controllers and operate at 100Hz, the drive commands use encoder readings for feedback, and the alignment command uses 6-DOF IMU readings that are fused into a global quaternion provided by the BNO055. If there is a consistent global reference frame, then a unit vector is specified by the alignment command. These are then converted into local robot coordinates so that the robot can then orient itself appropriately, in which it aligns its transverse axis with the vector specified. It is important to note that because the robot is cylindrical, local yaw does not have any effect on the output, and so controlling yaw is not important. However, yaw must be tracked so that the robot can adjust along its tracks appropriately.

If the robots are used in outdoor environments without magnetic interference, then the BNO055 can be used in 9-DOF mode. In this mode, magnetometer readings are incorporated into the output parameters, so a global frame of reference is established where the X-axis is aligned with gravitational North and the Z-axis is aligned with gravity. This is sufficient to establish a shared global reference frame that can be used by all the robots.

However, because the magnetometer caused significant drift due to interference of nearby buildings, we opted to only use the fused 6-DOF data. Because there is now no global alignment, if the robots are simply allowed to use the 6-DOF fused data, yaw is no longer accounted for (gravity still serves as a single alignment for all the robots), so while a single tube may be correct, they cannot be made in parallel or in the same workspace.

The procedure is then, before construction, all robots follow a calibration routine, where they are all aligned with some global feature (for example perpendicular to a sidewalk). From there, each robot i saves a local version of the reference frame R_i^vas

received by the IMU. Another reference frame R_i^w rotates this IMU-given frame into the set shared global reference frame (simply put, it is the inverse of R_i^v when we are in the calibration phase). From here, at every time step t, a robot can transform between intermediate local reference frames $R_i^l(t)$ and the shared global reference frame by

$$R_i^s(t) = R_i^w(t)R_i^v(t)R_i^l(t)$$

Where $R_i^l(t)$ is the rotation matrix from local coordinates to an intermediate reference frame as defined by the IMU. $R_i^s(t)$ is thus a rotation matrix used to transform between local coordinates and the shared global coordinates. A desired vector in the shared global workspace v^s, centered at robot i's local origin, can be represented as

$$v_i^l = R_i^s(t)v^s$$

By saving R_i^w, and reloading R_i^v on startup on a new robot j, robot j can replace robot i, as long as robot j is physically oriented in the same way as robot i was without undergoing the full calibration process. In this way, robots were replaceable if a catastrophic failure occurred, as long as the reference frames were saved and could be retrieved.

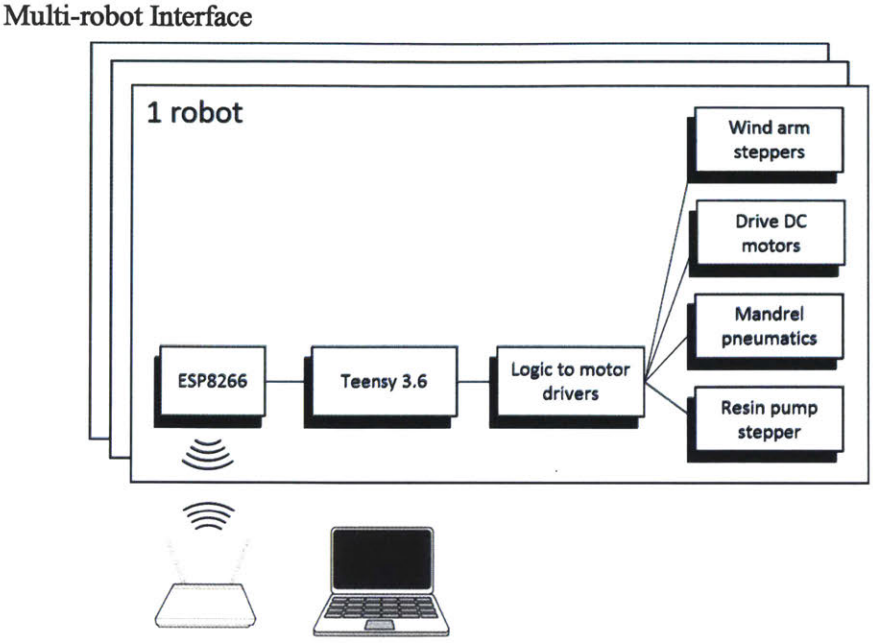

Figure 36: Overview of the communication system between the central controller and all of the robots and how commands are passed along.

During the construction process, all the robots were coordinated through a central computer on a local area network with fixed IP addresses, outlined in Figure 36. Every robot is assigned a unique ID, and is associated with a fixed starting location and tube to fabricate. The computer runs a multi-threaded, custom Python server that listens over 802.11 wireless for heartbeat commands from the robots. These heartbeat commands contain the current state of the robot and the last instruction ID that it executed. If the server is in "play" mode, if it detects that a robot is an IDLE state, and there are remaining commands associated to the robot, the computer will send the next available command to it. Once a robot has finished executing that command, it will return to the IDLE state.

Note that it is possible to modify this architecture to be "decentralized" by pre-loading all instructions to the robots ahead of time. Then when playing, all robots can simply execute their commands. The primary reason to use the centralized model was to aid in debugging and allow for easy ad-hoc adjustments to the paths when necessary. Though we did not use this capability during the final print, it was helpful earlier on during development when instruction sequences were not finalized.

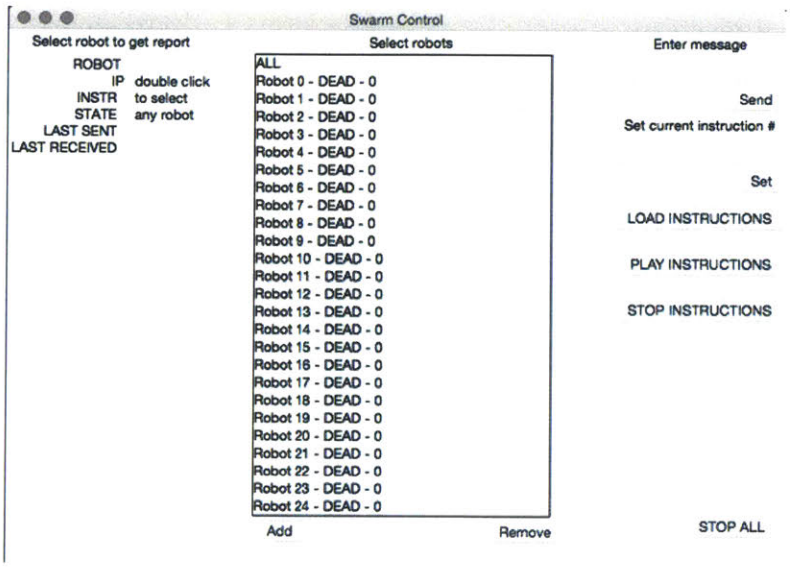

Figure 37: Human interface provided to monitor and coordinate up to 24 robots. On the left, a single robot's state can be viewed. In the middle is a list of all robot IDs, their state, and the segment number that they are currently fabricating. On the right, instruction sequences can be loaded, and commands can be sent to subsets of robots by selecting from the middle menu.

A human-interface, seen in Figure 37, was also developed that ran alongside the server. This interface allowed us to monitor progress of the robots, check for errors, and perhaps most importantly, pause and/or command a subset of robots without interfering with the operation of other robots. This feature proved invaluable for debugging without halting progress across the entire system.

3.2.5 Results

Several tests were conducted with the robots throughout the development process. The first test was a single straight tube before tilting and encoder capabilities were fully functioning. Later, we also performed tests with 1 robot creating controlled curves, and finally 2 and 4 robots creating full structures with controlled curvature. Finally, as a culminating test, we aimed to create a large-scale structure with at least a dozen robots operating simultaneously.

Architectural Scale Print with Multiple Robots

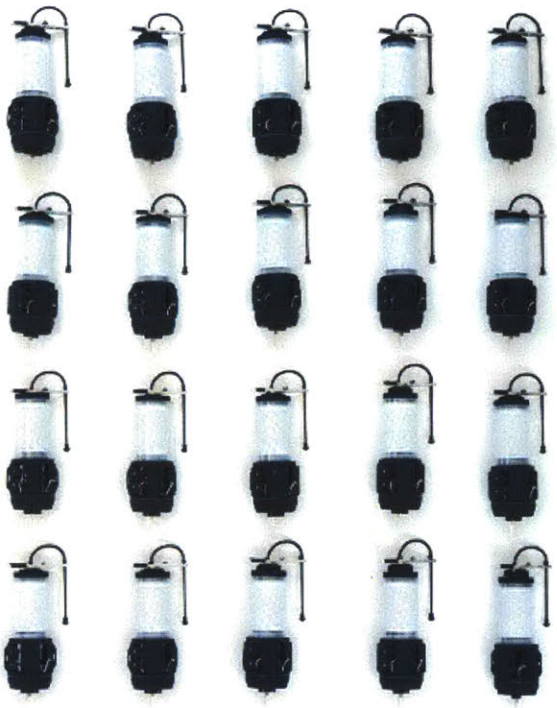

Figure 38: We built a total of 22 robots (20 pictured), with mostly 3D printed parts, a waterjet arm, custom machined rotary unions, and off-the-shelf parts.

The goal was to demonstrate that our system is capable of producing architectural-scale structures (at least 3 m tall) using a team of robots that could operate in the same workspace and at the same time.

To do this, we produced 20 identical robots, shown in Figure 38. Most of the parts for the robots were 3D printed using Selective Laser Sintering of nylon to produce roughly 600 individual parts. The fluid rotary union, used in the winding arm, was custom machined in-house for each robot, and the winding arms themselves were waterjet with aluminum. The silicone membranes were also assembled in-house. The rest of the parts were off-the-shelf components, though some required modifications. All the parts were manually assembled by us. We also built 20 steel bases that served as foundations for each of the tubes to be created. Not including labor, shipping, or research, each Fiberbot cost under $1500 USD.

Figure 39: Design of the final structure using the flocking technique, these are 3 different viewpoints of the same structure. PC: Christoph Bader.

A final design of the output structure was produced using the flocking-based approach outlined in Section 3.2.3. The high-level requirements of the structure were that 4 clusters of 4 robots were to be placed separately from each other, at 1.75 m apart. The robots should then curl within a cluster until about 4 m, before they begin to globally attract towards each other to create a roof-like enclosure. The idea was that a person could stand comfortably in the middle of the structure.

For construction materials we used Vetrotex glass fiber yarn, which was selected for its thickness and resin uptake. For the resin we used Solarez Vinyl Ester Epoxy Resin, which has a 5-minute total cure time. These were selected after empirical tests showing combinations of strength, but also aesthetics.

We chose days to perform the test when the weather was sunny with minimal wind or rain. Though our system is capable of building at night, which it predominantly did, it was ideal for the sun to cure the bottom layers more thoroughly. The steel bases were manually measured and placed in the correct orientations and the robots were initialized by aligning the robots using a simple jig and running the global reference sequence.

Then, over the course of 2 days, our system built a 4.5 meter structure using 16 robots simultaneously (8 each day due to mechanical difficulties on the first day), with an overall build-time of about 12.5 hours. The results can be seen in Figure 40. There were no collisions during the build process, and the final structure stood outside in rain, wind, and snow conditions for roughly 7 months.

During the build sequence, all robots operated autonomously. However, on several occasions, a small subset of robots needed to be stopped for maintenance. During these

periods, only the subset of problematic robots were paused, and the rest were left running. Many of these failures were minor mechanical failures. The only other period where human intervention was required was to refill resin tanks, but operation did not have to be halted for those periods.

Figure 40: At the bottom, a timelapse of the construction process over 2 days. At the top, the final structure after remaining outside in typical New England weather after several months.

3.2.6 Discussion & Conclusion

Figure 41: The pre-designed structure is shown on the left (designed up to 10 m tall), and the final structure in the middle (roughly 4.5 m), and photogrammetry of the actual structure overlayed on the designed structure on the right, it is clear that drift occurred, estimated at about 0.5-1 m or so over the entire length. Photogammetry credit to Silas Hughes.

With the Fiberbot project, to our knowledge, we demonstrated one of the first examples of fully autonomous construction with several mobile robots operating simultaneously in a shared workspace, and most importantly, at architectural scales. In the process, we also introduced a novel filament winding system that allowed for controlled fiber patterning, fiber-to-resin ratio, controlled curvature, and near-arbitrary lengths. We also co-developed a flocking-based design strategy that was fabrication-aware and simplified the design process for a human user.

However, the ultimate goal of the project is to enable ad-hoc behaviors with little to no human oversight. This requires higher accuracy motion, external sensing capabilities, and better understanding and analysis of the material and structural properties of the tubes. To start, as seen in Figure 41, the final output structure did not completely match the pre-designed structure. Using a drone, we did a photogrammetry scan of the output tubes and overlaid it on the pre-designed tubes in order to gain insight into the drift errors incurred during the process. There is clear drift, on the order of 0.5-1 m over the 4.5 m tube. More detailed analysis needs to be done on both the photogrammetry and comparison methods.

While the design methodology used is scalable, as flocking is inherently simple to scale, it does not provide guarantees that all robots will not get trapped. Now, the solution is to simulate robots in sequence (start one robot slightly earlier than another robot), and

introduce them in an outward fashion (ones nearer to the center of the structure), but this does not work in all scenarios, and may adversely affect the "interwovenness" of a structure. This strategy also provides no structural guarantees, only that one area of the structure will more likely be denser and more interwoven than another. For situations where all tubes are self-supporting, this may be fine, but if the curling is an important structural feature, then this is not a sufficient strategy.

In the future, we would like to deploy the Fiberbots without a pre-designed structure or pre-existing knowledge of the terrain. This requires external sensors (which we have already included ports for on the robot arm) to detect obstacles at build-time. And even further, we would like to create a system with hundreds, or thousands, of robots at once.

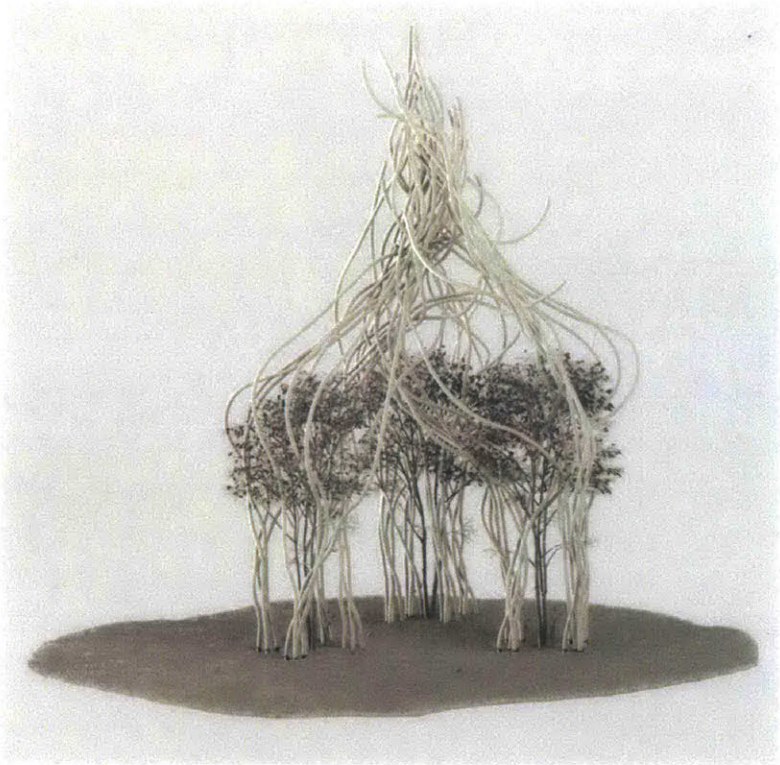

Figure 42: Far future vision, Fiberbots can detect and avoid arbitrary obstacles, the flocking based design method can still work at build-time.

4 The Future, Biological Swarms with Natural Materials

4.1 Vision

As climate change becomes an increasing threat to the planet, human society must find more sustainable means of fabrication. These must take into account utility just as much as ethics, and touches every aspect from how we design and build to what materials we select and how we extract them. In [85], Neri Oxman lays out a unifying ideology that she terms *Material Ecology*, to study the relations between form and function across disciplines in biology to computational design, all at once. That each aspect must consider its impact on the others, how they in turn relate back to nature.

This section will be far more speculative, but hopes to lay out a framework for which we can begin to achieve truly sustainable fabrication methods, from the materials we use, to the actual systems we use to fabricate.

4.1.1 Natural Materials

The research and industry communities are increasingly interested in natural materials that can be used in construction. The common goal is find materials, and corresponding material processes, that do not generate significant waste and can be decomposed naturally. However, one common issue is that such materials are difficult to create in strong, robust ways, and are difficult to control from a design perspective.

One strategy has been to look into the fabrication methods of indigenous people, using materials such as wood, adobe, clay, etc. and find ways to scale them. Rammed earth is similar, and uses local, composite organic materials, such as dirt or limestone , "rammed" into moulds to create strong structures such as flooring or walls [86], [87]. One issue is that this may not be consistent across regions depending on environmental conditions and available material, and transporting significant amounts of resources may counteract the environmental benefits of it.

Other approaches have looked directly at using living materials, or materials used in living organisms. Combinations of chitosan and pectin, found in shrimp shells and other shelled animals, are being investigated for use in architectural scale project [88]. Perhaps most popular is the use of the mushroom, mycelium, to create bricks, which has been already used to create large-scale structures [89].

However, all of these materials are still not fully understood and can be difficult to control.

4.1.2 Biological Agents

Biological systems however have figured out how to utilize natural materials to create robust structures that are also adaptable. Organisms ranging from termites to beavers to birds are all capable of building large, complex structures with seeming ease using only local or self-produced materials [90]–[94]. None are perhaps as well studied as the class of eusocial organisms, which include bees, wasps, ants, and termites. These insects are the most successful organisms in the world by biomass, and have colonies in a wide range of terrains. What is most astounding to researchers is how large and sophisticated their structures are compared to them. For instance, the *Macrotermes*, while only measuring several millimeters in length, can construct mounds that are several meters above ground [95].

Even for organisms that are not considered eusocial, a range of social behaviors exists, stretching from solitary to quasisocial to eusocial [96], [97]. It seems, however, that as one shifts along the social scale, the fabrication capabilities increase as well. Inspired by these accomplishments, this section seeks to understand how we can reproduce these behaviors using new materials and new fabricating agents, and how we might be able to collaborate with them in the future.

4.1.3 Framework: Designing new social behaviors

At a high-level, our goal is to understand the components that are necessary to form robust collective behaviors in order to inform how we might be able to replicate, and ultimately create, our own. This is driven by an assumption that sociality is a key ingredient towards developing truly scalable systems for large-scale autonomous construction and that biology serves as an idealized model of such systems.

Stigmergy

Before we dive into other details, it is important to provide some historical context and introduce a concept that will recur throughout this section—*stigmergy*. Preceding the 1980's, social behavior, across all living organisms, was considered a sophisticated trait that required an enormous amount of complexity and coordination, on the part of the organisms, to achieve. This debate was highly rooted in discussion around innate vs.

learned or evolved vs. taught behaviors. It was thus paradoxical that organisms that were considered simple, like insects, could exhibit highly organized social behaviors. In fact, in the case of eusocial organisms, their sociality is crucial to their overall success as an organism and can build structures with surprising details like chambers and control of airflow.

This confusion persisted until the early 1980's when Grasse [98], perhaps fortuitously to this thesis, was studying construction in termite colonies and proposed how some complex social behaviors could be distilled into a combination of much simpler behaviors or mechanisms. Some collective behaviors can be fully explained as the response of an individual towards passive stimuli left in the environment by another individual, usually of the same species. When this passive response-stimuli effect occurs across a colony, it can result in high-level collective behaviors, which he termed stigmergy. In this particular instance, termites leave pheromonal signals on dirt that causes other termites to be attracted to it, and either pick it up or deposit more dirt next to it. This creates a positive feedback loop, where increased construction activity leads to recruiting additional termites to increase it even more. Combining this with other pheromonal signals, such as a repellent from the queen [91], more complex structures can emerge. While this does not explain all social and collective phenomena, it is crucial to our understanding of construction behaviors in insects. Perhaps more important though, it enabled us to study and understand complex social behaviors as the composition of much simpler components and forms the basic ideas that will be presented here.

How are social behaviors formed in simple organisms?

Before we can understand how to create new, robust collective behaviors, it can be helpful to study how existing ones are formed first. The study on the origin of sociality is still an active area research with many perspectives and goals. Among them, there is a distinction between what mechanisms enable social behaviors to emerge locally, and a separate issue of how they are persisted in a species across generations, genetically or taught.

The latter issue has a complicated history and is also based on a paradox that has generated significant debate [99]. This paradox is based on the observation that insects are genetically identical within a colony and says that eusocial insects individually seem to express altruistic behavior, which goes against the competitive nature of evolution presented by Darwin [100]. They sacrifice the ability to produce their own offspring,

compete genetically, and completely submit to their specific role in a colony. An initial idea, called "inclusive fitness theory" or kin selection, was proposed by Hamilton [101], [102] as a potential explanation. This theory states that altruistic behavior will persist in a species if $rB > C$, where r is relatedness of individuals, B is the benefit of the social behavior and C is the cost of the behavior to an individual. However, more recent accumulation of evidence may suggest that this theory is either false, or at least inadequate to resolve the paradox fully [99].

This debate is adjacent to, and distinct from, the one that fueled the ideas behind stigmergy, which has less to do with *why* sociality persists and more to do with *how* short-term mechanisms enable sociality to begin with. The latter being more immediately important to our discussion of designing new social behaviors.

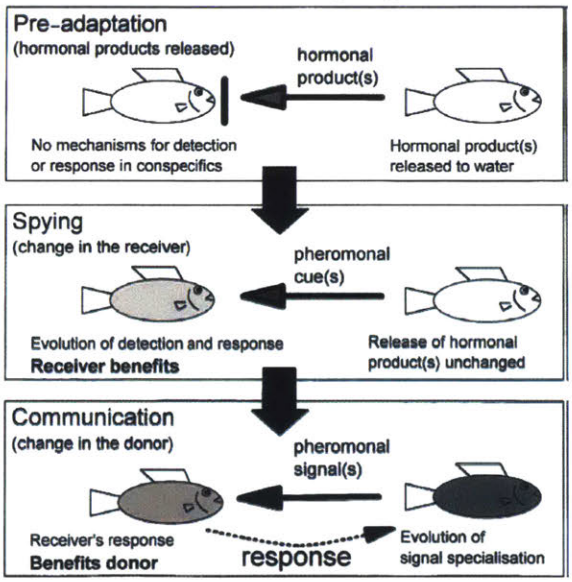

Figure 43: Illustration of the evolution of hormone to pheromone, original figure from [103], and re-adapted and reproduced here from [104].

An initial mechanism by which simple social behaviors develop was proposed when studying aggregation behaviors in fish. At a high-level, the idea is that some fish historically may have produced a hormone that was specific to that species. Then, further along the evolutionary timeline, fish of the opposite gender either develop sensors that detect the hormone, or already could detect it, but now are slightly drawn to it. Because this helps the fish find mates, this sense is selected for over time, and the hormone

producer is also selected to amplify the hormone. This continues until this becomes an established aggregation behavior [103], [104]. The process is illustrated in Figure 43.

A similar experiment was performed in an evolving population of artificial agents, where their goals were to wander around the environment and maximize mating potential [105]. A light source is provided in the environment and the agents are provided with sensors that give them their relative angle and distance to the source, but no other evolutionary benefits or pressures are added. Eventually, the population evolves a stable behavior that leads them to follow the light source, which can be explained by an evolutionary advantage for mating gained by aggregation with the light providing an indirect means for coordinating that behavior.

The unifying theme that we can then exploit is that social behaviors can emerge by creating a *linking benefit* between an *existing sense* and *existing environmental cue*, that did not have to be affiliated previously. What is even more promising perhaps, is that some of these behaviors may be enabled across sensory modes. Given that similar aggregation behavior emerged in the example of fish, where chemotaxis was used, and in the artificial agent, where phototaxis was used instead.

Wyatt [104] states that many different species can use the same chemical signals for different purposes, which suggests that they are perhaps interchangeable. He further classifies signals into chemical (ie. pheromones), tactile (ie. procession caterpillars), visual (ie. fish schooling), and acoustic (ie. bird calls), where each is used to achieve different spatiotemporal goals, such as repeated long-range communication over short time frames, or gradual communication over long time spans. This gives us a potential roadmap on how to look for potential *links* that can be created between behaviors. Just because one organism does not have a particular sense or behavior, does not mean it does not have an analog.

What approaches are there to study the physical mechanisms of sociality?

Most approaches to studying biological social behaviors are usually either invasive, intrusive, or observant, note that these lie on a spectrum and are not clear distinctions. These can be either in-situ, ex-situ, or simulated. Invasive methods are often described as "against will" of an organism, intrusive perhaps just annoying, and observant is just that and requires no direct interference with the organism.

Thus far, a popular method for studying, and confirming, the underlying mechanisms that enable more complex social behavior, in existing biological organisms, is through destructive means. Generally, a hypothesis is formed that estimates a particular chemical

compound or characteristic that enables a collective behavior. In order to verify this hypothesis, the organism is modified such that the expression of that compound or trait is suppressed in some fashion. Then, if the collective behavior is no longer expressed, all other traits held constant, then it has been determined that that compound or trait is at least a major component to the overall behavior. This strategy does not necessarily identify all components of a single behavior, but can highlight whether an individual component is necessary. This was used to determine the compounds involved with the swarming behavior of locusts and the overall collective nature of some ants [106], [107]. Some work has been done at the cellular level, from a built approach, and is an active area of research, but will not be discussed here.

How is social behavior modelled?

In 1994, Grünbaum et al. [108] classified all approaches to modelling of aggregate social behaviors, those involving motion, as either Lagrangian or Eulerian models. They state that the Lagrangian perspectives, also known as individual or stochastic models, attempt to describe the model as social interactions that arise from the behaviors of individuals and are usually focused on describing local interactions, and then extrapolating to the larger collective. These methods are also, more often than not, discrete. Within the context of artificial models of social behavior, Reynolds' famous boids model [79] and cellular automata as described by Conway's game of life are examples [109]–[111].

The Eulerian approach then is to instead model collective behaviors in terms of densities and flows, often using partial differential equations to model effects and responses at a global scale. This approach operates in a more continuous domain, and use advection-diffusion-reaction equations frequently, such as Turing's reaction-diffusion models [112]. Ladley et al. [113] proposed a similar decomposition of methods, specifically in regards to his own models vs. those proposed by Deneuberg (discussed later) in relation to termite construction behavior specifically. Merging the ideas, we arrive on the definition that Lagrangian approach are "bottom up" and Eulerian approaches are "top down".

Within the context of this thesis, there is an assumption that these models are dualities, and can be useful to describe the same process in slightly different perspectives. In fact, I will explicitly state that the hypothesis that Lagrangian approaches are perhaps more useful for designing new social behaviors, when creating the fabricator, and that Eulerian approaches are better for the end-user, those that use the

collective behaviors to accomplish end-tasks, such as the actual design of the output structures.

How can we create new social behaviors?

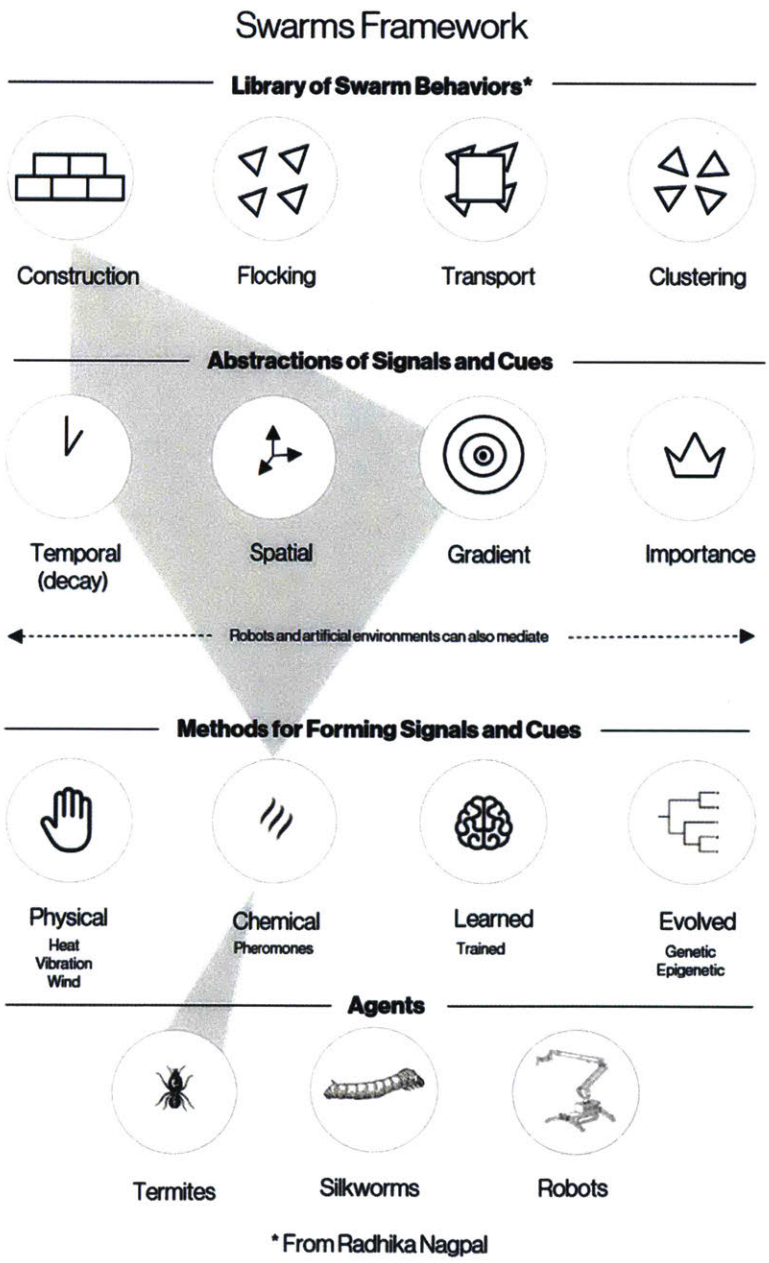

Figure 44: An abstract framework that balances top-down and bottom-up approaches to find pathways and linking behaviors to create new social behaviors.

These discussions lead up to our question, how can we go about creating new social behaviors? What lessons can we learn from biology that can translate into artificial or robotic contexts and vice versa. What strategies can we use to mediate between sensor and actuation modalities? To limit our discussion a little, these behaviors are focused on those do with motion, relying on taxes or kineses in biological terms. When do we need to be invasive, intrusive, or simply enabling?

Significant work has been done within the artificial and robotics communities, ranging from pure simulation with Boids [79], Conway's Game of Life [109], [111], to robotics [10], [11], [15], [16] and even artificial evolutionary standpoints [105]. On the biological side, not as much work has been done. Several instances of invasive tests have been performed to gain low-level control over insect mobility, and has been proposed that artificial algorithms can be used on top of these cyborg insects [114]–[117]. Perhaps the most related examples are those in domesticated animals herds, such as cows and sheep. More recently, artists have begun to form new types of interactions with social insects as fabricators of sculptures, such as [118]–[120].

The approach proposed here is not rigorous, and mostly outlines an abstract methodology that is summarized in Figure 44. It builds on the findings that many collective behaviors are composed of smaller simpler behaviors that were linked over time through evolution. These smaller behaviours in turn are composed of local responses and signals, many of which are interchangeable between species. The idea is then to take a high-level view on different pathways to achieve particular, robust, collective behaviors. It attempts to balance both top-down and bottom-up approaches to designing new systems. At a high-level, collective behaviors are broken down into known, abstract, enabling components, such as gradient following or evaporation of some signal. These in turn are mapped to their enabling mechanisms, such as known taxes and kinesis in biological organisms, or local algorithms for robots. Using this ideology, we can perhaps find new avenues for creating novel social behaviors.

4.2 Case Study: The Silkswarm

The work in this chapter builds on past work from our lab, the design of the heat platform is my own, with much assistance and advice from Dr. Markus Kayser, Jean Disset, João Costa, Sunanda Sharma, and Andrea Ling.

4.2.1 Overview & Approach

The short-term goal of this project is to induce basic social-like behaviors, specifically termite construction, in the *bombyx mori larva*, the domesticated silkworm, in a non-intrusive manner. Silkworms are selected as the model organism because they are (a) solitary, (b) natural fabricators when they are spinning silk, (c) well-studied, and (d) robust and safe in laboratory environments due to their heavy domestication. Termite construction is chosen both because of its interest in the larger scope of this thesis, but also because it relies on simple pheromone-driven interactions. For instance, with some probability, termites deposit material at areas where a certain pheromone is present with increasing probability the stronger the signal. They can also be repelled from certain areas, usually the queen, in order to create cavities within a structure [91].

I aim to recreate these behaviors by simulating pheromones using heat. Both being methods of environmental templating, and can be less intrusive. Silkworms are generally attracted to heat sources ranging from 30°-50°C, and are repelled by temperatures exceeding 80°C. Thus, at a high-level, by controlling temperature in highly localized ways, I hope to attract and repel silkworms in a similar strategy to those expressed in termites.

To do this, I present the design and development of a heat platform and, using the platform, propose methods for conducting these experiments. I will begin by introducing key concepts and experiments that were performed to understand silkworm behavior that are necessary for the development of this platform and overall strategy. Then I will describe

4.2.2 Background

To begin, one needs to understand some specific behavior of silkworms and their origins. Silkworms, the larva of the *bombyx mori* moth, have been domesticated by humans for thousands of years, no wild *bombyx mori* exist. They have evolved to be highly dependent on humans for survival, have very few developed senses, and their moths can no longer fly. Their primary function as worms then is to spin highly tuned silk cocoons, about 300-500 m of thread each, which are processed for human goods [121]. This process typically involves boiling the cocoons, with the silkworm still in it, and then

unraveling the cocoon to form a single thread. They are considered highly valuable to humans, and their genome has even been sequenced [122].

Even though the silkworms are raised in farms in close proximity, they have not evolved any behaviors that are considered social. The typical lifespan of a silkworm involves eating an exclusive diet of mulberry leaves, and over a period of several weeks, molts 5 times. Each time it molts, it enters a new *instar*. By the time it has reached its 5th instar, it feeds only briefly, before beginning to spin silk. Once it has started spinning silk, the silkworm will no longer feed, it loses its interest in the scent of food entirely, and roams around spinning silk in a figure 8 shape. Once it has found a suitable location, it will build a small scaffold, and then create a cocoon where it will turn into a pupa.

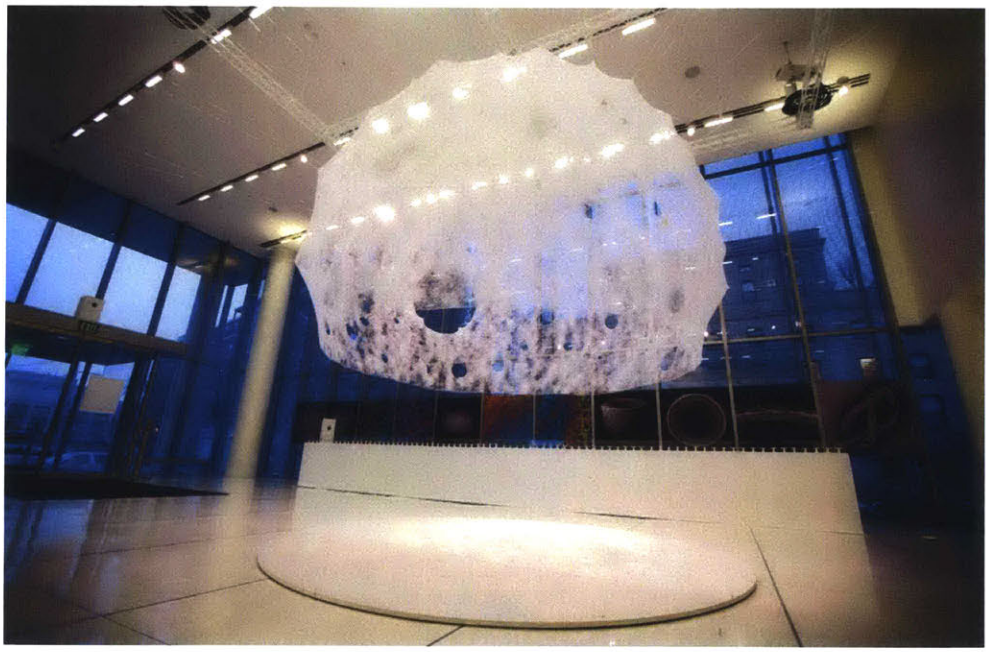

Figure 45: Silk Pavilion by the Mediated Matter Group. PC: Steven Keating.

Originally inspired by the intelligent construction abilities of termites and the adaptability and strength of silk used by silkworms and spiders, the Mediated Matter group was interested in what it might mean to merge these capabilities—to create a "silkmite". The approach was to use the silkworm as an individual fabricating agent, to build an understanding of their local behaviors, and to try to compose those behaviors into a larger collective behavior. These studies resulted in the creation of a large, cocoon-based structure, known as the Silk Pavilion, using nearly 6500 silkworms to create a

single monolithic structure [123]. However, these silkworms did not necessarily inform the construction itself, as a robot arm was used to wind a scaffolding layer of silk, which determined where silkworms could or could not reach. This work hopes to involve the silkworm's own behaviors more. This original work resulted in several important findings that this project will build on:

1. **Silkworms do not form cocoons on convex or "nearly convex" surfaces**

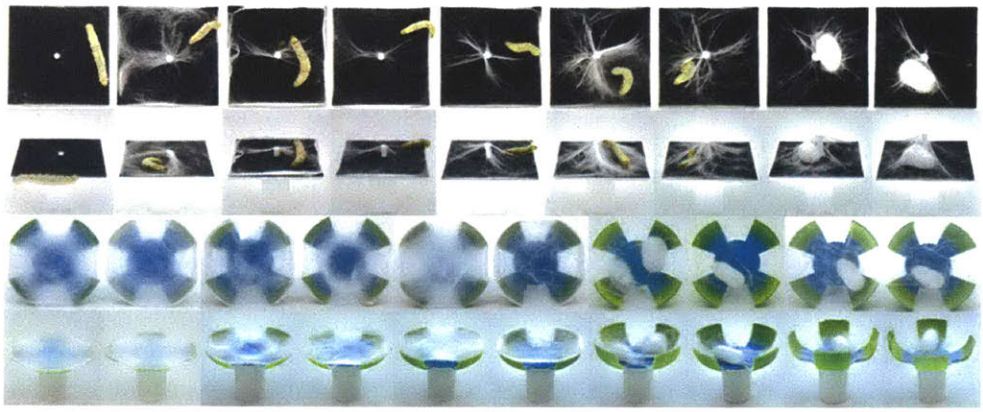

Figure 46: Experiments demonstrating that silkworms do not form cocoons on surfaces without sufficient "height" or concavity. On the top rows, from left to right, poles are provided with varying height, and on bottom row, increasing concavity. Cocoons only form at sufficient height/concavity. Published in [124].

The first observation was that silkworms form cocoons by creating a scaffolding first. This scaffold requires a "z-axis" to be present, though not necessarily accurate, one can think of this as needing at least 4 anchor points, roughly organized in a tetrahedron. Without this type of setup, they are unable to form a scaffold, and are consequently unable to cocoon. However, they do not stop spinning silk, and continuously deposit silk and wander the environment searching for a suitable scaffolding region. If none are found, they will simply deposit all their silk on the surface that they are on, and continue to pupate normally. Therefore, as long as surfaces are sufficiently convex (can be slightly concave), then silkworms can be thought of as depositing silk onto a mold or surface, see Figure 46. Other groups have since made similar discoveries, or have built slightly on this idea to create larger flat sheets or more complex geometries [125], [126].

2. Silkworms are attracted to heat

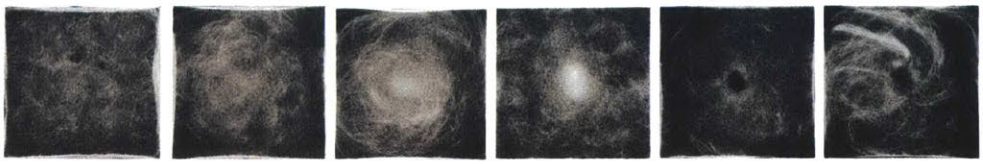

Figure 47: Silkworms are attracted to higher temperatures, but are repelled from extremely high temperatures. Small heating elements (resistors) producing localized heat were placed under a flat plastic surface, in the center, with heat isolation properties. One silk spinning silkworm was placed on each. From left to right, temperatures range from 30°C to 80°C in increments of 10°C. PC: João Costa.

The second observation was originally that silkworms are attracted by heat, but precise temperatures were not known. Since then, we have conducted a more controlled study and found that they are attracted to temperatures between 30°C and 60°C and repelled by temperatures exceeding 70°C, shown in Figure 47. According to the basic experiments, they can at least sense high temperature regions greater than 10 mm in diameter. These behaviors, one attractant and another repellant, will serve as separate artificial behaviors that can be exploited.

4.2.3 Artificial Pheromones and Control

Macrotermes Construction Models

The termite species *Macrotermes* is known for building some of the largest termite mounds in the world, several orders of magnitude larger than themselves. This has made them popular research subjects, and extensive literature is available on their building behaviors, as summarized by [127]. This makes them a reasonable starting point for this experiment.

The earliest model for termite construction behaviors came from Grassé in his discovery of stigmergy [98]. This was followed up by Deneubourg [128] who created a series of differential equations that modelled flow of termites in and out of a construction area subject to the presence and strength of pheromones, and how this positive feedback mechanism could result in construction. Bruinsma [129] observed that the queen termites emit *building pheromones* which templates or restricts an area over which builder termites will construct the "royal chamber". The builders themselves use *cement pheromones*, which are deposited into grain of soil that are used in construction. This pheromone helps to attract, or recruit, other builders as well as increase density of

deposited soil in a region. These concepts were shown to be sufficient to recreate simple 2D construction behaviors in simulations. Further studies by [113], [127], [129]–[131], extended these models to incorporate other parameters such as 3D behaviors, the effects of wind, excavation, additional pheromones, and agent-based methods (as opposed to continuous differential equation-based).

For the purposes of simplicity, we focus on reproducing the 2D variations of pheromone-based construction behaviors. At a high-level, these models all use *emission*, *diffusion*, and *evaporation* of pheromones (usually one or two) and analyze them spatiotemporally in order to fully determine the construction behaviors in termites. Intuitively and abstractly, emission controls the strength, diffusion creates gradients, and evaporation controls the rate of diminishing strength of a single pheromone.

To then apply this to the silkworm context, we attempt to treat heat as an analog for pheromones, and artificially control the emission, diffusion, and evaporation parameters. Temperatures between ambient and 60°C can mimic a cementing pheromone and higher temperatures can be used for restricting or templating pheromones. In order to create a positive feedback loop, as an example, one can increase heat, up to the 60°C threshold, wherever silk has been deposited. This may require the use of a camera in order to autonomously monitor the silk deposition and be able to react accordingly with the appropriate artificial pheromone response.

Other Forms of Control

In addition to the positive feedback control loops inspired by termite construction. We are also interested in how artificial control strategies can be used in conjunction with emergent behaviors to create systems that humans can meaningfully interact with. We thus hope to investigate the potential to use both feed-forward and negative feedback and understand to what extent certain behaviors can be controlled. For instance, rather than silkworms begin attracted to where other silkworms have deposited silk, we can attempt to lure silkworms to where a human requires additional silk to be deposited, or prevent them from reaching a certain region.

4.2.4 The Heat Platform

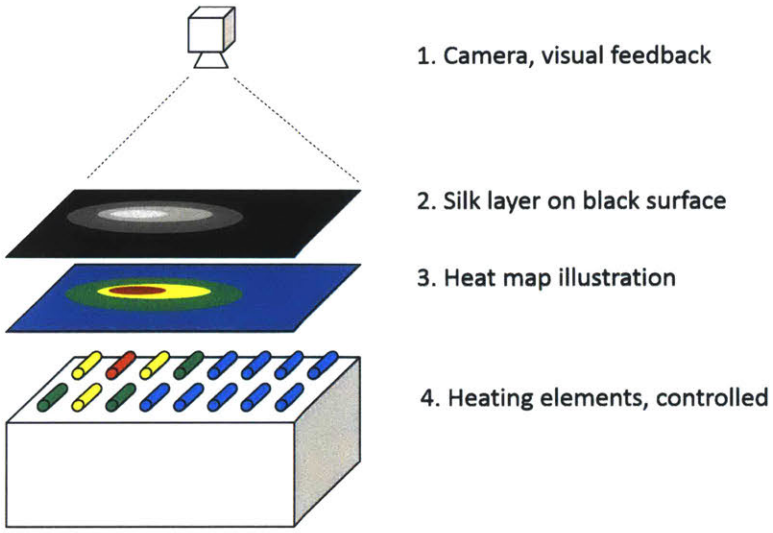

Figure 48: Overall vision for the heat platform. An overhead camera provides feedback on silk deposition and silkworm locations. Underneath, a panel containing heating elements are controlled in response to the silk deposition.

The purpose of the heat platform is to create a testbed to simulate pheromone behaviors using heat, a high-level vision is shown in Figure 48. From a positive feedback standpoint, the idea is to be able to mimic the emission, diffusion, and evaporation of at least one pheromone, the cement pheromone, and potentially introduce a second, the templating pheromone/behavior caused by the queen.

To mimic emission the platform must be able to, relatively rapidly, increase temperature in specified locations by controlled amounts. Diffusion by either natural diffusion of heat across a surface, or, by controlling the temperature of nearby localities as a gradient. And evaporation as cooling at a controlled rate. The templating behavior in termites, which controls the minimum distance at which soil will be placed from the queen, can be mimicked as a repellant within that radius. This can be achieved with high heat in local areas, above 70°C.

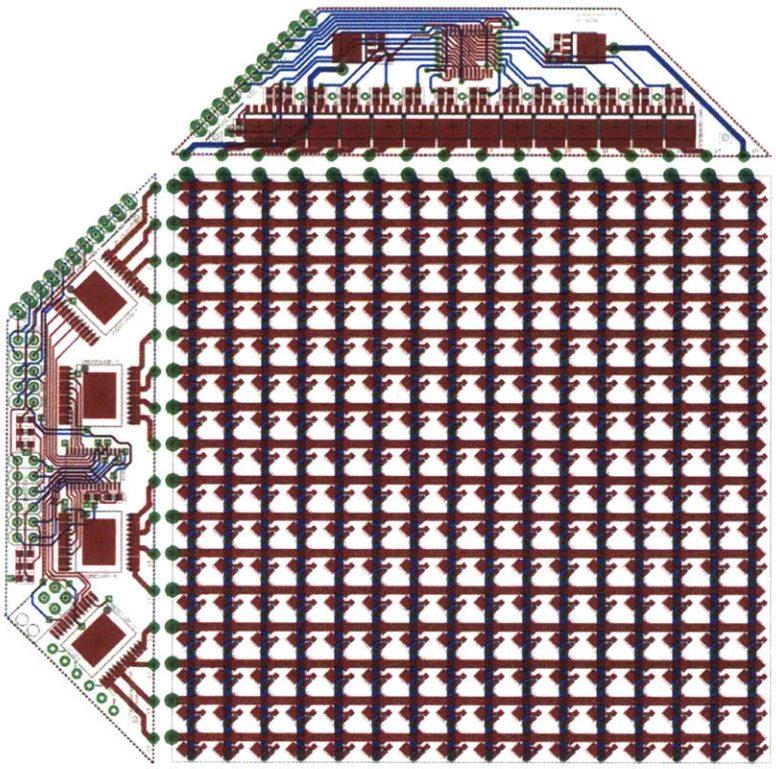

Figure 49: CAD of all 3 boards are shown here to control a single 16x16 resistor/heating element array, measuring 96x96 mm. The top trapezoid contains the low-side transistors and the left trapezoid contains the high-side transistors.

Two possible strategies were considered. The first was to raster heat onto a surface using a laser with mirror galvanometer and the second was to, effectively, build an LED matrix where the resistors are used as heating elements and the LEDs are replaced with standard diodes. The latter approach was chosen because precise control of the heat seemed simpler.

The primary difference between the heating matrix and an LED matrix is that the resistors are chosen and operated near their power rating, as they generate significant heat at those points. This means, however, that power consumption is potentially much higher than standard components, used in LED matrices, are designed for, and so a new panel must be developed with higher power components. It is also fortuitous that standard SMD resistors can safely operate up to 150°C, but often have a power decay starting at 70°C to 80°C, which is precisely the temperature ranges required in this application.

Component selection and board design then follows as (1) selecting "pixel" size, the resistor package, and board size, (2) the operating voltage and power requirements, which dictate the resistor value, and (3) the rest of the components are selected based on the previous.

First, the pixel size was chosen to be approximately 5mm. This was determined by slightly increasing resolution on the previous experiments in Figure 47, from 10mm. We fit both a diode and resistor within the pixel area, so a standard 1206 SMD resistor package was chosen. Each panel was decided to be 96x96 mm, so that the resolution was 16x16 and the cost per board was low. This way, several panels can be daisy chained to create arbitrarily large panels while remaining affordable.

Next, an operating voltage and power consumption are selected, which dictate the value of the resistor. Before this, it is important to note the general operation of the panel. The architecture that is used is the same that is used in scanning, or multiplexed, LED matrices. These pull a single column to ground at a time, and within an entire column, each resistor can be PWMed to an appropriate heat value. This means that at any given time, only 1 of the 16 columns can be turned on. By cycling through every column very quickly, it gives the illusion of persistence, but it means that the peak power consumption is that of a single column that is fully on. We can thus arrive at the equations:

$$R = \frac{V^2}{P_R * N}$$

$$I_{max} = \frac{V * N}{R}$$

Where R is the resistance of a single resistor, V is the operating voltage, P_R is the power required by a single resistor, and N is the number of resistors in a column. By selecting $P_R = ½W$, and $V = 24V$, based on cost and available components and power supplies, we arrive at a resistor value of $R = 48\Omega$.

By using a demux and a PCA9685, which is a i2c-based LED driver that can PWM select channels at once, a single panel is thus controllable with 12 wires: 24V, GND, demux enable, PCA9685 i2c lines, and 4 select channels for the demux. While this is quite a large number to be controlled from a single controller, each additional panel only requires 1 additional pin, which is the demux enable. By toggling the enable pin, a controller can cycle through a large number of panels and share all other wires. This makes the design of the board easy to scale. A sample for a single 16x16 panel is shown

in Figure 49. A modular design also allows us to modify resistor values and diodes easily.

The limiting factors for scaling beyond a 16x16 resolution then, as is needed for large-scale tests with potentially hundreds of silkworms, are the overall power requirements for all the panels, and the controller speed. On a Raspberry Pi 3, it was experimentally determined that the outer control loop could be run at roughly 8Hz max and PWM signals can be pulsed at about 1500Hz max. The easiest way to scale then is to use either faster embedded processors or add processors for every fixed number of panels.

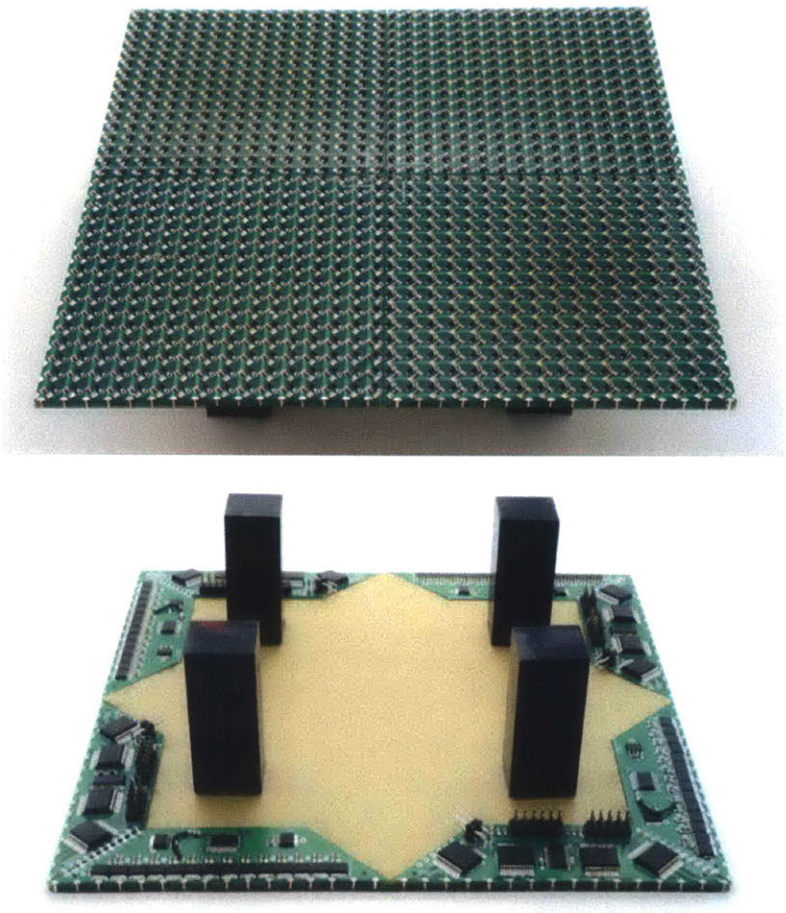

Figure 50: The heat platform, composed of 4 panels with 16x16 resistors each. An arbitrary number of panels can be added together, limited only by power consumption and computational

speed of the embedded controller. Total resolution is 32x32 "pixels", where each pixel is roughly 5x5mm and can reach temperatures between the ambient and about 75°C.

4.2.5 Results

Overall, the electrical architecture works to create a highly controllable, reactive, and easily extensible heating platform. The platform was characterized based on the maximum temperature achievable and the rate at which it could react, which indicates how effective it can be used to generate various emission effects and templating effects. While operating at the full 24V with 100% PWM, we can reach 70°C within 50 seconds, which is the temperature at which silkworms are repelled. Between 10 to 20 seconds, we can achieve the full range of attractive temperatures. Given that silkworms can move between 1-3 mm/s on average, this is likely sufficient to cover most behaviors that one might wish to replicate in terms of emission (having a high heat source track a silkworm travelling at full speed). These results are shown in Figure 51.

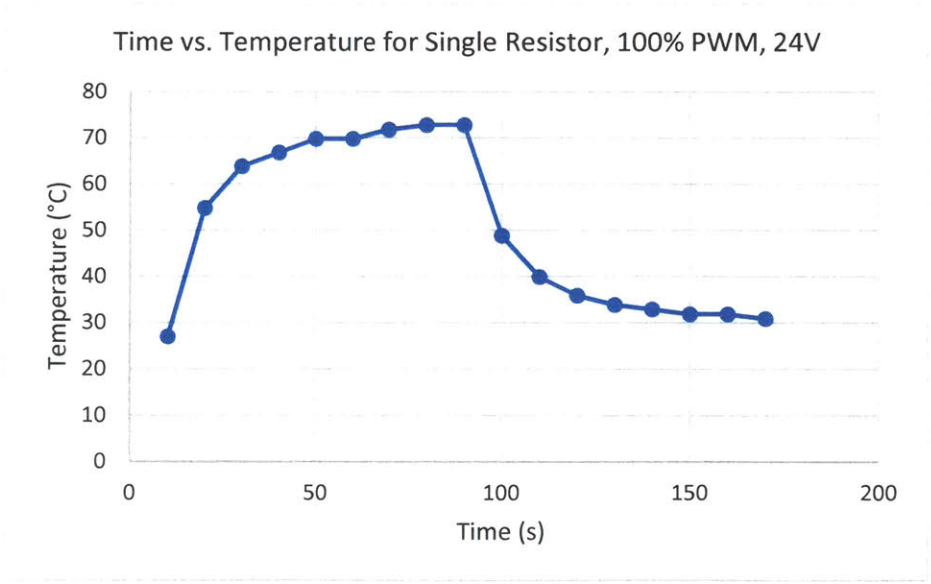

Figure 51: Shows the fastest reaction time of the platform for a single resistor. Measured using a contact-based heat probe at 30 second intervals.

Another basic set of experiments was performed while the heat matrix was still under developments. This was a passive feed-forward experiment, where temperatures are fixed during the duration of the experiment, to verify the attractive behaviors and

repellant behaviors using several silkworms on a single platform of the same size as a heating matrix with 32x32 resolution. 4 large 10W resistors were used to create an attractive and repellant ring at the center of the platforms, as shown in Figure 52.

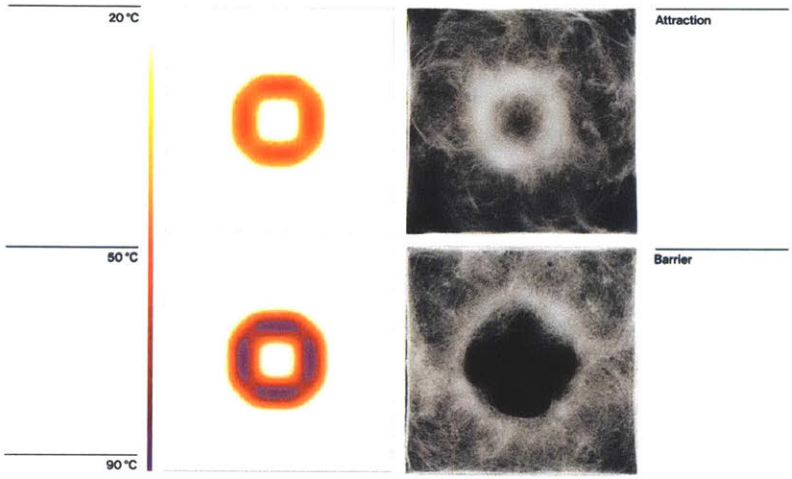

Figure 52: These experiments were done on a separate platform where the heating elements could be easily isolated, using thick sheets of silicone. The arrangement of the heating elements are shown on the left. 5 spinning silkworms, for 3 days, were used on each experiment, the platforms were roughly 25x25cm.

Figure 53: Timelapse over 3 days of the attraction experiment shown in Figure 52. PC: João Costa.

Once the platform was completed, 2 feed-forward experiments, shown in Figure 54, were performed to better characterize the resolution and behaviors on more complex, rectilinear patterns. The hypothesis was that ambient temperatures could have an affect on the overall behaviors and could improve attraction results. This was tested by leaving

one 32x32 resolution heat matrix at ambient room temperature and another was placed inside a custom cooled container that maintained an ambient temperature of 18°C a standard passive feed-forward pattern was applied, running with the exact same settings on both.

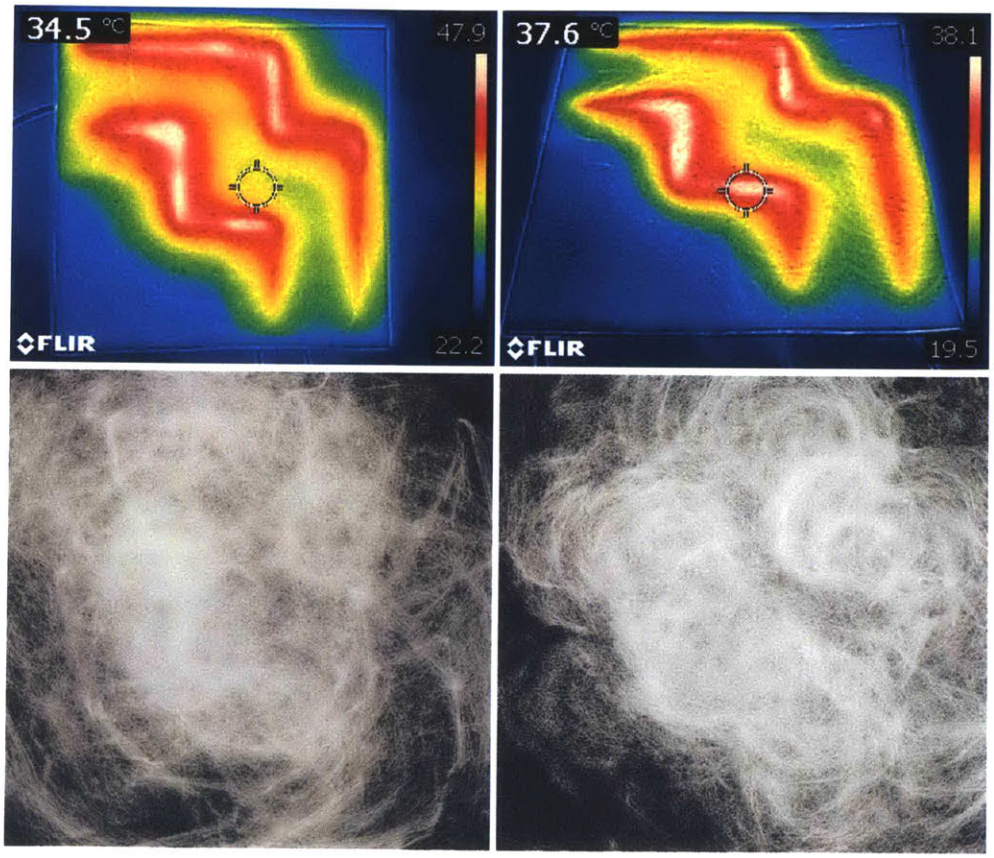

Figure 54: Here, feed-forward experiments were done to verify basic control of the system, both images were generated on a 32x32 platform running at 17.5V with 100% PWM. Both also used 5 silkworms in their 5th instar over the course of 3 days. On the left, the platform was kept at ambient room temperature (roughly 22 to 23°C), while on the right the platform was kept in a custom-built fridge with ambient temperature around 18°C. The resulting silk deposition on the right is more pronounced, demonstrating the effect of ambient temperatures. The green and hotter temperatures correspond with silk deposition, suggesting that diffusion, or unintentional spread, of heat has large impact on the output behaviors.

4.2.6 Discussion & Conclusion

While the base platform satisfies the overall requirements, and basic results have been achieved, much of the proposed experiments still need to be attempted and feedback, provided by an overhead web camera, using OpenCV on the Raspberry Pi 3, has not been fully implemented yet.

As shown in a combination of Figure 52 and Figure 54, the ability to isolate pixels, such that the heat does not diffuse across the surface in an uncontrollable way is desirable and can have dramatic effects. This also is suggestive that silkworms may equally prefer a range of temperatures, or experience them in a discrete manner. Additional experiments with higher temperatures would be required.

The two experiments performed in Figure 52 are suggestive that the overall methodology works and can be applied to create similar 2D construction patterns as seen in some simulations done in [127].

Overall, more work needs to be done to better insulate heating effects across the platform surface and feedback from an overhead camera must be included in order to proceed with further experiments. However, these initial results show a promising avenue to explore development of artificial social behaviors in a generally solitary insect. The pathway currently explored begins with a "bottom-up" analysis of existing behaviors in silkworms and develops a control architecture that is "top-down", which provides feedback based on output material density rather than individually controlling each insect.

5 Conclusions and Future Work

Within this thesis I have presented a potential roadmap for achieving scalable, on-site and autonomous fabrication at architectural scales that are feasible today, tomorrow, and in the far future. I have argued that to develop effective fabrication systems, considerations must be given to the *structural designer*, the design of the *fabrication system*, the *materials and processes* used in the structure, and finally the requirements of the *final structure* itself. I argue that in order to match all these considerations, it is important to try to balance "bottom-up" and "top-down" approaches to designing new autonomous systems. Focus was given to mobile systems and how to scale them in output size and build speed using various methods of control and system architecture to augment individual machine capabilities. For each time period discussed I helped

implement these controls strategies on real-world demonstrations. I proposed control strategies for a compound arm approach to develop a fabrication platform composed of existing platforms and code certified material processes. I then explored methods by which multiple robots can work in parallel to use composites, which are an up and coming class of construction materials. And finally, I present a methodology that we can use to study how biology accomplishes incredible construction feats, and how we might be able to cooperate with them at some point in the future.

However, we are still a long way away from truly scalable and truly autonomous fabrication systems, and very few are used currently. In each of the projects demonstrated, a clear need for better external sensing, such as camera-based or LIDAR-based, for feedback arose. Better swarm algorithms and systems, perhaps those considering heterogeneous teams, that can provide structural guarantees that can be used on a wider range of platforms is also needed.

And finally, there is still an incredible amount left to explore in how nature is able to achieve balance and scale, all while creating complex architectures that we still cannot even mimic. A better understanding of these could help us achieve a healthier relationship with the environment and a *material ecology*.

6 References

[1] "BAAM - Big Area Additive Manufacturing," *Cincinnati Incorporated*. [Online]. Available: https://www.e-ci.com/baam/. [Accessed: 23-Apr-2018].

[2] "Contour Crafting," *CC-Corp*. [Online]. Available: http://contourcrafting.com/. [Accessed: 13-May-2018].

[3] "RFL." [Online]. Available: http://www.ita.arch.ethz.ch/archteclab/rfl.html. [Accessed: 18-Apr-2018].

[4] J. Atkinson, "NASA Langley Debuts ISAAC — an 'Impressive Machine,'" *NASA*, 06-Mar-2015. [Online]. Available: http://www.nasa.gov/larc/nasa-langley-debuts-isaac-an-impressive-machine. [Accessed: 06-May-2018].

[5] "Winsun," *Future of Construction*. [Online]. Available: https://futureofconstruction.org/case/winsun/. [Accessed: 05-May-2018].

[6] M. Giftthaler *et al.*, "Mobile robotic fabrication at 1:1 scale: the In situ Fabricator," *Constr. Robot.*, vol. 1, no. 1–4, pp. 3–14, Dec. 2017.

[7] V. Helm, S. Ercan, F. Gramazio, and M. Kohler, "Mobile robotic fabrication on construction sites: DimRob," in *2012 IEEE/RSJ International Conference on Intelligent Robots and Systems*, 2012, pp. 4335–4341.

[8] "Home - Fastbrick Robotics." [Online]. Available: https://www.fbr.com.au/. [Accessed: 05-May-2018].

[9] F. Augugliaro *et al.*, "The Flight Assembled Architecture installation: Cooperative construction with flying machines," *IEEE Control Syst.*, vol. 34, no. 4, pp. 46–64, Aug. 2014.
[10] Q. Lindsey and V. Kumar, "Distributed Construction of Truss Structures," in *Algorithmic Foundations of Robotics X*, Springer, Berlin, Heidelberg, 2013, pp. 209–225.
[11] M. Dogar, R. A. Knepper, A. Spielberg, C. Choi, H. I. Christensen, and D. Rus, "Multi-scale assembly with robot teams," *Int. J. Robot. Res.*, vol. 34, no. 13, pp. 1645–1659, Nov. 2015.
[12] "Minibuilders." [Online]. Available: http://robots.iaac.net/. [Accessed: 05-May-2018].
[13] M. Doerstelmann *et al.*, "ICD/ITKE Research Pavilion 2014–15: Fibre Placement on a Pneumatic Body Based on a Water Spider Web," *Archit. Des.*, vol. 85, no. 5, pp. 60–65, Sep. 2015.
[14] "Mobile Robotic Fabrication System for Filament Structures | Institute for Computational Design and Construction." .
[15] L. Cucu, M. Rubenstein, and R. Nagpal, "Towards self-assembled structures with mobile climbing robots," 2015, pp. 1955–1961.
[16] K. Petersen, R. Nagpal, and J. Werfel, "TERMES: An Autonomous Robotic System for Three-Dimensional Collective Construction," 2011.
[17] N. Melenbrink, P. Michalatos, P. Kassabian, and J. Werfel, "Using local force measurements to guide construction by distributed climbing robots," 2017, pp. 4333–4340.
[18] "ICD/ITKE Research Pavilion 2016-17 | achimmenges.net." .
[19] Q. Lindsey, D. Mellinger, and V. Kumar, "Construction of Cubic Structures with Quadrotor Teams," 2011.
[20] "Chinese workers build railway station in just nine hours | The Independent." [Online]. Available: https://www.independent.co.uk/news/world/asia/chinese-workers-productivity-build-nanlong-railway-station-nine-hours-longyan-a8173881.html. [Accessed: 25-Apr-2018].
[21] "Project Escher - Autodesk." [Online]. Available: https://technologycenters.autodesk.com/locations/pier9/research/escher/. [Accessed: 05-May-2018].
[22] M. Allwright, "An autonomous multi-robot system for stigmergy-based construction," p. 158.
[23] M. Dogar, A. Spielberg, S. Baker, and D. Rus, "Multi-robot grasp planning for sequential assembly operations," 2015, pp. 193–200.
[24] "Table of Contents | ICC publicACCESS." [Online]. Available: https://codes.iccsafe.org/public/document/IBC2018. [Accessed: 13-May-2018].
[25] "MX3D Bridge," *MX3D*. [Online]. Available: http://mx3d.com/projects/bridge-2/. [Accessed: 05-May-2018].
[26] G. Gardiner, "SFMOMA façade: Advancing the art of high-rise FRP." [Online]. Available: https://www.compositesworld.com/articles/sfmoma-faade-advancing-the-art-of-high-rise-frp. [Accessed: 13-May-2018].

[27] K. C. Galloway, R. Jois, and M. Yim, "Factory floor: A robotically reconfigurable construction platform," in *2010 IEEE International Conference on Robotics and Automation*, 2010, pp. 2467–2472.
[28] W. Doggett, "Robotic assembly of truss structures for space systems and future research plans," 2002, vol. 7, pp. 7-3589-7–3598.
[29] A. S. J. Suiker, "Mechanical performance of wall structures in 3D printing processes: Theory, design tools and experiments," *Int. J. Mech. Sci.*, vol. 137, pp. 145–170, Mar. 2018.
[30] S. Camazine, J.-L. Deneubourg, N. R. Franks, J. Sneyd, E. Bonabeau, and G. Theraula, *Self-organization in Biological Systems*. Princeton University Press, 2003.
[31] N. Ayanian, P. J. White, Á. Hálász, M. Yim, and V. Kumar, "Stochastic Control for Self-Assembly of XBots," 2008, pp. 1169–1176.
[32] E. Klavins, "Programmable Self-Assembly," *IEEE Control Syst.*, vol. 27, no. 4, pp. 43–56, Aug. 2007.
[33] B. Sparrman *et al.*, "Large-Scale Lightweight Transformable Structures," p. 10, 2017.
[34] S. Tibbits, C. McKnelly, C. Olguin, D. Dikovsky, and S. Hirsch, "4D PRINTING AND UNIVERSAL TRANSFORMATION," *Mater. AGENCY*, p. 10, 2014.
[35] L. Mahadevan and S. Rica, "Self-Organized Origami," *Science*, vol. 307, no. 5716, pp. 1740–1740, Mar. 2005.
[36] M. Rubenstein, A. Cornejo, and R. Nagpal, "Programmable self-assembly in a thousand-robot swarm," *Science*, vol. 345, no. 6198, pp. 795–799, Aug. 2014.
[37] N. Mathews, A. L. Christensen, R. O'Grady, F. Mondada, and M. Dorigo, "Mergeable nervous systems for robots," *Nat. Commun.*, vol. 8, no. 1, p. 439, Sep. 2017.
[38] G. Jing, T. Tosun, M. Yim, and H. Kress-Gazit, "An End-To-End System for Accomplishing Tasks with Modular Robots," 2016.
[39] D. Saldana, B. Gabrich, G. Li, M. Yim, and V. Kumar, "ModQuad: The Flying Modular Structure that Self-Assembles in Midair," p. 8.
[40] M. Yim *et al.*, "Modular Self-Reconfigurable Robot Systems [Grand Challenges of Robotics]," *IEEE Robot. Autom. Mag.*, vol. 14, no. 1, pp. 43–52, Mar. 2007.
[41] J. W. Romanishin, K. Gilpin, and D. Rus, "M-blocks: Momentum-driven, magnetic modular robots," in *2013 IEEE/RSJ International Conference on Intelligent Robots and Systems*, 2013, pp. 4288–4295.
[42] J. Paulos *et al.*, "Automated Self-Assembly of Large Maritime Structures by a Team of Robotic Boats," *IEEE Trans. Autom. Sci. Eng.*, vol. 12, no. 3, pp. 958–968, Jul. 2015.
[43] K. Kotay and D. Rus, "Efficient Locomotion for a Self-Reconfiguring Robot," in *Proceedings of the 2005 IEEE International Conference on Robotics and Automation*, 2005, pp. 2963–2969.
[44] "Apis Cor. We print buildings." [Online]. Available: http://apis-cor.com/. [Accessed: 13-May-2018].
[45] "Home — Built Robotics." [Online]. Available: http://www.builtrobotics.com/. [Accessed: 05-May-2018].

[46] S. J. Keating, J. C. Leland, L. Cai, and N. Oxman, "Toward site-specific and self-sufficient robotic fabrication on architectural scales," *Sci. Robot.*, vol. 2, no. 5, p. eaam8986, Apr. 2017.
[47] S. J. (Steven J. Keating, "From bacteria to buildings : additive manufacturing outside the box," Thesis, Massachusetts Institute of Technology, 2016.
[48] J. L. Bell, "Development of an Experimental Platform for Architectural-Scale Robotics: The Digital Construction Platform," p. 232.
[49] *dcpctrl_v1: Code developed 2015-2016 to control the second iteration of the Digital Construction Platform.* MIT Media Lab, 2018.
[50] S. J. (Steven J. Keating, "Renaissance robotics : novel applications of multipurpose robotic arms spanning design fabrication, utility, and art," Thesis, Massachusetts Institute of Technology, 2012.
[51] S. Keating, N. A. Spielberg, J. Klein, and N. Oxman, "A Compound Arm Approach to Digital Construction," in *Robotic Fabrication in Architecture, Art and Design 2014*, Springer, Cham, 2014, pp. 99–110.
[52]: : "Concrete Buildings :: Commercial Construction Concrete Buildings, Design for Tilt Up and ICF (Insulated Concrete Forms) ::" [Online]. Available: http://www.concretebuildings.org/icf/faq.html. [Accessed: 02-May-2018].
[53] H. Lipkin, "A Note on Denavit-Hartenberg Notation in Robotics," pp. 921–926, Jan. 2005.
[54] J. I. Quinones, "Applying acceleration and deceleration profiles to bipolar stepper motors," p. 7, 2012.
[55] T. W. Yang, W. L. Xu, and J. D. Han, "Dynamic Compensation Control of Flexible Macro #x2013;Micro Manipulator Systems," *IEEE Trans. Control Syst. Technol.*, vol. 18, no. 1, pp. 143–151, Jan. 2010.
[56] A. Sharon, N. Hogan, and D. E. Hardt, "The macro/micro manipulator: An improved architecture for robot control," *Robot. Comput.-Integr. Manuf.*, vol. 10, no. 3, pp. 209–222, Jun. 1993.
[57] "Magnetostrictive linear position sensors." [Online]. Available: http://www.balluff.com/local/us/products/sensors/magnetostrictive-linear-position-sensors/. [Accessed: 10-May-2018].
[58] "Robotics Toolbox – [petercorke.com]." .
[59] "Control of a Macro-Micro Robot System Using Manipulability of the Micro Robot." [Online]. Available: https://www.jstage.jst.go.jp/article/jsmec/49/3/49_3_897/_article. [Accessed: 11-May-2018].
[60] M. Schneider and M. Hiller, "VIBRATION SUPPRESSING FOR HYDRAULICALLY DRIVEN LARGE REDUNDANT MANIPULATORS," p. 8.
[61] I. Duleba, "Modeling and Control of Mobile Manipulators," *IFAC Proc. Vol.*, vol. 33, no. 27, pp. 447–452, Sep. 2000.
[62] S. Chitta, B. Cohen, and M. Likhachev, "Planning for autonomous door opening with a mobile manipulator," 2010, pp. 1799–1806.

[63] W. F. Carriker, P. K. Khosla, and B. H. Krogh, "Path planning for mobile manipulators for multiple task execution," *IEEE Trans. Robot. Autom.*, vol. 7, no. 3, pp. 403–408, Jun. 1991.
[64] "ICD/ITKE Research Pavilion 2012 | achimmenges.net." .
[65] P. Fratzl and R. Weinkamer, "Nature's hierarchical materials," *Prog. Mater. Sci.*, vol. 52, no. 8, pp. 1263–1334, Nov. 2007.
[66] M. LeGault, "Architectural composites: Rising to new challenges." [Online]. Available: https://www.compositesworld.com/articles/architectural-composites-rising-to-new-challenges. [Accessed: 02-May-2018].
[67] M. LeGault, "SkyPath: Scenic bikeway/walkway a winner with composites." [Online]. Available: https://www.compositesworld.com/articles/skypath-scenic-bikewaywalkway-a-winner-with-composites. [Accessed: 05-May-2018].
[68] "High Strength 3D Printing – Markforged." [Online]. Available: https://markforged.com/. [Accessed: 13-May-2018].
[69] "Impossible Objects," *Impossible Objects*. [Online]. Available: http://impossible-objects.com/. [Accessed: 13-May-2018].
[70] J. R. Raney, B. G. Compton, J. Mueller, T. J. Ober, K. Shea, and J. A. Lewis, "Rotational 3D printing of damage-tolerant composites with programmable mechanics," *PNAS*, 2018.
[71] "Plethora." [Online]. Available: https://www.plethora.com. [Accessed: 05-May-2018].
[72] A. H. Bermano, T. Funkhouser, and S. Rusinkiewicz, "State of the Art in Methods and Representations for Fabrication-Aware Design," *Comput. Graph. Forum*, vol. 36, no. 2, pp. 509–535, May 2017.
[73] H. Pottmann, "Architectural Geometry and Fabrication-Aware Design," *Nexus Netw. J.*, vol. 15, no. 2, pp. 195–208, Aug. 2013.
[74] Y. Schwartzburg and M. Pauly, "Fabrication-aware Design with Intersecting Planar Pieces," *Comput. Graph. Forum*, vol. 32, no. 2pt3, pp. 317–326, May 2013.
[75] P. Funes and J. Pollack, "Evolutionary Body Building: Adaptive Physical Designs for Robots," *Artif. Life*, vol. 4, no. 4, pp. 337–357, Oct. 1998.
[76] J. FRAZER, J. FRAZER, L. Xiyu, T. Mingxi, and P. JANSSEN, "Generative and evolutionary techniques for building envelope design," p. 17, 2002.
[77] S. Jing, "Architectural evolutionary system based on Genetic Algorithms," *Interactive Architecture Lab.* .
[78] "PROJECTS," *STUDIO ROLAND SNOOKS*. [Online]. Available: http://www.rolandsnooks.com/. [Accessed: 03-May-2018].
[79] C. W. Reynolds, "Flocks, Herds, and Schools: A Distributed Behavioral Model," p. 13.
[80] M. Munro, "Review of manufacturing of fiber composite components by filament winding," *Polym. Compos.*, vol. 9, no. 5, pp. 352–359, Oct. 1988.
[81] J. V. Anderson, "Automated Manipulation for the Lotus Filament Winding Process," p. 143.
[82] J. Rousseau, D. Perreux, and N. Verdière, "The influence of winding patterns on the damage behaviour of filament-wound pipes," *Compos. Sci. Technol.*, vol. 59, no. 9, pp. 1439–1449, Jul. 1999.

[83] Y. Zhang, Z. Xia, and F. Ellyin, "Two-scale analysis of a filament-wound cylindrical structure and application of periodic boundary conditions," *Int. J. Solids Struct.*, vol. 45, no. 20, pp. 5322–5336, Oct. 2008.
[84] M. L. Skinner, R. R. Roser, and K. J. Samowitz, "Computer Control of Fiber Glass Filament Winding Machines," *IEEE Trans. Ind. Appl.*, vol. IA-21, no. 4, pp. 1057–1063, Jul. 1985.
[85] N. Oxman, "Material Ecology," p. 7.
[86] admin_yourhome, "Rammed earth," 29-Jul-2013. [Online]. Available: http://www.yourhome.gov.au/materials/rammed-earth. [Accessed: 13-May-2018].
[87] "GreenSpec: Environmental Advantages of Rammed Earth Construction." [Online]. Available: http://www.greenspec.co.uk/building-design/rammed-earth/. [Accessed: 13-May-2018].
[88] L. Mogas-Soldevila and N. Oxman, "Water-based Engineering & Fabrication: Large-Scale Additive Manufacturing of Biomaterials," *MRS Proc.*, vol. 1800, 2015.
[89] G. Arthur, "Making houses out of mushrooms," *BBC News*, 30-Aug-2014.
[90] T. Guy, B. Eric, and D. Jean-Louis, "The origin of nest complexity in social insects," *Complexity*, vol. 3, no. 6, pp. 15–25, Jul. 1998.
[91] A. Greene, J. A. Coddington, N. L. Breisch, D. M. De Roche, and B. B. Pagac, "An Immense Concentration of Orb-Weaving Spiders With Communal Webbing in a Man-Made Structural Habitat (Arachnida: Araneae: Tetragnathidae, Araneidae)," *Am. Entomol.*, vol. 56, no. 3, pp. 146–156, 2010.
[92] B. Krafft and L. J. Cookson, "The Role of Silk in the Behaviour and Sociality of Spiders," *Psyche: A Journal of Entomology*, 2012. [Online]. Available: https://www.hindawi.com/journals/psyche/2012/529564/. [Accessed: 05-May-2018].
[93] O. Feinerman and A. Korman, "Individual versus collective cognition in social insects," *J. Exp. Biol.*, vol. 220, no. 1, pp. 73–82, Jan. 2017.
[94] N. E. COLLIAS and E. C. COLLIAS, "WEAVERBIRD NEST AGGREGATION AND EVOLUTION OF THE COMPOUND NEST," p. 15.
[95] C.-C. Lee, K.-B. Neoh, and C.-Y. Lee, "Caste Composition and Mound Size of the Subterranean Termite Macrotermes gilvus (Isoptera: Termitidae: Macrotermitinae)," *Ann. Entomol. Soc. Am.*, vol. 105, no. 3, pp. 427–433, May 2012.
[96] "Sociobiology — Edward O. Wilson | Harvard University Press." [Online]. Available: http://www.hup.harvard.edu/catalog.php?isbn=9780674002357&content=reviews. [Accessed: 15-May-2018].
[97] L. Avilés, G. Harwood, and W. Koenig, "A Quantitative Index of Sociality and Its Application to Group-Living Spiders and Other Social Organisms," *Ethology*, vol. 118, no. 12, pp. 1219–1229, Dec. 2012.
[98] U. Göllner, "Grassé, Pierre-P.: Fondation des Société – Construction. Termitologia. 2. 624 S., 452 Fig., 28 Tab., Masson, Paris, New York, Barcelona, Milan, Mexico, Sao Paulo, 1984," *Dtsch. Entomol. Z.*, vol. 32, no. 4–5, pp. 379–379.

[99] B. Cepelewicz, "The Elusive Calculus of Insects' Altruism and Kin Selection," *Quanta Magazine*. [Online]. Available: https://www.quantamagazine.org/the-elusive-calculus-of-insects-altruism-and-kin-selection-20180410/. [Accessed: 03-May-2018].
[100] "On the Origin of Species, 1st Edition by Charles Darwin." [Online]. Available: https://www.gutenberg.org/files/1228/1228-h/1228-h.htm. [Accessed: 09-May-2018].
[101] W. D. Hamilton, "The genetical evolution of social behaviour. I," *J. Theor. Biol.*, vol. 7, no. 1, pp. 1–16, Jul. 1964.
[102] W. D. Hamilton, "The genetical evolution of social behaviour. II," *J. Theor. Biol.*, vol. 7, no. 1, pp. 17–52, Jul. 1964.
[103] P. W. Sorensen and N. E. Stacey, "Evolution and Specialization of Fish Hormonal Pheromones," in *Advances in Chemical Signals in Vertebrates*, Springer, Boston, MA, 1999, pp. 15–47.
[104] T. D. Wyatt, "Pheromones and Animal Behaviour: Communication by Smell and Taste," p. 404.
[105] N. Bredeche, J.-M. Montanier, W. Liu, and A. F. T. Winfield, "Environment-driven distributed evolutionary adaptation in a population of autonomous robotic agents," *Math. Comput. Model. Dyn. Syst.*, vol. 18, no. 1, pp. 101–129, Feb. 2012.
[106] M. L. Anstey, S. M. Rogers, S. R. Ott, M. Burrows, and S. J. Simpson, "Serotonin Mediates Behavioral Gregarization Underlying Swarm Formation in Desert Locusts," *Science*, vol. 323, no. 5914, pp. 627–630, Jan. 2009.
[107] W. Trible *et al.*, "orco Mutagenesis Causes Loss of Antennal Lobe Glomeruli and Impaired Social Behavior in Ants," *Cell*, vol. 170, no. 4, pp. 727-735.e10, Aug. 2017.
[108] D. Grünbaum and A. Okubo, "Modelling Social Animal Aggregations," in *Frontiers in Mathematical Biology*, vol. 100, S. A. Levin, Ed. Berlin, Heidelberg: Springer Berlin Heidelberg, 1994, pp. 296–325.
[109] S. Wolfram, "Computation theory of cellular automata," *Commun. Math. Phys.*, vol. 96, no. 1, pp. 15–57, Mar. 1984.
[110] "Cellular Automata and Complexity: Collected Papers, by Stephen Wolfram." [Online]. Available: http://www.stephenwolfram.com/publications/cellular-automata-complexity/. [Accessed: 13-May-2018].
[111] E. R. Berlekamp, J. H. Conway, and R. K. Guy, *Winning Ways for Your Mathematical Plays, Volume 4*, 2nd edition. Natick, Mass: A K Peters/CRC Press, 2004.
[112] A. M. Turing, "The chemical basis of morphogenesis," *Phil Trans R Soc Lond B*, vol. 237, no. 641, pp. 37–72, Aug. 1952.
[113] D. Ladley, "Models of Termite Nest Construction," p. 76.
[114] "The RoboRoach Bundle." [Online]. Available: https://backyardbrains.com/products/roboroach. [Accessed: 03-May-2018].
[115] "DragonflEye Has Liftoff," *Draper - Engineering Possibilities*, 31-May-2017. [Online]. Available: http://www.draper.com/news/dragonfleye-has-liftoff. [Accessed: 03-May-2018].

[116] A. Verderber, M. McKnight, and A. Bozkurt, "Early Metamorphic Insertion Technology for Insect Flight Behavior Monitoring," *JoVE J. Vis. Exp.*, no. 89, pp. e50901–e50901, Jul. 2014.
[117] "Video: DARPA's Remote-Controlled Cyborg Beetle Takes Flight," *Popular Science*. [Online]. Available: https://www.popsci.com/military-aviation-amp-space/article/2009-09/darpa-project-releases-video-remote-controlled-cyborg-beetle. [Accessed: 13-May-2018].
[118] "Hybrid Webs - Projects - Tomás Saraceno." [Online]. Available: http://tomassaraceno.com/projects/hybrid-webs/. [Accessed: 13-May-2018].
[119] "Sculpture," *TOMAS LIBERTINY*. [Online]. Available: http://www.tomaslibertiny.com/sculpture/. [Accessed: 03-May-2018].
[120] M. Rao, "Chinese Artist Exhibits Gorgeous 'Sculptures' Built By Bees," *Huffington Post*, 05-Jul-2014.
[121] K. K. Hirst, "Who Invented Silk, and Did That Really Involve Silkworms?," *ThoughtCo*. [Online]. Available: https://www.thoughtco.com/silkworms-bombyx-domestication-170667. [Accessed: 13-May-2018].
[122] J. Duan *et al.*, "SilkDB v2.0: a platform for silkworm (Bombyx mori) genome biology," *Nucleic Acids Res.*, vol. 38, no. suppl_1, pp. D453–D456, Jan. 2010.
[123] "Silk Pavillion Environment |CNC Deposited Silk Fiber & Silkworm Construction | MIT Media Lab." [Online]. Available: http://matter.media.mit.edu/environments/details/silk-pavillion. [Accessed: 03-May-2018].
[124] N. Oxman, J. Laucks, M. Kayser, and C. D. G. Uribe, "Biological Computation for Digital Design and Fabrication," p. 10.
[125] L. B. Garay *et al.*, "New Technique to Produce Large Amount of Flat Silk by Biospinning," *Agric. Sci.*, vol. 05, no. 14, pp. 1483–1490, 2014.
[126] R. Iwasaki *et al.*, "Silk Fabricator: Using Silkworms As 3D Printers," in *SIGGRAPH Asia 2017 Posters*, New York, NY, USA, 2017, pp. 46:1–46:2.
[127] Institute for Complex Systems Simulation, University of Southampton, UK, SO17 1BJ, N. Hill, and S. Bullock, "Modelling the Role of Trail Pheromone in the Collective Construction of Termite Royal Chambers," 2015, pp. 43–50.
[128] J.-L. Deneubourg, "APPLICATION DE L'ORDRE PAR FLUCTUATIONS A LA DESCRIPTION DE CERTAINES ETAPES DE LA CONSTRUCTION DU NID CHEZ LES TERMITES," *Insectes Sociaux Paris*.
[129] O. H. Bruinsma, "An analysis of building behaviour of the termite Macrotermes subhyalinus (Rambur)," phd, Bruinsma, Wageningen, 1979.
[130] B. Green, P. Bardunias, J. S. Turner, R. Nagpal, and J. Werfel, "Excavation and aggregation as organizing factors in de novo construction by mound-building termites," *Proc. R. Soc. B Biol. Sci.*, vol. 284, no. 1856, p. 20162730, Jun. 2017.
[131] D. Feltell, L. Bai, N. N. Bb, and H. J. Jensen, "An individual approach to modelling emergent structure in termite swarm systems," *Int J Model. Identif. Control*, vol. 3, 2008.